

THESIS FOR THE DEGREE OF DOCTOR OF PHILOSOPHY (PHD)

**Synthesis of multivalent glycomimetics, carbohydrate-containing chimeras
and antibiotics with potential biological relevance**

by **Son Thai Le**

UNIVERSITY OF DEBRECEN
DOCTORAL SCHOOL OF PHARMACEUTICAL SCIENCES

DEBRECEN, 2022

THESIS FOR THE DEGREE OF DOCTOR OF PHILOSOPHY (PhD)

**Synthesis of multivalent glycomimetics, carbohydrate-containing chimeras
and antibiotics with potential biological relevance**

by **Son Thai Le**

Supervisor: **Dr. Magdolna Csávás**



UNIVERSITY OF DEBRECEN

Doctoral School of Pharmaceutical Sciences

Debrecen, 2022

Table of contents

List of abbreviations	5
1. Introduction	6
2. Literature review	8
2.1. Importance of carbohydrate-specific proteins: Lectins	8
2.2. Anti-adhesion therapy	13
2.3. Chimeric strategy	17
2.4. Structure and mechanism of fluoroquinolones	19
2.5. Structure and mechanism of pleuromutilin	22
2.6. Methods for chemical synthesis	24
2.6.1. Copper-catalyzed azide-alkyne cycloaddition	24
2.6.2. Thiol-ene radical addition	26
2.7. The objectives of the work	28
2.7.1. Anti-adhesive therapy with lectin inhibitors	28
2.7.2. Inventing novel chimeric antibiotics	29
2.7.3. Structural modification of pleuromutilin and lefamulin	29
3. Laboratory synthesis	30
3.1. Synthesis of carbohydrate-based lectin inhibitors	30
3.2. Synthesis of chimeric antibiotics	36
3.3. Semisynthetic modification of pleuromutilin	39
3.4. Semisynthetic modification of lefamulin	41
4. Results	43
4.1. Lectin-carbohydrate interaction results	43
4.2. Antibacterial results of chimeric antibiotics	49
4.3. Antibacterial results of pleuromutilin derivatives	51
4.4. Antibacterial results of lefamulin derivatives	53
5. Discussion	54
6. Summary	56

7. Methods and experimental data	57
7.1. Antibacterial measurement	57
7.2. Hemagglutination inhibiton assay (HIA)	57
7.3. Surface plasmon resonance (SPR)	58
7.4. General methods for synthesis	59
7.5. Experimental data	61
8. References	88
8.1. References	88
8.2. List of publications	101
9. Keywords	103
10. Acknowledgement	103
11. Appendix	104

List of abbreviations

ABR = antibiotic resistance

ABS= antibiotics

SA= *Staphylococcus aureus*

MRSA= methicillin-resistant *Staphylococcus aureus*

VRSA=vancomycin-resistant *Staphylococcus aureus*

MIC=minimum inhibitory concentration

PA= *Pseudomonas aeruginosa*

MGC = multivalent glycoconjugate

CuAAC=copper-catalyzed azide-alkyne cycloaddition

DIPEA= N,N-diisopropylethylamine

DPAP= 2,2-dimethoxy-2-phenylacetophenone

MAP= 4-methoxyacetophenone

DMF = N,N-dimethyl-formamide

TFA= trifluoroacetic acid

DCM = dichloromethane

equiv. = equivalent

HIA = hemagglutination inhibition assay

SPA = surface plasmon resonance

MALDI-ToF MS = Matrix-Assisted Laser Desorption and Ionization - Time of Flight Mass Spectrometry

NMR = nuclear magnetic resonance spectroscopy

rt = room temperature

TLC = thin layer chromatography

1. Introduction

Antibiotic resistance (ABR) is an alarming multifaceted problem, and it is predicted to be one of the greatest threats to human health in the next few decades, which requires immediate action to tackle before it is too late. Since the first introduction in the late 1940s, antibiotics (ABS) were effective to treat serious infections and saved millions of lives, but resistance was quickly developed and recognized shortly thereafter. In 2004, more than 70% of pathogenic bacteria were estimated to be resistant to at least one type of antibiotic. Should this problem remain unsolved, it would cause more than 10 million deaths by 2050 [1]. Lack of drug development in recent decades and inadequacy of meticulous infection control further contributed to the threat of resistance [2-5]. The emergence and spread of new resistance may have been greatly accelerated by the overuse and misuse of ABS. In many countries, ABS are easily given without professional control and are inappropriately used in both humans and animals. For instance, patients usually take ABS for common viral sicknesses, for which these medicines are ineffective. Moreover, ABS are also consumed in a large amount in agriculture and may give rise to cross-resistance. The reports of antimicrobial resistance and multi-resistance indicated that bacterial resistance needs to be addressed as a global problem as it presents in every territory [6-8] and is estimated to cause more deaths than cancerous diseases in the next few decades. This rising issue poses both a clinical threat and an economical burden on patients and the health care system, as the bacterial resistance not only limits the therapeutic options, decreases the treatment efficacy, but also leads to more infectious complications, longer hospital stay, higher medical cost, and increases mortality and morbidity of the diseases [9-12]. Resistance can occur spontaneously through mutation, but exposure to antibiotics hastens this process further. This particularly happens in hospital settings where obvious relationships between the use of antibiotics and the appearance of multiresistant strains can be detected. ABS will eradicate drug-sensitive bacteria but leave resistant strains behind, and these resistant ones will continue to grow and reproduce as a result of natural selection. Resistant genes then can be inherited (by vertical transfer) from relatives or can be acquired (by horizontal transfer) from nonrelatives on mobile genetic elements such as plasmids and transposons. This type of horizontal gene transfer allows ABR to be transferred among individuals of the same strain or different strains of Gram-positive and Gram-negative organisms. For instance, at the beginning of the 1950s penicillinase-producing *Staphylococcus aureus* (SA) caused many clinical problems that were subsequently solved by the introduction of methicillin, cloxacillin, and then flucloxacillin, which has resulted in a significant decrease of these strains. But methicillin-resistant *Staphylococcus aureus* (MRSA) strain was detected very shortly after the introduction of methicillin in 1960,

and this event marked the start of the long battle against MRSA. Moreover, the dramatic increase of MRSA infections has led to the utilization of vancomycin, which later resulted in the thickened cell wall of MRSA that represents a sign of mild resistance. The biggest dread is that glycopeptide-resistant *enterococci*, a gram-positive strain, can transfer vanA gene complex into SA to produce vancomycin-resistant *Staphylococcus aureus* (VRSA) strain. Between 2002-2007 in the USA, six clinical isolates of VRSA have been reported, all carrying the vanA gene complex. As a consequence, the more antibiotics are used, the more serious the resistance is. Especially when the first and then second-line of antibiotic treatments are unavailable or ineffective, patients have to resort to using drugs that are more expensive and more toxic [13-14].

In general, bacteria can resist antibiotic actions by either intrinsic or acquired pathways, and it is the latter that we must worry about because the bacteria which were initially susceptible to antibiotic treatments now become untreatable. Resistance can be achieved through a variety of mechanisms including enzymatically inactivating the ABS, altering the target sites for the ABS, blocking the transport of the ABS into the bacterial cell, enhancing the efflux of the ABS out of the cell, and bypassing the metabolic pathways inhibited by the ABS. Multiple resistance mechanisms may be encoded on a single plasmid, transposon, integron, or cassette. In addition, bacteria may possess more than one mechanism of resistance to a single class of drugs. Mutations or horizontal genetic transfer, in combination with selective pressure from antimicrobial agents (either natural or synthetic antimicrobial agents), particularly in suboptimal concentrations, enable many bacterial species to adapt quickly to the ABS. While a single mutation only reduces the susceptibility of the bacteria to one antibiotic agent slightly, this might be just enough to allow them to survive until they acquire further mutations or additional genes which would result in full-fledged resistance to that antibiotic agent. However, in rare circumstances, a single mutation can be enough to grant high-level and clinically significant resistance to an organism. Ultimately, this can lead to *multidrug-resistant*, *extensively drug-resistant*, and *pandrug-resistant bacterial* strains. Multi-drug resistance refers to bacteria that are resistant to one antibiotic in three or more antibiotic classes. Extensively drug resistance is a more serious problem when bacteria are only vulnerable to one or two antibiotic classes, and pandrug resistance is the most dangerous complication as bacteria are not susceptible to any antibiotic classes [15-19]. One striking illustration is *Pseudomonas aeruginosa* (PA), one of the most deadly opportunistic Gram-negative pathogens that is responsible for many acute and chronic nosocomial infections including pneumonia, urinary tract infection, gastrointestinal infection, skin and soft tissues infection, burn infection, and blood infection. This species is intrinsically

resistant to many ABS such as macrolides, tetracyclines, β -lactams, and many fluoroquinolones. PA is typically found in cystic fibrosis and immunocompromised patients whose immune system is weakened, and this bacterium is also classified in the “critical” category according to the World Health Organization, for which research and development of new ABS is an urgent need. This pathogen is outrageously dangerous as it is not only associated with high mortality and morbidity when compared to other bacterial infections but also able to develop a variety of resistant mechanisms through multidrug efflux pumps, β -lactamases, target mutations, decreased membrane permeability, and biofilm formation. These factors together render PA the potential to become multidrug-resistant and more difficult to treat than before [20-26]. Once ABR is allowed to continue uncontrollably, we may enter a ‘post-antibiotic era’ of medicine, in which even a minor infection may become lethal. In the light of this global problem, we aimed to tackle ABR through three approaches during my doctoral research including building multivalent glycomimetics, developing chimeric antibiotics, and modifying mutilin-type antibiotics.

2. Literature review

2.1 Importance of carbohydrate-specific proteins: Lectins

Lectins have long been molecules of interest in the field of glycobiology, as they can be found in most organisms and have a wide range of applications in biology and medicine [27]. They are involved in several physiological processes including cell-cell interactions, cell transport, biosignaling, immunological response, and toxicity. Particularly, lectins are of special importance in cellular recognition [28]. They are proteins or glycoproteins of non-immune origin with no catalytic activity that interact non-covalently and reversibly with their carbohydrate ligands via carbohydrate recognition domains (CRD). They may need metal ion such as Ca^{2+} or Mn^{2+} for their binding activity. Usually, the cations are chelated by the oxygen atoms of the hydroxyl groups from carbohydrates and by the amino acids. And the metal ions perform a critical task in detecting the stereospecificity of carbohydrates by recognizing the relative stereochemistry of two neighbouring hydroxyl groups (cis or trans) [**Figure 1**].

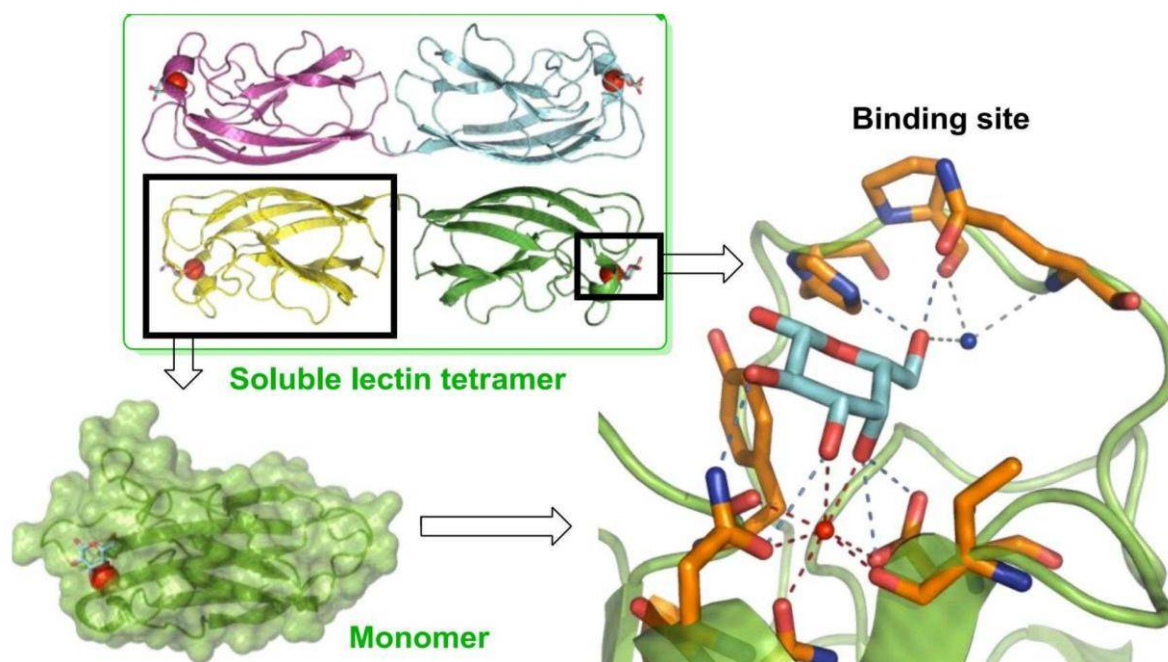


Figure 1. Schematic description of lectin and its interactions with carbohydrate ligand [61].

Depending on the biological structure and the type of organism, each type of lectin has a different CRD and displays different affinity and specificity for its mono- or oligosaccharide ligands, with higher binding affinity for the latter as oligosaccharides are more flexible and most likely the natural ligands of lectin. Thus, elucidating the three-dimensional structure of lectin based on the spatial arrangement of amino acids is of special interest, as it provides a basis for comprehending how lectin recognizes and binds to its natural ligand through a network of hydrogen bondings and hydrophobic interactions. Hydrogen bonding is constituted by the binding of hydroxyl groups of carbohydrate to the polar groups of the lectin. Hydrophobic interactions are made up of the hydrophobic patches of the sugar structure and the aromatic residues present in the lectin. Since lectins are able to bind to carbohydrate ligands specifically and hence act as recognition determinants, especially in the world of microbes, they are considered as invaluable tools for the examination of the pathogen-host cell recognition-adhesion process. Therefore, studying lectins and their role in cellular recognition is making significant contributions to the improvements of glycobiology [29-30]. In nature, bacteria, viruses, and parasites use their lectins to recognize and bind to sugar moieties of glycoconjugates on the surface of host cells [31-33] and thus mediate pathogen-host cell adhesion [Figure 2]. Viral lectins are usually called hemagglutinins, and bacterial lectins are classified into two classes: lectins (adhesins) which locate on the outer surface of bacteria and facilitate bacterial adhesion-colonization, and the other is secreted bacterial toxins. Such specific recognition-adhesion is the initial step in pathogenesis, and it is usually

followed by invasion and infection [34-35]. This also accounts for the preference of certain pathogens in selected tissues—a phenomenon called tissue tropism— and selected species, similarly.

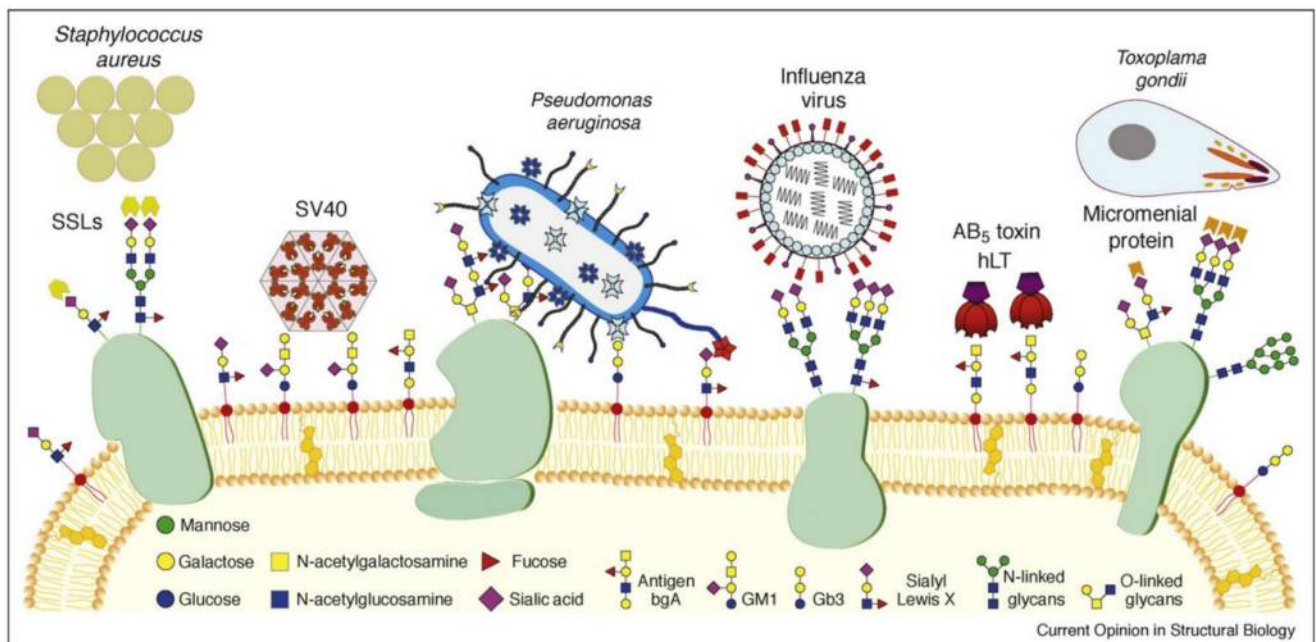


Figure 2. Some of the strategies used by pathogens for host glycoconjugates recognition and adhesion [31].

An interesting illustration of the role of bacterial lectins in the recognition of host cells is provided by *Escherichia coli* (*E.coli*) K99. This organism binds to *N-glycolylneuraminic acid* but not to *N-acetylneuraminic acid*; these two sugar molecules only differ in a single hydroxyl group, which presents in the former molecule but absent in the latter. *N-glycolylneuraminic acid* is typically found on piglets' intestinal cells but normally disappears when they grow up and develop. This type of compound is also not normally formed in human beings. This phenomenon explains why *E.coli* K99 causes diarrhoea (usually lethal) in newborn piglets, but not in adult pigs nor humans. Another illustration is a prejudiced lung infection caused by *Influenza viruses*, both *Human influenza* and *Avian influenza* strains use hemagglutinin to bind to sialic acid moieties on the host cell surface. The former strain preferentially binds to α -2,6-linked sialic acid, whereas the latter strain binds to α -2,3-linked sialic acid. α -2,6-linked sialic acid receptors are found at higher levels on epithelial cells, including ciliated cells and, to a lesser extent, on goblet cells in the upper respiratory tract. α -2,3-linked sialic acid receptors are found at higher levels on nonciliated bronchiolar cells and alveolar type II cells in the lower respiratory tract. As a result, *Human influenza* viruses primarily bind to ciliated epithelial cells and infect the upper respiratory tract, whereas *Avian influenza* viruses generally bind to nonciliated epithelial cells and infect the lower respiratory tract [36-38]. One

more notable example is that the *Coronaviruses* (*SARS-CoV* in 2003 and *SARS-CoV-2* in 2019) use the receptor-binding domain (RBD) of S protein (a glycoprotein) to specifically bind to angiotensin-converting enzyme 2 (ACE2) to mediate viral binding. X-ray crystallography of the RBD-ACE2 complex was used to analyze the interactions between these two components at the molecular level and suggested that there was a RBD-glycan interaction. And this interaction was proposed to have important roles in the binding of *Coronaviruses* to ACE2. This explained why *Coronaviruses* mainly infected those cells that expressed ACE2 such as lung, trachea, small intestine, kidney, pancreas, and heart [39-41]. And the converse is true in some cases, in which pathogens use their surface polysaccharide to bind to lectin on the host cell to media host cell-pathogen adhesion. Basically, lectins can be categorized into 5 groups, dependent upon the monosaccharide they display the highest affinity [28]:

1. *D-mannose*
2. *D-galactose/N-acetyl-D-galactosamine*
3. *N-acetyl-D-glucosamine*
4. *L-fucose*
5. *N-acetylneuraminic acid*

or 3 classes, based on structural features:

1. *simple*
2. *multidomain (mosaic)*
3. *macromolecular assemblies*

Simple lectins have molecular weights of around 30kDa constituted from a small number of sub-units, and undergo aggregation to dimers and/or tetramers to become active. On the other hand, most animal lectins and viral hemagglutinins display *multidomain* structures composed of different types of protein domains, but only one domain presents a carbohydrate binding site. The families of the animal lectins have conserved CRD and largely have variable carbohydrate specificities. *Macromolecular assembly* structures of lectins are made up of polymers of major subunits and are commonly expressed on the surface of many bacterial species. Only one of the subunits presents a carbohydrate binding site and is accountable for carbohydrate binding activity and specificity. Each lectin typically contains at least two or more CRD, i.e., di- tri- or polyvalent. Therefore, when lectins react with cells, for example red blood cells (erythrocytes), lectins not only combine with the carbohydrates on one cell's

surface, but they will also cause cross-linking among many cells, a phenomenon called cell agglutination and hemagglutination in the case of red blood cells. Lectins are also able to form cross-links among glycoprotein or polysaccharide molecules, and thus induce their precipitation. These two aforementioned reactions of lectins can be inhibited by using the sugars to which they are specific. Unfortunately, the binding affinity of lectins for their monosaccharides is selective but weak, and thus it requires a high sugar concentration for inhibition, normally in the millimolar range. On the contrary, the affinity of lectins for oligosaccharides is usually very high because of their flexibility around the glycosidic bonds and they are more likely to be the natural ligands of lectins [28]. Moreover, covalent linkage of carbohydrates or decoration of scaffold with monosaccharides to create multivalent carbohydrates was proved to significantly enhance lectin binding potency. Besides that, attachment of pathogens to the cell surface also prevents pathogens from being washed away by host cleansing mechanisms such as secretions, ciliary action, salivation, and swallowing. In the normal state, fluid flow is more rapid than the rate of multiplication of bacteria, unattached organisms are simply eliminated along with the luminal contents, by the mechanical cleansing mechanisms, leaving the firmly attached organisms remaining on the surface. Thus, they will have better access to nutrients, form colony, and induce tissue damage and inflammation. As mentioned earlier, pathogen-host cell adhesion initiated by lectin-carbohydrate binding phenomenon [42-43] is the key step of bacterial colonization, from which the next stage is the formation of the biofilm. The biofilm layer helps bacteria to attach irreversibly and firmly to other bacteria, leading to the production of a carbohydrate mucous layer that maintains the integrity of the biofilm. Moreover, the biofilm matrix, which consists of substances like proteins and polysaccharide alginate, acts as a physical barrier that helps to protect bacteria against the host defence system as well as antibiotic action. This usually leads to recurrent or chronic infection, and thus requires prolonged treatment [44]. In addition to lectin-carbohydrate interaction, pathogen-host cell adhesion is also comprised of other interactions such as protein-protein interaction and hydrophobin-protein interaction. Nevertheless, lectin-carbohydrate interaction, due to multiple receptor-ligand interactions between host and pathogen, plays a crucial role not only in recognition-adhesion but also in infection specificity. Taking into consideration, lectins stand out as novel targets for inhibiting lectin-carbohydrate interaction which is a crucial factor in bacterial/viral adhesion, and this inhibition may lead to a new, promising strategy in the fight against bacterial/viral infection.

2.2 Anti-adhesion therapy

In addition to pathogen-host cell recognition-adhesion, the lectin-carbohydrate binding also engages in numerous biological processes such as inflammation, immunological response, cancer metastasis, and cell proliferation. From these points of view, taking advantage of the specific binding between lectin and its ligand proposes many biomedical applications [45-46] such as lectin-based drug carrier [47], pathogen detection [48], anticancer therapy [49-50], lectin-based [51] or carbohydrate-based [52] vaccine production, drug design [53], and most important anti-adhesion therapy [54]. As mentioned previously, adhesion and colonization are the most important steps in pathogenesis, as to trigger infection the pathogens need to stick to the host surface strong enough. From this aspect, blocking the pathogen attachment is a crucial tactic to prevent or treat infection, since unattached organisms are easily eliminated by host cleansing mechanisms or host defence systems. Thus, anti-adhesion refers to any methods that prevent the pathogens from attaching to cell surface, and potentially prevent microbial infection from the beginning. The anti-adhesion therapy therefore can be achieved in several potential approaches:

1. *using sub-lethal concentration of antibiotics to alter physicochemical property of the bacterial surface and decrease bacterial adhesion* [43, 54],
2. *developing lectin-based antibodies and vaccines* [43, 54-55],
3. *using dietary supplements or probiotics* [43, 54],
4. *using isolated lectins, or synthetic or recombinant fragments binding to host glycoconjugates to block the bacterial/viral adhesion* [43, 54],
5. *using saccharides binding to bacterial/viral lectin as competitive inhibitors* [55-58].

Among the aforementioned methods, using saccharides to inhibit bacterial/viral lectins is the most feasible method and has been supported by plenty of *in vitro* evidence. For example, co-injection of *E. coli* (which expresses the mannose-specific lectin) together with methyl- α -D-mannoside into the mice bladder was able to prevent the colonization of bacteria by 90% compared to the experimental groups that received only the infected bacteria or methyl- α -D-glucoside, a type of carbohydrate which is not recognized by the mannose-specific lectin [59]. But the major drawback of anti-adhesion therapy is that blocking only one type of adhesin is not sufficient to prevent colonization and symptomatic infection, since most pathogens possess more than one type of adhesin. That is why for effective anti-adhesion therapy, it is essential to use multiple compounds to simultaneously inhibit all types of lectins

of the pathogen, or use a single compound that displays a wide range of anti-adhesion activity. The second problem is that pathogens express several hundreds of lectin molecules on the outer layer for multiple ligand-receptor interactions, thus inhibition of lectin usually requires a high concentration of monovalent ligands, but this could lead to side effects or resistance. These problems could be overcome by linking monovalent ligands to a structured scaffold, for instance polymer, dendrimer, or fullerene [Figure 3] to create a multivalent carbohydrate inhibitor. With this multivalency strategy, such inhibitors can be used at much lower concentration (within micromolar or even nanomolar scale) with higher binding affinity and avidity, as the first binding of receptor-ligand will facilitate the second binding and so forth. For example, the application of α -D-mannosyl glycoclusters in *E.coli* [60] proved to be excellent bacterial lectin inhibitors with a much stronger binding affinity compared to standard α -D-mannose. Another interesting example of multivalency inhibition is provided by PA, a dangerous opportunistic bacterium which displays both LecA (PA-IL), which is specific to galactose, and LecB (PA-IIL), which is specific to fucose. Both lectins are involved in bacterial adhesion and infection process. In *in vitro* and *ex vivo* experiments, tetravalent galactosylated and fucosylated glycoclusters with calix[4]arene scaffold were synthesized and proved to inhibit both bacterial aggregation and bacterial adhesion better than monovalent compounds [61].

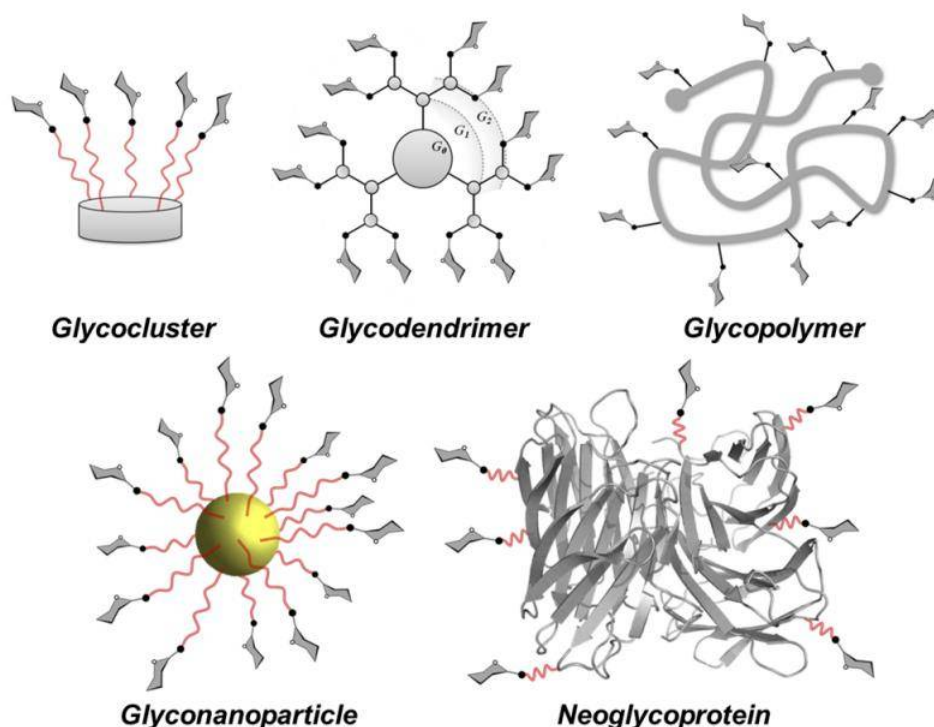


Figure 3. Different types of multivalent glycoconjugates [65].

Moreover, only tetravalent glycoclusters were able to constrain bacterial biofilm formation and display protection against lung injury, whereas monovalent compounds could not. On the other hand, only multivalent carbohydrates which contain multiple sugar units were able to bind to one lectin at multiple binding sites or to several individual lectins (of the same type) at the same time, thus synergistically increasing the binding affinity and binding avidity of the compounds. Another advantage of using multivalent glycoclusters is that their interactions with lectins mimic the interactions that take place in natural biological processes, and in turn, lead to increased binding strength and kinetic stability. Glycoclusters exhibit a restricted but synthetically manipulated amount of epitopes and thus can reach higher valencies, although the drawback is the toxicity of the polymer backbone, size distribution, and valency control. Glyconanoparticles can provide a larger amount of valencies (50–150 valencies). Neoglycoproteins display carbohydrate epitopes at specific positions of proteins and are interesting candidates for drug discovery, although their design is challenging due to toxicity and optimal valency for biomedical applications [62]. The multivalent interactions between multivalent glycoclusters and lectin binding sites can take place through several mechanisms [Figure 4] [63-65]. The first type is *chelate association mechanism* [Figure 4a]. This is among the most investigated mechanisms and can induce significant avidity effects, a phenomenon referred to as multivalency-driven increase of affinity. The second type is *receptor clustering* [Figure 4b]. The third mechanism is *subsite association* [Figure 4c], in which a heterobivalent ligand can bind to a second binding site. The fourth mechanism is *statistical reassociation*, in which multivalent glycosylated structures, when being available in higher density and in close proximity to the binding sites, can interact with monovalent lectin with improved affinity [Figure 4d]. Thus, understanding the structure of lectin receptor and mode of binding at the molecular level is the first priority for designing multivalent scaffolds. A ligand-based design that begins with the natural ligand and then designs an optimized structure is an efficient method. But this strategy is extremely complicated because of the difficulties of completely understanding the topology, valency, and density of carbohydrates. In contrast, the most broadly adopted method begins with the lectin, and then creates a multiglycosylated ligand which would appropriately suit the structure of lectin, so-called "lectin-based design". Careful considerations should be given to the geometry of the scaffold, the number of valencies, and the nature and the length of the linker. Other important factors that must be taken into account include the chemical synthetic pathway which is appropriate for building the multivalent structure, the effectiveness of the synthesis, purification methods, protecting group strategies, and complete regio- stereoselectivities of the reactions. Such careful selections of multivalent scaffolds and conjugation methods are crucial for the success of the project.

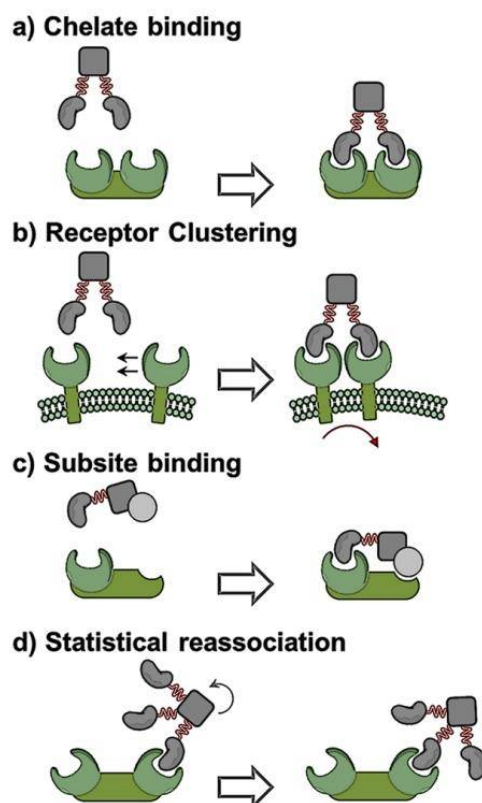


Figure 4. *Interaction between multivalent ligands and multivalent receptors [65].*

One remarkable method is building multivalent glycoconjugate (MGC) from optimized glycomimetic monovalent units. Such an approach will indubitably provide a big success because affinity and selectivity have improved in a synergetic manner [65-67]. Over the past decades, numerous multivalent glycoconjugates with different scaffolds, spacers, and valencies were designed and tested with their corresponding lectins. In most cases, the binding affinity of MGC is greatly enhanced due to the multivalent effect, sometimes the binding affinity of tri- or tetravalent compounds could be increased up to several hundredfolds or even a thousandfold. For example, glycopeptide dendrimer that uses lysine as a branching unit was synthesized and evaluated for binding to LecA of PA. It contained four tripeptide spacers and four galactoside end-groups. This compound, which is a tetravalent ligand, was found to be the best binder to LecA, with a K_d of 0.1 μM , a 219-fold improvement over monovalent D-galactose. In the context of infection, this compound can prevent the formation of biofilms and disperse existing ones [68]. The interactions are highly dependent on the nature of multivalent compounds and their targets. So, the structure of scaffolds, length of spacers, the conformation of carbohydrates, and topology and rigidity of MGC products are of utmost importance as they have the potential to act as selective inhibitors, which are able to discriminate between lectins with closely related sequences [69-77]. Moreover, MGC was

also proved to inhibit bacterial biofilm formation, aggregation, and adhesion, thus reducing the spread of infection better than monovalent compound. The effectiveness of adhesion inhibition suggests that MGC has the potential to improve or even replace antibiotic treatments. The biggest advantage of antiadhesion therapy over traditional antimicrobial treatment is that it does not result in the development of resistance, as the viability of pathogens is not affected since these anti-adhesion agents do not kill or interrupt the growth of bacteria. However, it is inevitable that resistance to anti-adhesion agents would occur but at a significantly lower rate than that of resistance to antimicrobial agents. Hence, anti-adhesion therapy is a noteworthy, novel strategy that can be used in the fight against microbial resistance.

2.3 Chimeric strategy

As discussed above, ABR is a global problem that needs immediate solutions. Especially with multidrug-resistant and extensively drug-resistant infections, the treatment is usually so complicated that health care professionals need recourse to last line ABS such as polymyxin or colistin, but these agents are more toxic and thus often lead to serious side effects. Another milder approach is to use antibiotics in combination such as amoxicillin-clavulanic acid, piperacillin-tazobactam, or combine two or three currently available ABS with different modes of action [78-85]. These combination therapies proved to be effective in many cases, yet the biggest problem is the emergence of new resistant mechanisms against each of ABS used in these therapies, particularly when it is not used at optimal concentration. Therefore, in order to combat bacterial resistance and to prepare an arsenal of potential ABS for future resistance, we need new ABS with improved activity, or new modes of action, or a new class of drugs with new target interactions. From the perspective of medicinal chemistry, there are three possible strategies that can be employed:

1. *finding new ABS from natural or synthetic resources*
2. *modifying the structure of currently available ABS*
3. *developing of hybrid ABS.*

While *finding new ABS from natural or synthetic resources* is a long, costly process that needs to go through pre-clinical and clinical trial procedures that normally take 10-15 years, *modifying the structure of ABS* has led to the development of new generation ABS with improved pharmacokinetic-dynamic properties and better spectrum and resistance profile. For instance, vancomycin, which is a natural antibiotic, binds to the terminal dipeptide D-alanine-

D-alanine, a precursor of the peptidoglycan chain of the bacterial cell wall, thus inhibiting cell wall synthesis. Telavancin, a more lipophilic derivative of vancomycin, was approved for the treatment of bacterial skin infections [Figure 5]. It is derived from the chemical modification of vancomycin by attaching a (decylaminoethyl) lipophilic tail on the vancosamine sugar and a hydrophilic [(phosphonomethyl)aminomethyl] group on the 4' position of aromatic amino acid. The former modification improves potency against a range of Gram-positive pathogens, whereas the latter provides favourable pharmacokinetic properties [86].

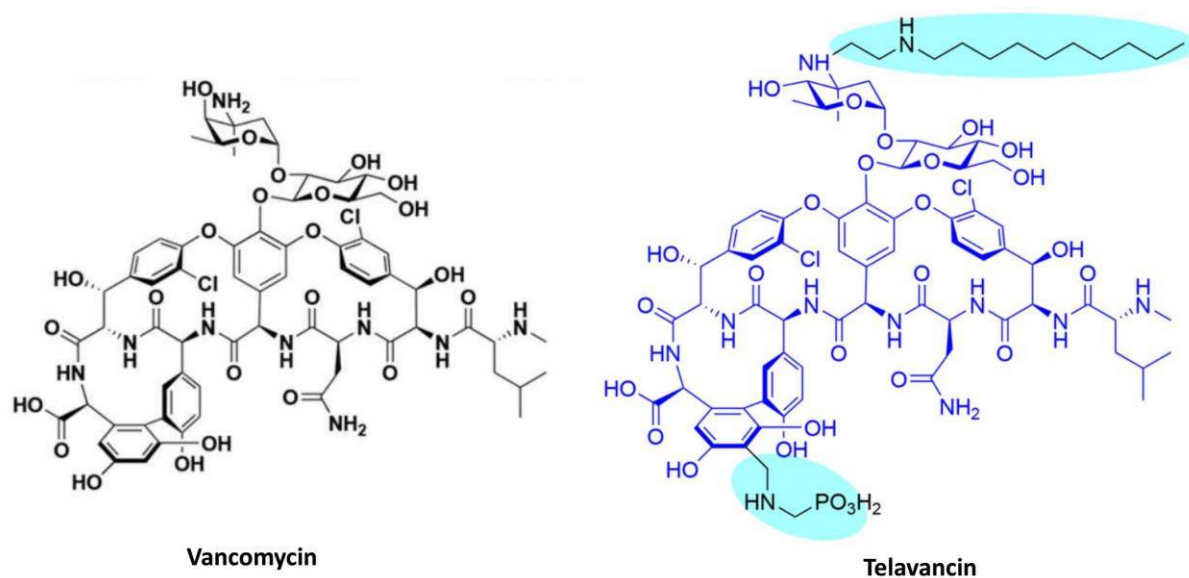


Figure 5. Structure of Vancomycin and Telavancin [86].

Oritavancin is significantly more potent, also binds to D-Ala-D-Ala as primary and cell membrane as secondary interaction. The lipophilic structural features of this agent not only increase its half-life in humans but also provide additional target interactions accounting for improved potency. However, synthesizing new antibiotics with improved spectrum and resistance properties through chemical modification is facing significant challenges due to the lack of modifiable chemical sites. As the pharmacophore structure remains untouched, the biggest threat is the class-based resistance or cross-resistance [87] such as β -lactamase or efflux pump, once occurred, may quickly abate the new agents' efficacy. Alternatively, the invention of *hybrid ABS* by joining the two or three ABS of different antibiotic classes or their pharmacophore groups into one chemical entity (with or without a linker) has opened up a new therapeutic approach to bacterial resistance. The key concept of building a hybrid molecule is that it is less likely to develop resistance when bacteria are attacked at multiple target sites. Moreover, the hybrid molecule is also expected to have a wider spectrum and stronger antibacterial activity. For example, hybrids of tobramycin and ciprofloxacin are highly potent molecules against PA infections [88-89]. At low concentrations, tobramycin

binds to the 30S ribosomal subunit and inhibits protein synthesis, while at higher concentrations it disrupts the outer membrane. Ciprofloxacin, like other fluoroquinolones, targets both DNA gyrase and topoisomerase IV, and inhibits bacterial DNA synthesis. The hybrid candidates showed improved antibacterial activity compared to tobramycin or ciprofloxacin alone. Moreover, when used in combination, the hybrid molecules were able to enhance the effect of other ABS that have poor penetration such as moxifloxacin, erythromycin, or trimethoprim, as the hybrid agents promote the uptake of those ABS via disrupting bacterial membrane. This phenomenon was not observed if tobramycin and ciprofloxacin were used in combination, not as a hybrid molecule. Even the *in vitro* results boded well for the future of hybrid drugs, yet the main drawback related to physicochemical property, poor pharmacokinetic-pharmacodynamic profile, low drug bioavailability due to high molecular weight, and potential drug-drug interactions [90]. The problem with ABS is that there are no "ideal" ABS as resistance is an inevitable event, and the average time for one antibiotic from introduction to resistance recognition is just 5 years. Old ABS then have to be replaced by newer ones when they become ineffective. While the pressure of bacterial resistance is increasing and the therapeutic options are narrowing, the need for new ABS or new alternatives to overcome ABR is paramount [91-94].

In our research, in addition to the synthesis of new anti-adhesive agents, we also introduced a new concept to combat bacterial resistance: chimeric strategy. We chose PA as the main target since this Gram-negative pathogen expresses two soluble lectins on the outer membrane, the two key virulence factors LecA and LecB, which are ideal targets for lectin-carbohydrate interactions [95-97]. On the other hand, this infamous pathogen is only susceptible to a few ABS such as fluoroquinolones or aminoglycosides which makes the treatment challenging, but the treatment is more effective when these ABS were used in combination with sugar therapy [98-100]. We proposed that combining sugar and antibiotic into one single molecule could improve the anti-infective properties of the compound. By taking the advantages of anti-adhesion therapy and hybrid antibiotics together, we developed novel chimeric ABS by conjugating multivalent glycomimetics with conventional antibiotics [101-104].

2.4 Structure and mechanism of fluoroquinolones

Quinolones quickly became the centre of scientific and clinical interest since their discovery in the early 1960s. They possess many attributes of being an ideal antibiotic class such as great potency, wide spectrum, favourable bioavailability, and low incidence of side

effects. They were primarily used for the treatment of uncomplicated urinary tract infections. Over the past decades, numerous chemical modifications were carried out on the parent molecule and led to the structural evolution with four generations of fluoroquinolones, as the newer drugs have enhanced pharmacokinetic-pharmacodynamic profile. This development has shifted the indication of these agents from uncomplicated urinary tract infections to more systemic use, and currently to respiratory tract infections. Generally, the newer quinolones possess enhanced activity against *Mycoplasma pneumoniae* and other atypical bacteria, and some agents have increased activity against Gram-negative anaerobes, for example *Bacteroides fragilis*. Nevertheless, many newer quinolones such as gatifloxacin, gemifloxacin, garenoxacin and moxifloxacin, are less potent than ciprofloxacin against PA. One of the crucial developments in terms of potency is the enhanced activity against Gram-positive such as SA, *Streptococcus pneumoniae*, and Group A streptococci. The attachment of a fluorine atom at position -6 was one of the earliest modifications to the structure. This modification brought on more than a ten-time increase in gyrase inhibition and a hundred-time improvement in minimum inhibitory concentration (MIC). **Figure 6** shows the basic structure of fluoroquinolone molecule from which two major groups have been developed: quinolones and naphthyridones.

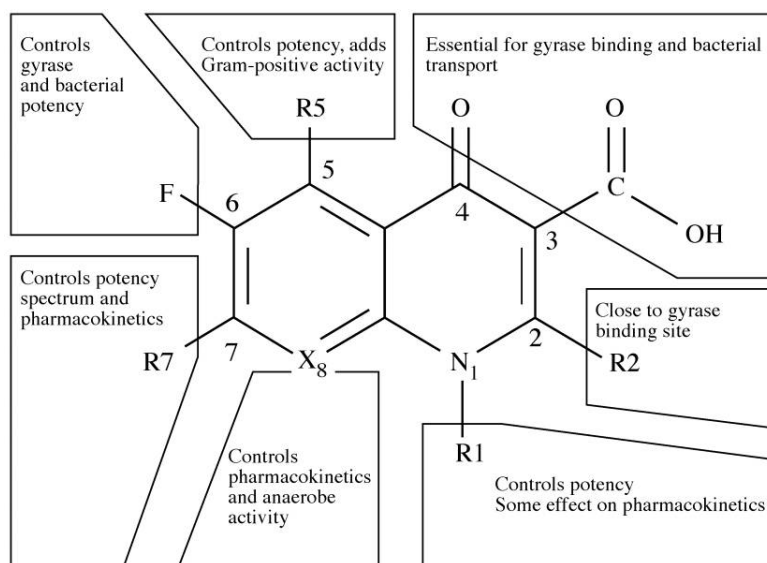


Figure 6. Basic structure of fluoroquinolones [105].

The quinolones and naphthyridones were further developed by modifications at the N-1, C-5, and C-7 positions of the molecules. The appearance of piperazine group at C-7 position enhanced anti-Gram-negative activity. This group is supposed to play a role in inhibiting efflux mechanisms, thus increasing the potency of the agents. The alterations at C-7 position were associated with many key features such as antibacterial spectrum, bioavailability, and side effects. The most common derivatives were cyclic amino groups

(piperazine or pyrrolidine), while other substituents were less potent. A cyclopropyl added to the N-1 position increased the potency of the drug. The addition of a 2,4-difluorophenyl group at N-1 position (trovafloxacin) enhanced potency and anti-anaerobes activity. Addition of primary amine group (-NH₂) at C-5 position generally increased activity against Gram-positive bacteria. Modifications at X-8 position might change oral pharmacokinetic properties, broaden the antibacterial spectrum, and reduce the selection of mutants. Especially, alkylation, which generally increases the lipophilicity, has further increased activity against Gram-positive, enhanced tissue penetration, and prolonged the half-life of the agents (grepafloxacin, levofloxacin and sparfloxacin) [105-106].

Quinolone antibiotics are classified into four groups based on clinical use, pharmacodynamic-pharmacokinetic properties, and their potency. The first group consists of older drugs which are active against the common *Enterobacteriaceae* and thus used in the treatment of urinary tract infection. The second group includes ciprofloxacin, levofloxacin, and ofloxacin that can be used for Gram-negative infections and *Pseudomonas* infections. The third group have a sufficiently broad spectrum against Gram-negative, Gram-positive, *Pseudomonas*, and anaerobic strains so that they can be used for a wide range of infections. The fourth group are respiratory agents such as moxifloxacin and garenoxacin; these drugs have good activity against *Streptococcus pneumoniae* and atypical bacteria but are weaker against PA. Regarding the action mechanism, fluoroquinolones inhibit bacterial DNA synthesis by inhibiting DNA gyrase (topoisomerases II) and topoisomerases IV, which are not present in human cells but are essential for bacterial DNA replication, thereby enabling these agents to be both bacterial specific and bactericidal. Fluoroquinolones tend to inhibit DNA gyrase (topoisomerase II) in Gram-negative organisms and topoisomerase IV in Gram-positive bacteria. These ABS interact with the enzyme-bound DNA complex to create conformational changes that inactivate the enzymes. As a result, the new drug–enzyme–DNA complex blocks DNA replication, thereby inhibiting DNA synthesis and ultimately resulting in rapid cell death. Bacteria can develop fluoroquinolone resistance through two main mechanisms: mutation of target enzymes and expression of efflux pumps. Mutations in DNA gyrase and topoisomerase IV commonly occur in Gram-negative and Gram-positive bacteria, respectively. Such mutations take place in enzyme subunits, thereby reducing the drug binding affinity and diminishing antibacterial effect. Another mechanism of bacterial resistance is the expression of membrane-associated efflux pumps, which actively pump drugs out from the bacterial cell [107-109]. In spite of the fact that bacteria can evolve and gain resistance, fluoroquinolones are apposite candidates for constructing novel chimeric antibiotics.

2.5 Structure and mechanism of pleuromutilin

Pleuromutilin is an unusual tricyclic diterpenoid bio-product with eight contiguous stereocenters [Figure 7] first extracted from *Pleurotus mutilus* and *Pleurotus passeckerianus* species in crystalline form in the early 1950s [110-111].

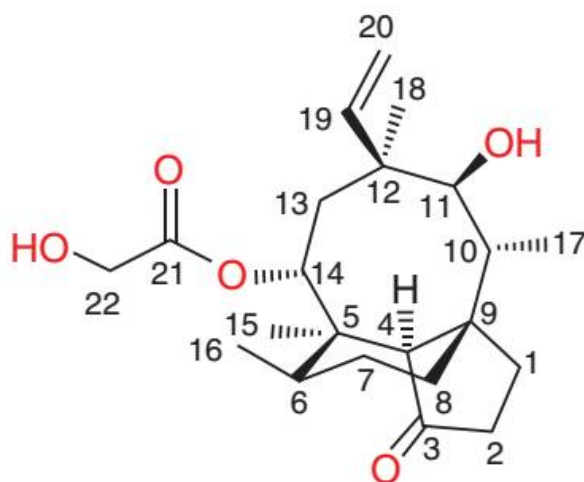


Figure 7. Structure of Pleuromutilin with Arigoni numbering system [124].

This natural compound was found to be active against *Staphylococcus aureus*, *Mycobacterium tuberculosis*, and some Gram-negative strains by binding to the 23S rRNA of the 50S bacterial ribosome subunit, preventing peptidyl transferase reaction, thereby inhibiting protein synthesis. The hydroxyl group of C-11 and the carbonyl oxygen of C-21 are suitable for hydrogen bonding [112]. This unique mode of action is different from that of currently available ABS, and it made pleuromutilin an ideal candidate in the battle against bacterial resistance as it has a low probability of resistance and rare cross-resistance with other ABS. In the past, the research and development for pleuromutilin were stopped due to its poor solubility in water and strong inhibition of human cytochrome P450. But nowadays, under the pressure of ABR as many drugs are losing their antibacterial effect, the need for new ABS with new mode of action is paramount. Therefore, numerous derivatives of pleuromutilin were synthesized and led to the success of tiamulin, valnemulin, retapamulin, and lefamulin [Figure 8].

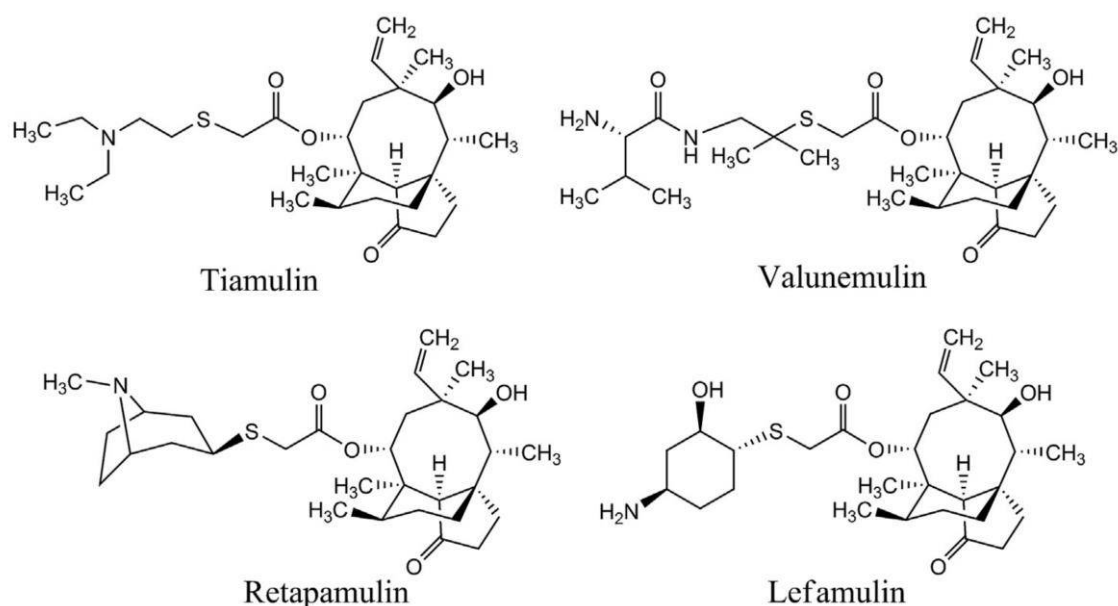


Figure 8. Structure of Tiamulin, Valunemulin, Retapamulin, and Lefamulin [122].

The first two mentioned pleuromutilin analogues are used in veterinary medicine, and the last two analogues are used to treat human diseases. Retapamulin is used topically to treat skin infection, and lefamulin is the only available antibiotic that has been accepted for internal treatment against community-acquired pneumonia. These compounds vary only at the C-14 side chain, in which a sulfur atom is connected to C-22 and followed by a two- or three-carbon linker before a basic nitrogen functionality. The introduction of a thioether at the C-22 position and the presence of a basic group enhanced antibacterial activity. Based on this interesting knowledge, numerous derivatives of pleuromutilin were synthesized by modifying the core structure, C-12, C-13, C-14, and especially at the C-22 side chain [113-114] with different nitrogen-bearing moieties [115-123], and these compounds were found to have improved activity against *Mycobacterium tuberculosis*, *Staphylococcus aureus*, MRSA. To date, only three mechanisms of resistance to pleuromutilin have been identified including mutations in 23S rRNA and *rplC* genes encoding the ribosomal protein L3, methylation of the nucleotide A2503 by *cfm* methyltransferase, and drug efflux by ATP-binding cassette (ABC) transporters. Despite the detection of resistance mechanisms, the overall rates of resistance to pleuromutilins still remain low and make this antibiotic a potential candidate for drug research and development [124].

Until now, lefamulin is the only mutilin antibiotic approved for human use. The biggest hurdle of pleuromutilin analogues was largely due to low water solubility and poor pharmacokinetic profile. To our best knowledge, whereas modifications at C-14 and C-22

side chains have been extensively conducted, there was only one report about modifications at the C-19-20 double bond, in which pleuromutilins were conjugated to a variety of amino-containing moieties [125]. Clinical data suggested that an ether or thioether bonding at this position is worth investigating. Therefore, in an attempt to explore potential activity at this position, we engaged in pleuromutilin and lefamulin structural modification by using thiol-ene click reaction at C-19-20 terminal alkene. Hence, we proposed photoinitiated thiol-ene radical addition would be an efficient strategy to synthesize a wide range of pleuromutilin-thioether analogues, which would be potential antibacterial candidates.

2.6 Methods for chemical synthesis

2.6.1 Copper-catalyzed azide-alkyne cycloaddition

Copper-catalyzed azide-alkyne cycloaddition (CuAAC) is a kind of Huisgen 1,3-dipolar cycloaddition, which is used for preparations of various heterocyclic compounds [126], yet the main disadvantages of Huisgen-reaction involve increased reaction temperature, prolonged reaction time, and formation of structural isomers due to the lack of selectivity. The concept of "click chemistry", which was first introduced in 2001, has upgraded the applications of Huisgen-reaction. This idea was based on a set of stringent criteria that a reaction must meet, and it must be modular, broad in scope, high in yields, low in inoffensive byproducts, and be stereospecific [127]. The "click chemistry" of CuAAC then became so popular and widely used in chemistry, life science, and materials science due to its mild or moderate reaction conditions, very good yields, fast reaction time, and formation of only one regioisomer, especially when azide and alkyne are among the least reactive functional groups in organic chemistry. Whereas the thermal azide-alkyne cycloadditions generally lead to the formation of mixtures of regioisomers, the copper-catalyzed reaction is very useful for the formation of a 1,4-disubstituted 1,2,3-triazoles ring between a terminal alkyne and an azide, so-called "click reaction" [Figure 9].

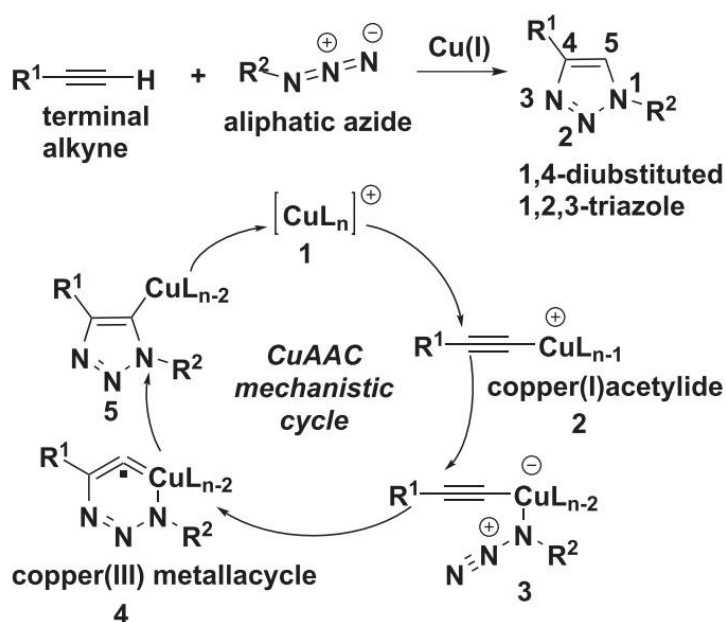


Figure 9. Proposed mechanism Cu(I)-catalyzed azide-alkyne cycloaddition [112].

The triazole rings not only serve as strong linkers but are also able to associate with biological targets through a network of hydrogen bondings and dipole interactions. In contrast to amides and benzenoids, triazole rings can not be cleaved hydrolytically, oxidized or reduced. Furthermore, click reaction has promoted the usage of organic reactions that connect two molecular building blocks in a facile, selective, and high-yielding reaction under mild conditions with few or no byproducts. On the other hand, the purification of the main product is generally easy and it is orthogonal with a wide range of protecting groups. And the applications of CuAAC are progressively employed in drug discovery and development, from lead finding to bioconjugation strategies for proteomics and DNA research [128-129]. The limitation of the CuAAC method in bioorthogonal reactions and chemical biology chiefly dues to the toxic nature of copper.

Regarding the reaction mechanism, CuAAC reaction takes place in a step-wise process in which copper forms acetylide via coordination with an alkyne in the initial step. In the next step, azide binds to the copper followed by the formation of an unconventional copper(III)metallacycle. The intermediate undergoes ring contraction to give copper-triazolyl derivative, which upon protonolysis gives the desired 1,2,3-triazole product. Copper, either as metal or in salt form (ionic or complex), has been employed as the most effective catalyst to promote the 1,3-dipolar addition reaction, and among copper halide catalysts, copper(I) iodide is frequently used in various transformations. Thanks to the advantages of "click chemistry",

CuAAC is a useful tool to conjugate two molecules into a single chemical/biochemical compound.

2.6.2 Thiol-ene radical addition

In addition to the CuAAC reaction, photoinduced thiol-ene radical addition, which also falls into the category of click chemistry and has been extensively studied over the last decades, is a powerful tool in synthetic chemistry to create a new robust C-S bond from free thiol -SH and electron-rich C=C double bond. Thiol-ene radical addition reaction possesses many key features of "click chemistry" such as high yield reaction with easily removable by-products, regio- and stereospecificity, mild reaction conditions, and ready availability to a wide range of starting compounds. These advantageous attributes enable the thiol-ene radical reaction to have a broad spectrum of applications ranging from polymer science to biochemistry/organic chemistry, especially in the field of material fabrication and molecular synthesis [130-136]. The rate of reaction is largely dependent on the chemical structures of the thiol and alkene. Another important factor is the steric hindrance of substitutions on double bonds, as singly substituted alkenes are more reactive than highly substituted alkenes; therefore, terminal alkene is the most reactive, whereas addition to internal C=C bond exhibits a much lower reaction rate. There are two basic rules about this radical addition reaction. Firstly, the conversion rate is related to the alkene's electron density, with electron-rich alkenes being consumed much more quickly than electron-poor ones, which are more favourable in thiol-Michael addition reaction [137]-an analogue to thiol-ene radical addition. The basic exception is that highly conjugated double bond compounds copolymerize very slowly with thiols, because of the high stability of the carboncentered radical formed upon the addition of thiyl radical to C=C double bond. Secondly, in several cases, thiol based on mercaptopropionate ester reacts with a given alkene more rapidly than thiol based on mercaptoacetate ester, which in turn reacts more quickly than simple alkyl thiol. Because hydrogen bonding between the thiol hydrogen and the ester carbonyl can weaken the sulfur-hydrogen bond, thus facilitates hydrogen abstraction from the thiol group [138].

The addition of the thiol across the double bond is exothermic and proceeds through a free-radical step-growth mechanism: radical initiation, chain propagation, and chain termination. Thiyl radicals are highly versatile reactive intermediates that are able to undergo a large number of addition reactions to unsaturated systems including alkenes, alkynes, thiocarbonyl, and isonitrile groups. Thiyl radicals are readily formed through homolytic cleavage of the sulfhydryl S-H bond due to low bond dissociation energies of around 87

kcal/mol. In the initiation step, a radical initiator is usually employed to generate a thiyl radical, either via direct hydrogen abstraction from a thiol or via addition across a double bond which generates a radical that then abstracts hydrogen from another thiol in the reaction medium. The produced thiyl radical adds across an alkene generating an intermediate carboncentered radical, which then abstracts hydrogen from another thiol to generate a thioether product that exhibits a high degree of anti-Markovnikov selectivity, and a new thiyl radical, and the cycle repeats-chain propagation [Figure 10] [139-141]. Thiols can also add to various alkynes either once or twice, consecutively-so called thiol-yne reaction but exhibits slower kinetics than the thiol-ene reaction. Radicals generated during the thiol-ene reaction can recombine or otherwise terminate, effectively stopping the reaction when new radicals are not generated-chain termination. Because of this reaction, photoinitiated thiol-ene reaction generally begins only when the light is turned on and stops almost immediately when the light is turned off.

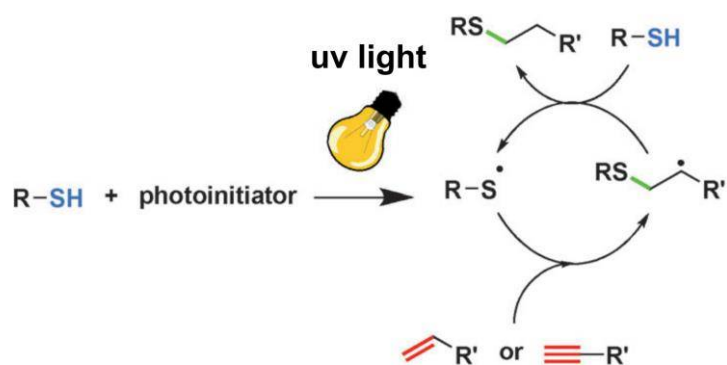


Figure 10. Mechanism of photoinduced thiol-ene/yne click reaction [139].

There are a number of ways to initiate a radical reaction. In our research work, we carried out photoinduced thiol-ene radical addition using a highly effective 2,2-dimethoxy-2-phenylacetophenone agent (DPAP) which gives a benzoyl radical and a tertiary carbon radical [Figure 11] upon the absorption of a photon of ultraviolet (UV) light. A rearrangement of the tertiary carbon radical occurs, yielding a methyl radical and methyl benzoate. The methyl and benzoyl radicals may insert into a C=C double bond directly or abstract a hydrogen from a thiol group. In either case, the two-step process characteristic of the thiol-ene free-radical chain reaction is initiated and repeated as in Figure 10.

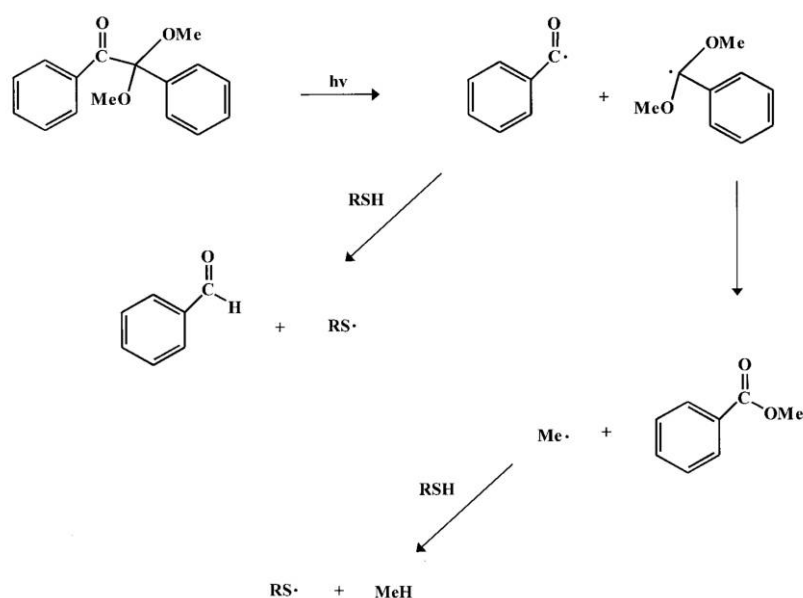


Figure 11. Mechanism for thiol-ene addition with excitation of cleavage photoinitiators [131].

There is no doubt that the use of the thiol-ene click reaction has increased over the past few years as a result of its simplicity, efficiency, and wide applicability. The photoinduced thiol-ene reaction can proceed at normal temperature without a need for metal catalyst and tolerates a number of functional groups, including alcohols, amines, amino acids, carbohydrates, carboxylic acids, and fluorinated compounds. Because the reaction is typically initiated by visible light, which is not harmful to biomolecules, and proceeds well under mild reaction conditions, this type of reaction is an ideal and broadly applicable method, specifically for bioconjugation and organic synthesis.

2.7 The objectives of the work

2.7.1 Anti-adhesive therapy with lectin inhibitors

The first part of my doctoral research mainly focused on developing anti-adhesive therapy by synthesizing a wide panel of carbohydrate-based ligands for bacterial lectins. In particular, L-fucopyranoside and D-galactopyranoside were chosen as monosaccharide units. These two monosaccharides are highly specific for a wide range of pathogens such as *Pseudomonas aeruginosa*, *Burkholderia cenocepacia*, *Aspergillus fumigatus*, *E.coli*. Especially, *Pseudomonas aeruginosa*, which is one of the most dangerous opportunistic pathogens in cystic fibrosis and immunocompromised patients, expresses LecA and LecB that are ideal targets for our potential inhibitors. Since the affinity of LecB for fucose is much higher than that of LecA for galactose, a series of L-fucose-containing compounds were

synthesized. The purpose of this synthesis is to find out the best inhibitor for LecB as well as the best universal inhibitor for fucose-specific lectins [142].

As a rule of nature, lectins generally display a high avidity effect towards their multivalent ligands. Therefore, I also built several trivalent and tetravalent glycoclusters containing α -L-fucopyranoside and β -D-galactopyranoside. The purpose is to find out the best scaffold, linker, and multivalent structure for bacterial lectins. The lectin binding potency of all synthesized compounds was tested via hemagglutination inhibition assay (HIA) with microscopic detection. And the best compounds were studied further in *ex vivo* bacterial adherent assay [142-143].

2.7.2 Inventing novel chimeric antibiotics

In addition to the anti-adhesive therapy, the second part of my dissertation is to invent new ABS to fight against bacterial resistance crisis by synthesizing novel chimeric antibiotics, which are built upon the most suitable multivalent glycoclusters and ABS. Hence, fluoroquinolones and trivalent glycoclusters were chosen. The chimeric ABS are expected to detach bacteria from the host cell, reduce bacterial infection, inhibit bacterial biofilm formation, and thus may enhance the effect of conjugated ABS. Moreover, as the rate of resistance against anti-adhesion therapy is much lower than that against ABS, the rate of resistance against new chimeric molecules is also supposed to remain low. The other advantage of chimeric molecules over conventional ABS is that upon binding to the carbohydrate moieties of the molecules, the conjugated antibiotics are delivered directly to the binding bacteria and exert antibacterial activity in a targeted therapy manner. This approach not only reduces the antibiotic side effects on the host but also increases the antibiotic concentration available to the bacteria, thus improving antibacterial efficacy.

2.7.3 Structural modification of pleuromutilin and lefamulin

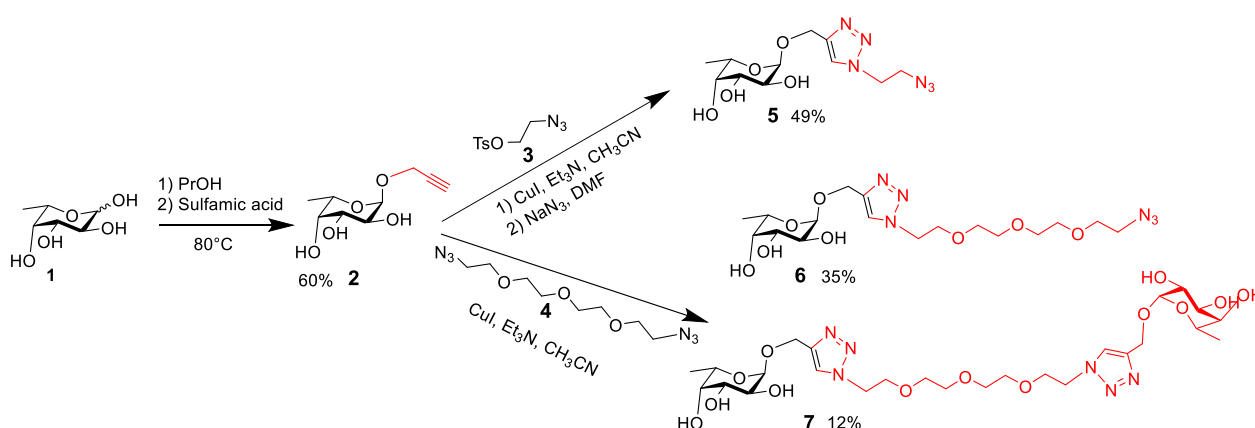
Finding new potential drug candidates based on currently available ABS is also a fast, convenient, and cost-efficient method. So the third part of my research concentrated on structural modification of pleuromutilin antibiotic at terminal alkene C-19-20. The goal of this synthesis is to create a series of new mutilin analogues in order to discover the better derivatives compared to parent mutilin as well as to find out new binding mode at this position. New compounds were tested against a wide range of bacteria and studied for structure-activity relationship. The same synthetic strategy was applied to lefamulin antibiotic.

3. Laboratory synthesis

3.1 Synthesis of carbohydrate-based lectin inhibitors

In the last 10-15 years there have been a huge number of synthetic molecules based on the structure of L-fucose, D-galactose, and other monosaccharides. These sugars are mainly conjugated with lipophilic side chains, aryl, biaryl, or biphenyl rings in order to create more optimized ligands. Monosaccharides are also linked with one another through different *O*- or *S*- glycosidic bonds, or through different linkers to create multivalent structures. The final purpose is to invent glycomimetic compounds that are capable of binding to bacterial lectins with stronger affinity, more selectivity, and more resistance to glycosidase enzyme by replacing *O*-atom of sugars with *S*-atom [144].

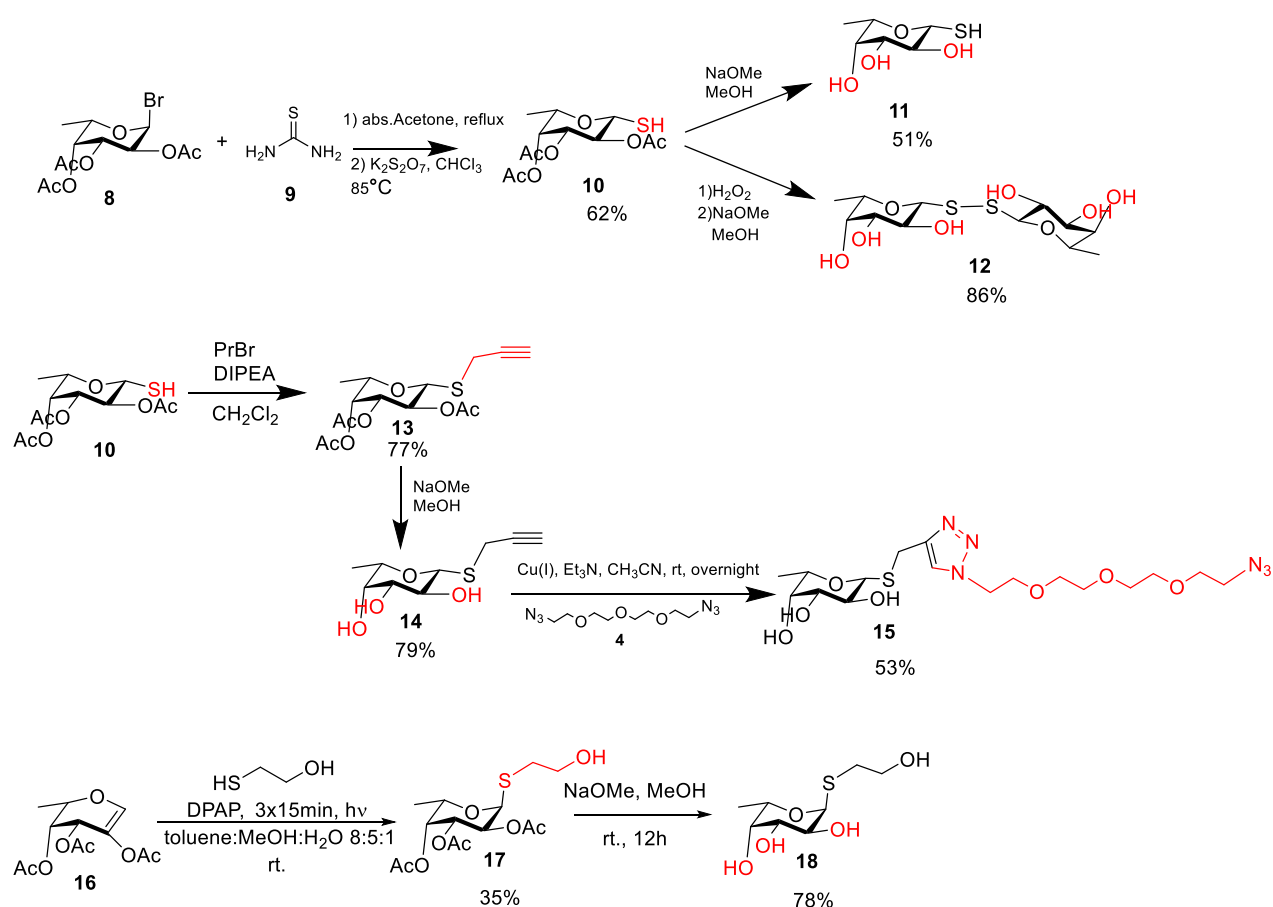
During my research, in order to study the effect of structural alterations and valency on lectin binding activity, I synthesized a wide panel of lectin-specific inhibitors. First, α -L-fucopyranoside was chosen as a basic carbohydrate unit. Compound **2** was prepared from unprotected form of L-fucose **1** by Fischer-type glycosylations using sulfamic acid and propargyl alcohol, with an α : β anomer ratio of approximately 3:1 [145-146]. Compounds **5**, **6**, and **7** were subsequently prepared by reacting compound **2** with heterobifunctionalized ethylene glycol and diazido tetraethylene glycol linker **3** and **4**, respectively, via CuAAC reaction. Tosyl group was then converted into azide to give compound **5** (49%), and compound **2** was reacted directly with diazido-tetraethylene glycol **4** to yield compounds **6** (35%) and **7** (12%) (**Scheme 1**).



Scheme 1. Synthesis of L-fuco-based lectin inhibitors

Another panel of 1-thio analogues from L-fucose compound were also prepared from per-*O*-acetylated-L-fucopyranoside. These thio-analogues are more stable than *O*-analogues as they are more resistant to degrading enzymes. Compound **11** was prepared from a reaction of 2,3,4-tri-*O*-acetyl- α -L-fucose bromide **8** with thiourea **9**, followed by a reduction of the

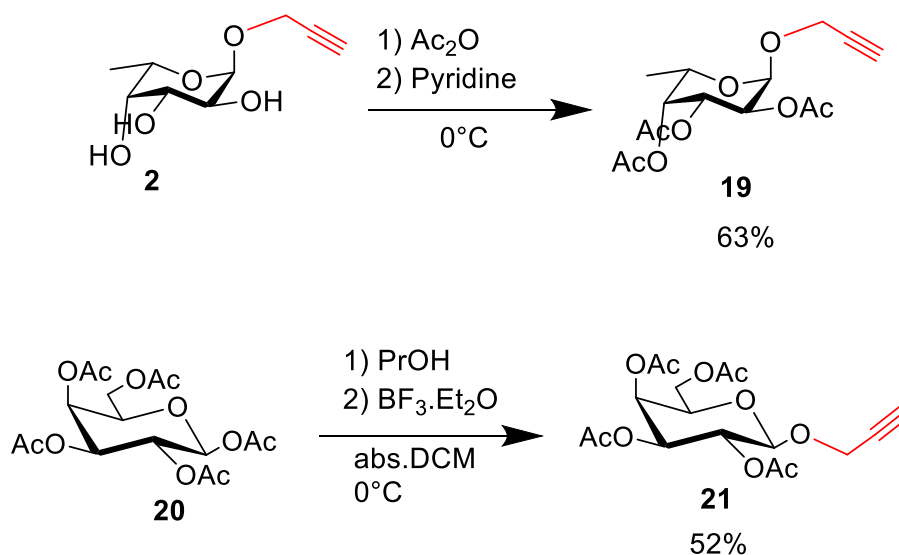
product to produce 2,3,4-tri-*O*-acetyl-1-*S*- β -L-fucose **10** (62%) [147], which was then subjected to *O*-deacetylation by Zemplén deacetylation [148] to give the desired compound **11** (51%) 1-*S*- β -L-fucose, or oxidized by H₂O₂ and then deprotected to give disulfide product **12** (86%) [149]. Compound **13** (77%) was also synthesized from compound **10** using propargyl bromide and DIPEA, this compound was then brought to *O*-deacetylation to give compound **14** terminal alkyne (79%). Unprotected compound **14** further reacted with diazido tetraethylene glycol **4** via CuAAC method to form compound **15** (53%). Furthermore, 2-acetoxy-3,4-di-*O*-acetyl-L-fucal **16** was allowed to react with 2-mercaptoethanol in a mixture of toluene:methanol:water with an added amount of DPAP catalyst at room temperature to give compound **17** in moderate yield (35%), which was then deacetylated to produce compound **18** (78%) in free hydroxyl form [142, 150] (**Scheme 2**).



Scheme 2. Synthesis of β and α -1-thiofucopyranoside derivatives

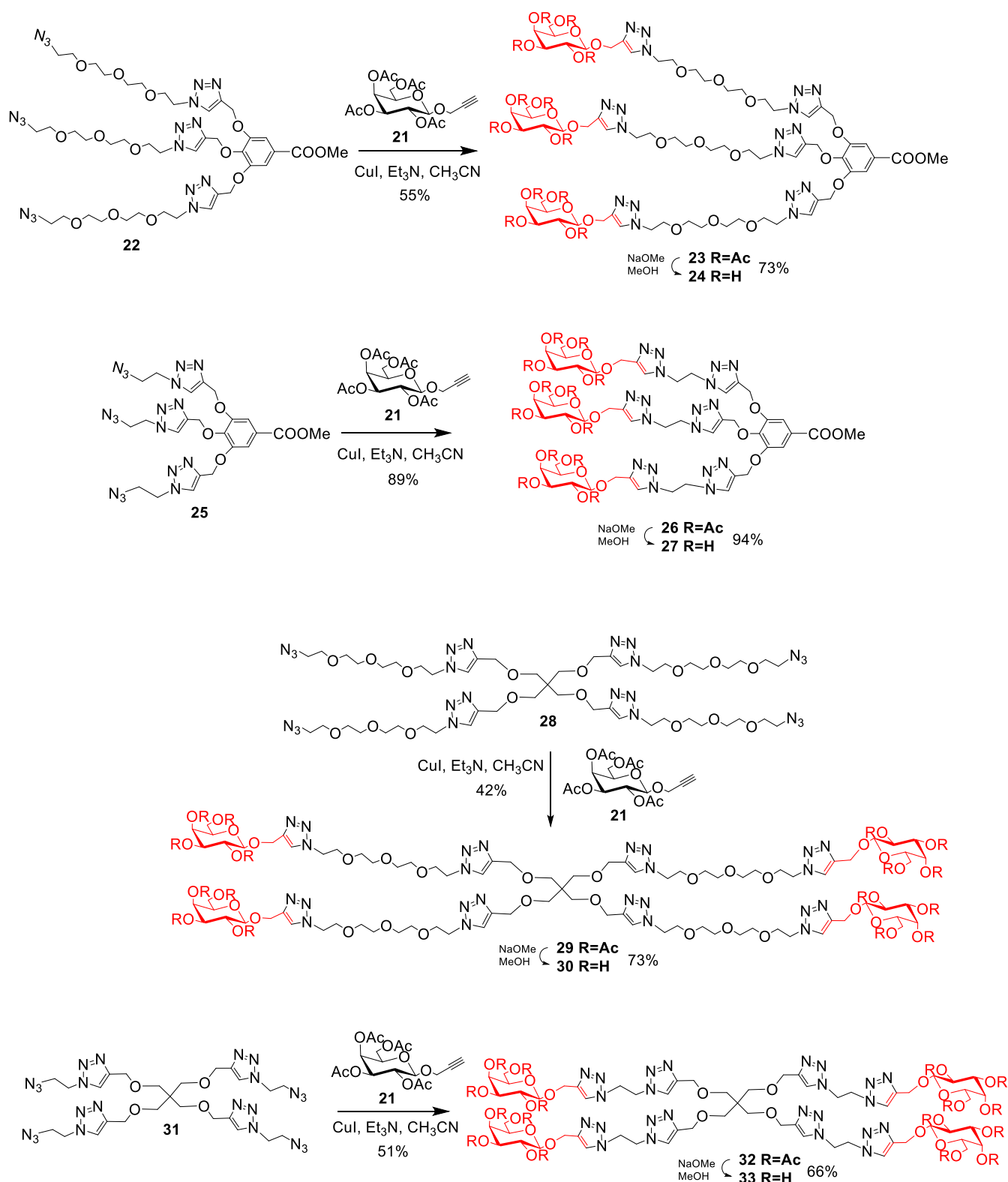
The ability of all 7 monovalent compounds **2**, **5**, **6** (α -*O*-fucosides), **11**, **14**, **15** (β -*S*-fucosides), **18** (α -*S*-fucosides), and 2 divalent compounds **7** and **12** to inhibit the selected fucose-specific lectins were determined by hemagglutination inhibition test and compared to that of standard L-fucose.

In order to build multivalent glycoclusters, we started from per-*O*-acetylated-D-galactose **20** and compound **2**. All three free hydroxyl groups of compound **2** were protected by acetylation in pyridine to give compounds **19** propargyl 2,3,4-tri-*O*-acetyl- α -L-fucopyranoside (63%). Compound **20** pentaacetyl-D-galactose was alkylated using boron trifluoride diethyl etherate and propargyl alcohol to produce compound **21** (52%) in good yield [151] (**Scheme 3**).



Scheme 3. Synthesis of **19** and **21**

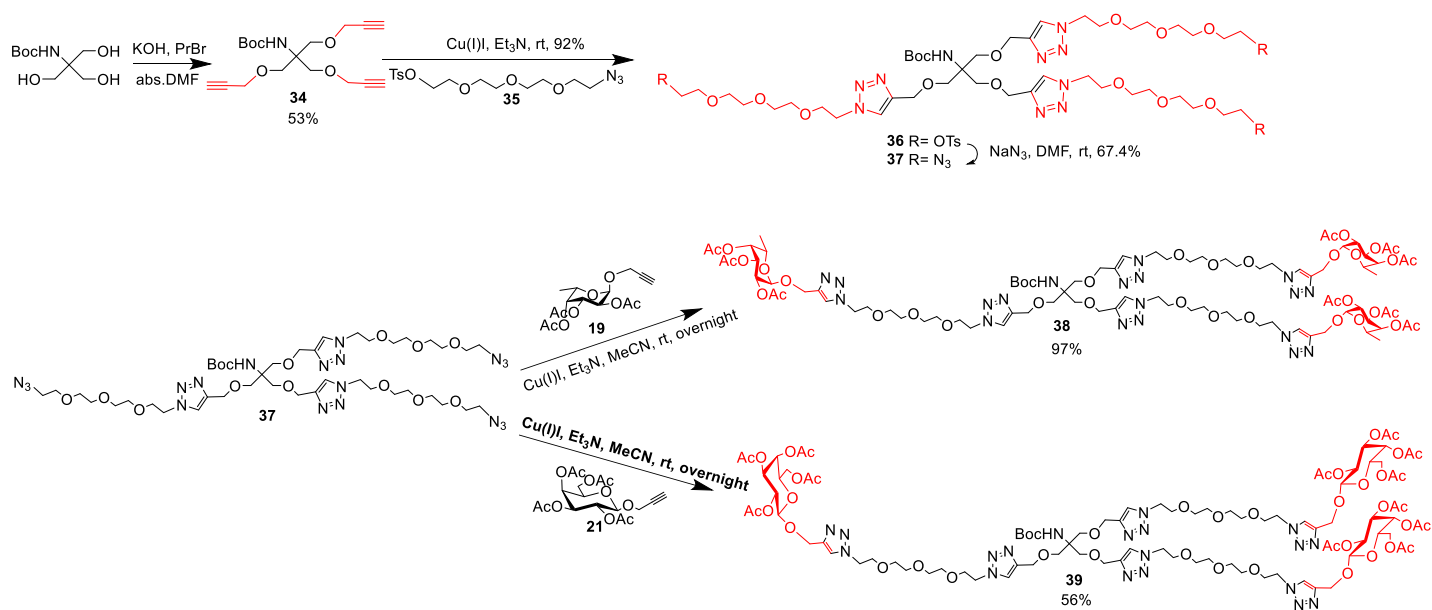
In order to find potential candidates to inhibit lectins of interest, several galactoside- and fucoside-containing multivalent compounds were planned to be synthesized. Firstly, a range of multivalent galactosylated compounds, including methyl gallate and pentaerythritol structures, were favoured as tri- and tetravalent scaffolds, respectively. These two scaffolds were decorated with tetraethylene (**22** and **28**) and ethylene glycol chains (**25** and **31**) [143]. These long and short linkers possessing azido group are suitable for CuAAC reaction with compound **21** 2,3,4,6-tetra-*O*-acetyl-1-*O*-propargyl- β -D-galactose in the next step (**Scheme 4**). Firstly, trivalent **22** and **25** were allowed to react with **21** to produce two trivalent galactoclusters **23** and **26**, respectively. Secondly, tetravalent **28** and **31** were also conjugated with **21** to produce two tetravalent galactoclusters **29** and **32**, respectively. As a result, four galactoclusters were synthesized with moderate (42%) to excellent yield (89%). Finally, the desired non-protected products **24**, **27**, **30**, and **33** were attained by Zemplén-deacetylation of **23**, **26**, **29**, and **32**, respectively.



Scheme 4. Synthesis of tri- and tetravalent β -D-galactoclusters

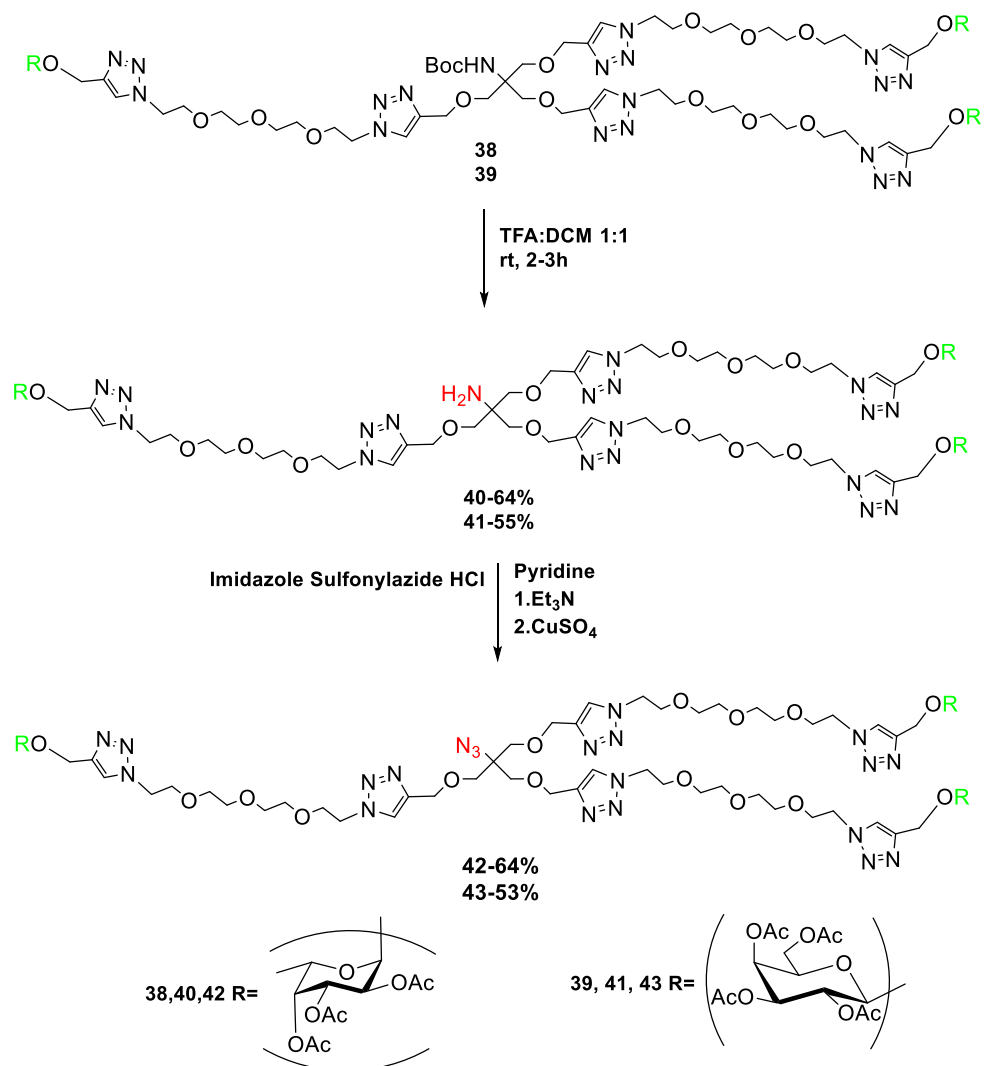
In addition to four multivalent galactoclusters, I also synthesized trivalent glycoclusters containing α -L-fucose and β -D-galactose as carbohydrate moieties [142]. *N*-(*t*-butyloxycarbonyl)-tris-(hydroxymethyl)-aminomethane was chosen to build the trivalent structure. First, this scaffold was alkylated using propargyl bromide in the presence of KOH

to result in compound **34** (53%) [152], which was reacted then with **35** tosylated *O*-(2-azidoethyl)-tetraethylene glycol linker via CuAAC reaction to produce **36** in high yield (92%). Tosyl group was later converted into azido functional group by nucleophilic substitution reaction to give **37** in good yield (67%). This azido-containing scaffold is now ready to couple with compound **19** propargyl 2,3,4-tri-*O*-acetyl- α -L-fucopyranoside- and **21** propargyl 2,3,4,6-tetra-*O*-acetyl- β -D-galactopyranoside to produce trivalent compound **38** in a high yield (97%) and **39** in a moderate yield (56%), respectively (**Scheme 5**).



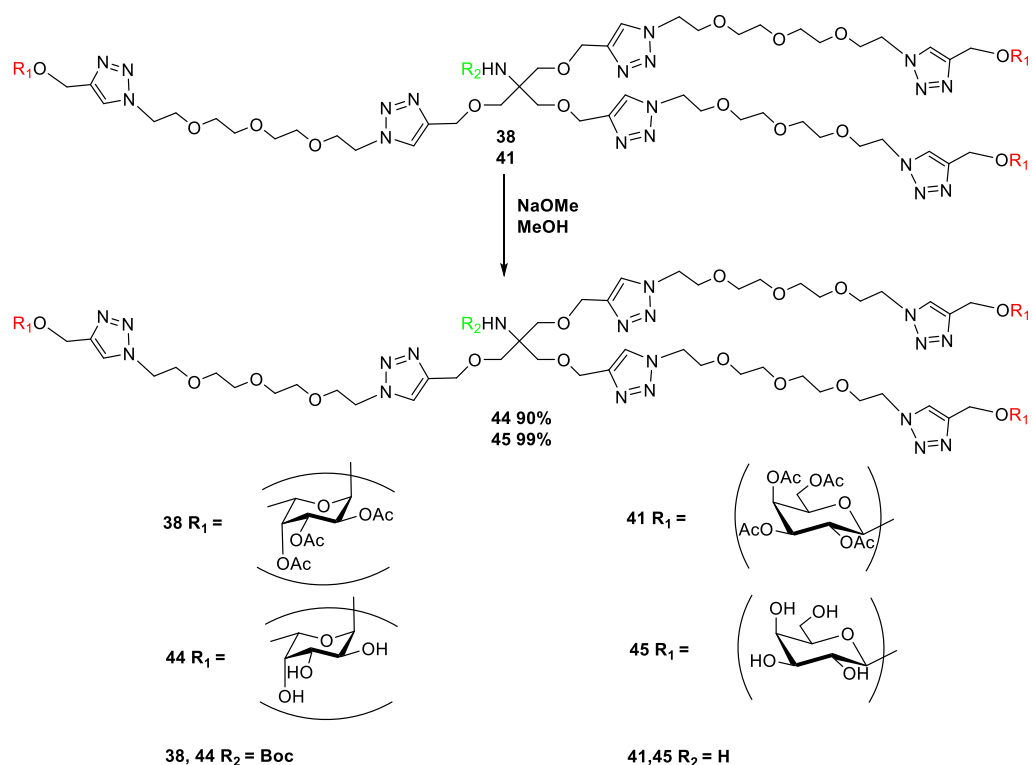
Scheme 5. Synthesis of trivalent α -L-fucose- and β -D-galactose-containing glycocluster

Both trivalent compounds **38** and **39** contain *Boc*-protecting group, which is suitable for acidic cleavage and further chemical modifications from $-NH_2$ group such as synthesizing chimeric compounds and glycoconjugates. The *Boc* protecting group of compounds **38** and **39** was then removed in a solution of TFA/DCM 1:1 at room temperature to generate a primary amine $-NH_2$ functional group of compounds **40** (64%) and **41** (55%), which was then converted into azido moiety in an amine-azide transfer reaction to give compound **42** (64%) and **43** (53%) [153-154], respectively (**Scheme 6**). These two new compounds are now ready to couple with propargyl-containing antibiotics via CuAAC click reaction to produce novel chimeric antibiotic molecules with a 1,4-disubstituted-1,2,3-triazole linker.



Scheme 6. Synthesis of primary amine and azido-containing trivalent glycoclusters

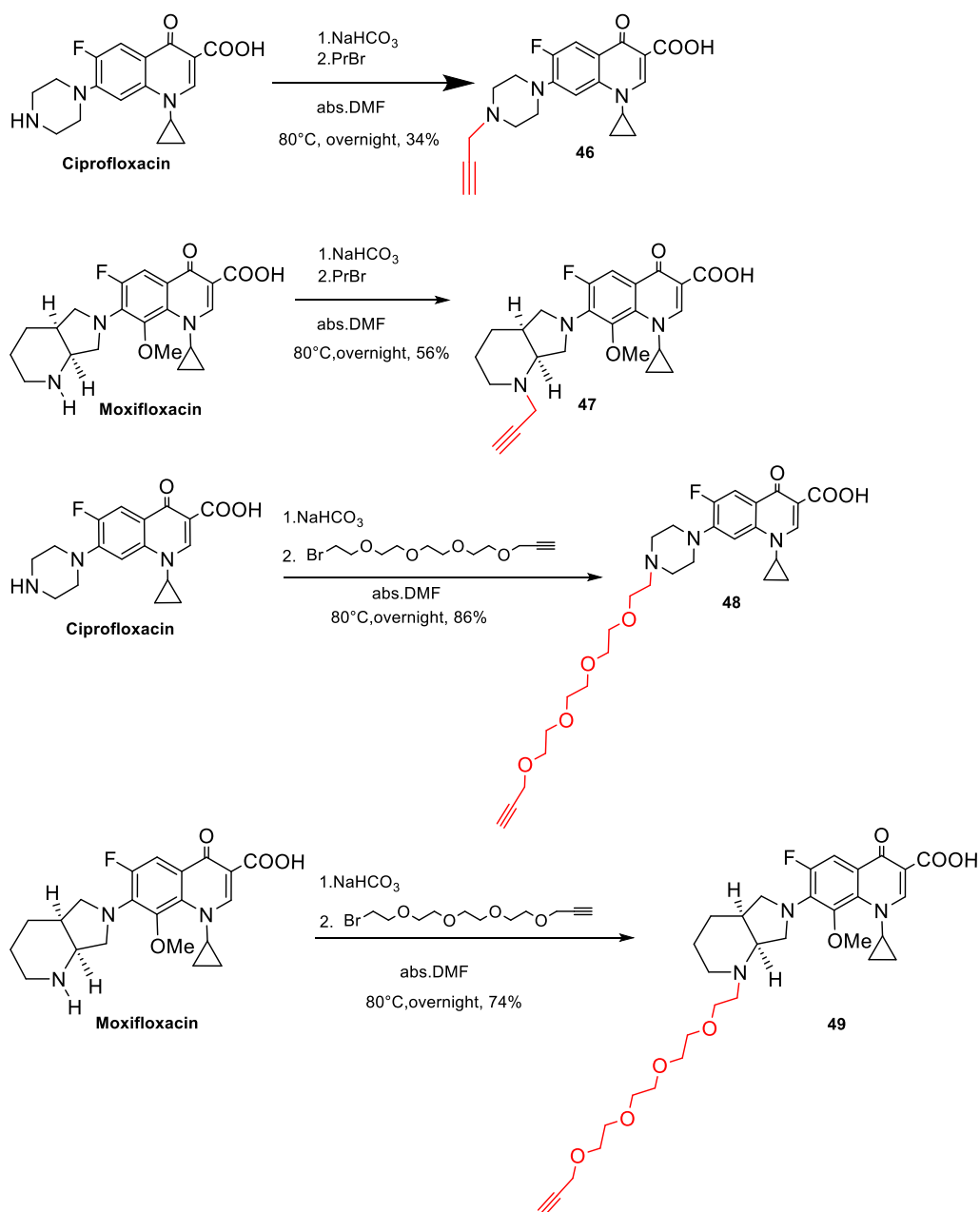
In order to examine the lectin binding potency of trivalent fuco- and galactocluster compounds, all the acetyl protecting groups must be hydrolyzed to give free hydroxyl –OH functional groups. Hence, compounds **38** and **41** were deacetylated according to the Zemplén method to give compounds **44** (90%) and **45** (99%) in excellent yield, respectively (**Scheme 7**). All six multivalent compounds **24**, **27**, **30**, **33**, **44**, and **45** were measured for their biological activities. Their inhibitory potency was determined by HIA and/or SPR methods. The best inhibitory compounds were further investigated in an *ex vivo* assay to test their capability to block the attachment of *Pseudomonas aeruginosa* to epithelial lung cells.



Scheme 7. Deacetylation of trivalent fucocluster **38** and galactocluster **41**

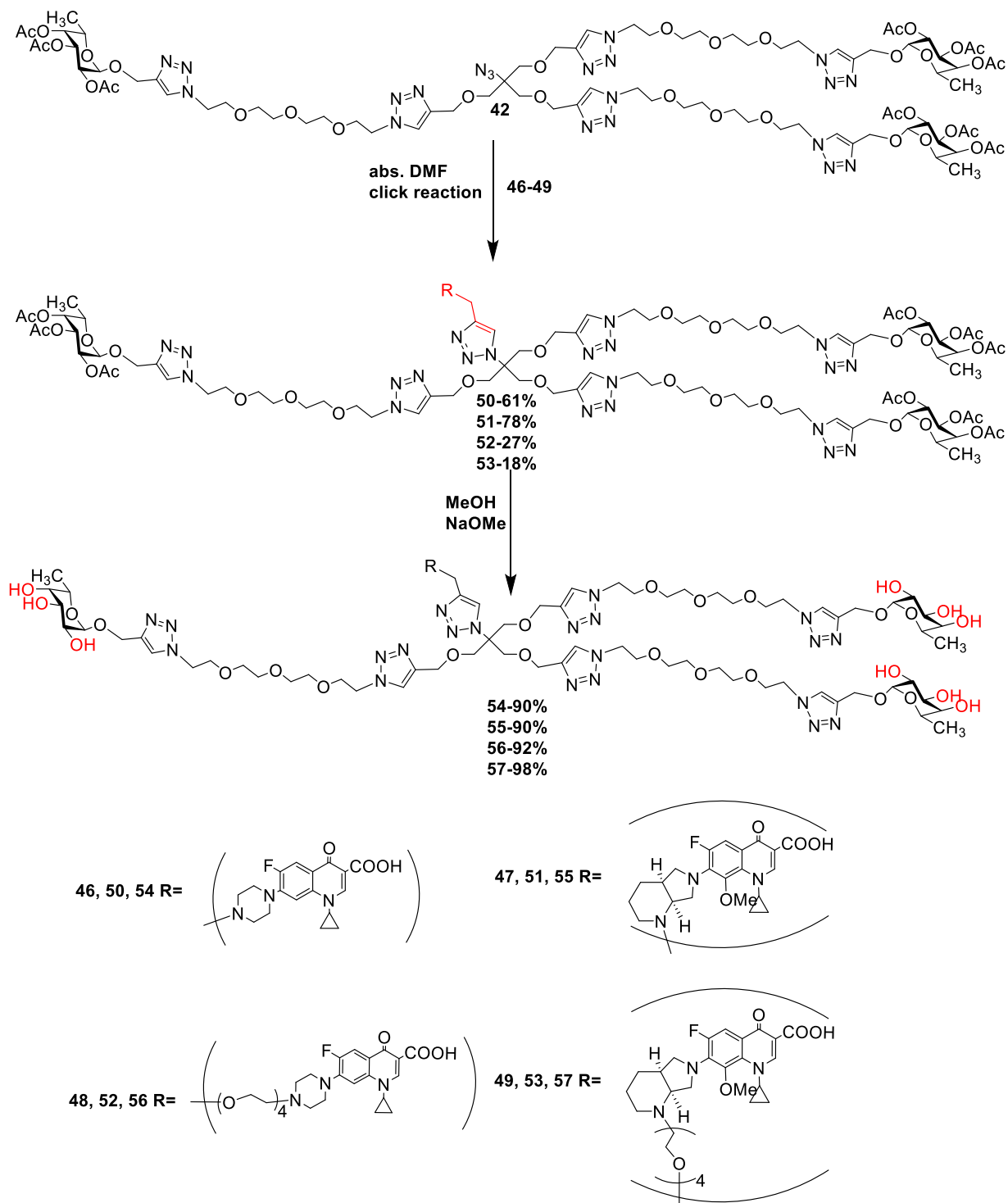
3.2 Synthesis of chimeric antibiotics

In an attempt to synthesize novel ABS, we came up with the concept of "chimeric" antibiotics by conjugating the multivalent glycoclusters with conventional ABS, thanks to the advantageous application of click-chemistry, azido-containing trivalent glycoclusters were able to couple with propargyl-containing ABS through CuAAC click reaction in just one step. In order to prepare *N*-propargyl derivatives of fluoroquinolone antibiotics, compounds **46** (34%) and **47** (56%) were synthesized from Ciprofloxacin and Moxifloxacin in moderate yield, respectively [155]. First, sodium bicarbonate was added to deprotonate the secondary amine, yielding an inorganic salt of fluoroquinolones. Subsequently, the antibiotics were alkylated in a nucleophilic substitution reaction using propargyl bromide. Compound **48** (86%) and **49** (74%) were prepared in a similar manner by conjugating with 1-bromo-3,6,9,12-tetraoxapentadec-14-yne linker to acquire more flexibility and more length in a good yield (**Scheme 8**).



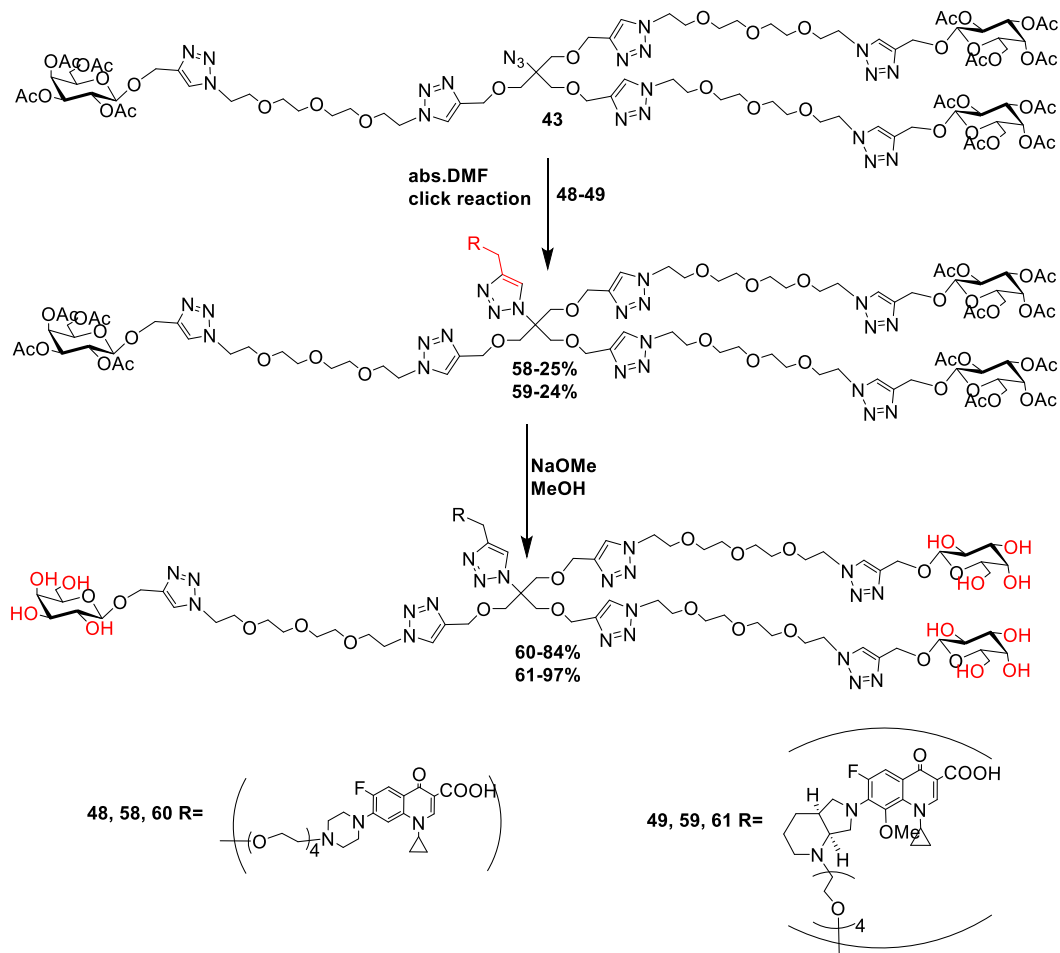
Scheme 8. Synthesis of propargylated derivatives of fluoroquinolones

In the first attempt to synthesize fucose-containing chimeric antibiotics, the four produced fluoroquinolones with terminal alkyne **46**, **47**, **48** and **49** were coupled with azido functional group of trivalent fucocluster **42** to give four chimeric compounds **50** and **51** in good yield, **52** and **53** in moderate yield, respectively. The acetyl protecting groups of compounds **50**, **51**, **52**, and **53** were then removed by Zemplén deacetylation to give compounds **54**, **55**, **56**, and **57** in high yield, respectively (**Scheme 9**).



Scheme 9. Synthesis of fucose-containing chimeric antibiotics

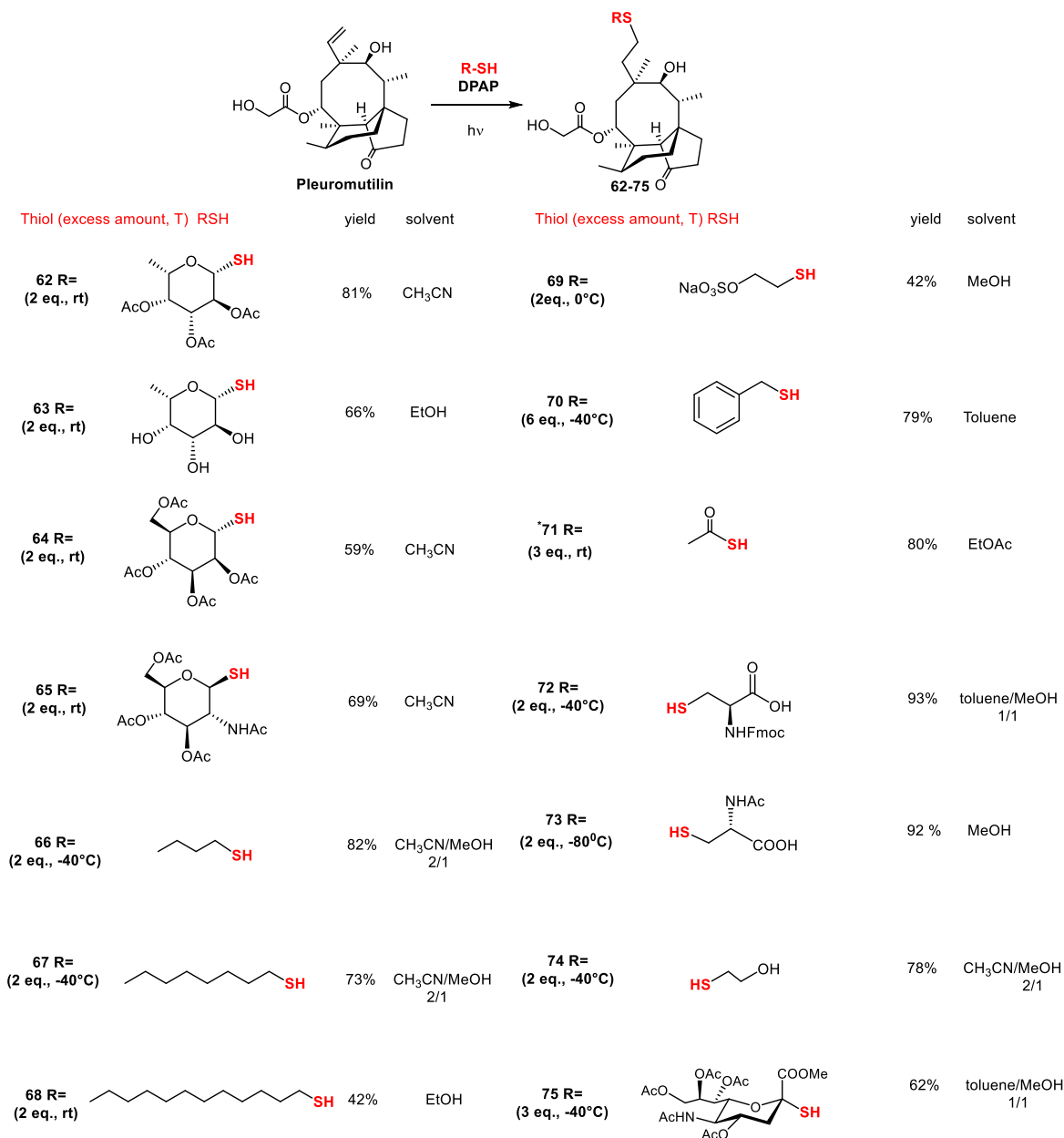
In the same synthetic route to synthesizing fucose-containing chimeric antibiotics, compound **43** was allowed to couple with **48** and **49** to give two new galactose-containing chimeric antibiotics **58** and **59** in moderate yield, respectively. Finally, compounds **58** and **59** were deacetylated to give compounds **60** and **61**, respectively (**Scheme 10**). Altogether, six newly synthesized chimeric antibiotics (4 fucosylated and 2 galactosylated chimeric antibiotics) were tested for hemagglutination inhibition and antibacterial activity.



Scheme 10. Synthesis of β -D-galactose-containing chimeric antibiotics

3.3 Semisynthetic modification of pleuromutilin

In addition to the synthesis of chimeric ABS, I also performed pleuromutilin and lefamulin structural modification by using thiol-ene radical addition reaction at C-19-20 terminal alkene in order to find out more potent antibacterial candidates from these two antibiotics. We proposed that photoinitiated thiol-ene radical addition would be an efficient strategy to couple a wide range of thiol-compounds to this reactive double bond (**Scheme 11**).

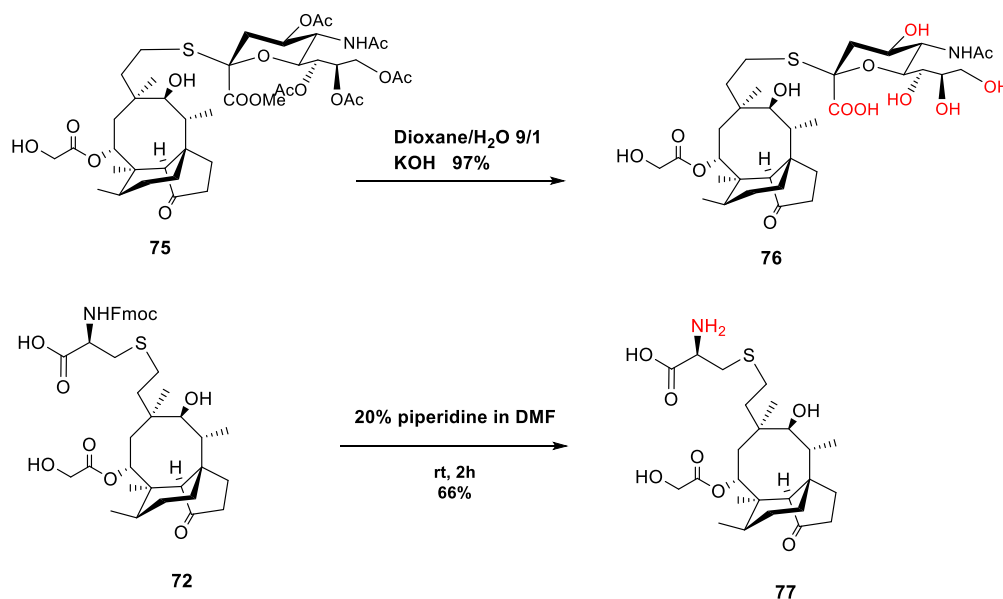


*combination of DPAP and MAP was used as synergistic initiators.

Scheme 11. Synthesis of thio-derivatives of pleuromutilin

As a result, 14 new pleuromutilin compounds were synthesized directly from pleuromutilin with moderate (42%) to excellent yield (93%) including sugar moieties **62-65**, lipophilic side chains **66-68**, sodium ethyl sulfonate (Mesna) **69**, benzylmercaptan **70**, thioacetic acid **71**, protected cysteines **72-73**, 2-hydroxyethylmercaptan **74**, and *N*-acetylneuraminic acid **75**. Compounds **75** and **72** were then deprotected to give **76** and **77** in good yield (**Scheme 12**), respectively. Interestingly, the internal ester bond at C-21 position was conserved under KOH condition. In general, a reaction carried out at low temperature (-40°C or -80°C) with 2-3 irradiation cycles would give a better overall yield. In case of thioacetic acid (compound **71**), the combination of **MAP** and **DPAP** reagents was necessary,

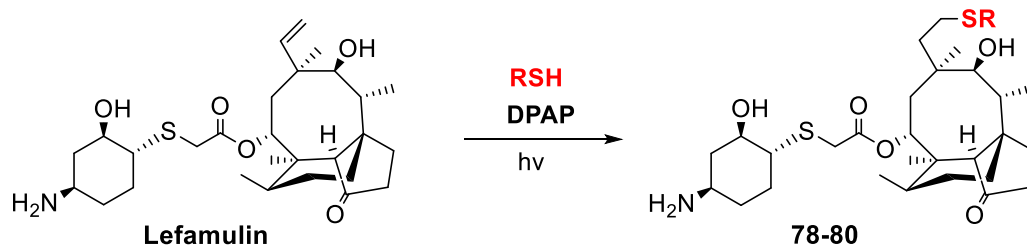
which acted as photosensitizer and photoinitiator, respectively [156]. All synthesized compounds were tested for antibacterial activity and studied for structure-activity relationship.



Scheme 12. Deprotection of **75** and **72**

3.4 Semisynthetic modification of lefamulin

Our preliminary results showed that compounds **73**, **74**, and **76** have much better antibacterial activity compared to the other thio-pleuromutilin derivatives. This result suggested that an anion that is capable of forming hydrogen bonds at this position could form new binding. As far as this discovery is concerned, compounds **78**, **79**, and **80** were then synthesized in the same procedure from lefamulin (**Scheme 13**).

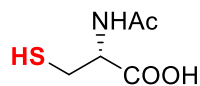


Thiol (excess amount, T) RSH

yield

solvent

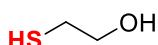
78 R=
2equiv., -80°C



86%

MeOH

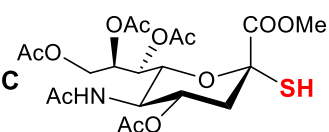
79 R=
4equiv., -80°C



60%

MeOH

80 R=
4equiv., -80°C

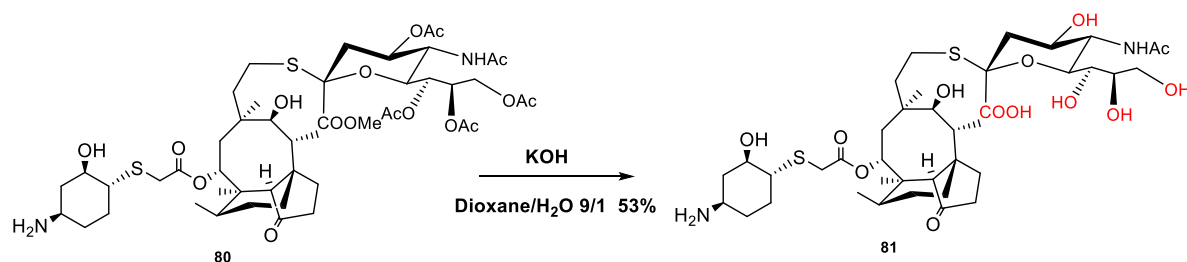


78%

MeOH

Scheme 13. Synthesis of thio-derivatives of lefamulin

Because lefamulin contains -NH_2 basic group in its structure, which could interfere with thiol reactant by abstracting a hydrogen atom from it and thus hindering the production of thiyl radical, the addition of trifluoroacetic acid to neutralize this basic group was necessary [157]. Compound **80** was then deprotected to give **81** (Scheme 14).



Scheme 14. Deprotection of **80**

4. Results

4.1 Lectin-carbohydrate interaction results

The binding potency of all tested compounds was measured against six fucose-specific lectins by mean of HIA with microscopic detection, and the inhibitory activity was also calculated semi-quantitatively. First, each type of bacterial lectin was dissolved in a separate buffer and mixed thoroughly with the tested compounds in a serial dilution order. A solution of red blood cells was then added, and the suspension mixture was incubated at room temperature. After incubating for five minutes, the mixture was shaken one more time, and transferred to a microscope slide for examination. The minimum inhibitory concentration (MIC) of compounds capable of suppressing hemagglutination produced by lectin and red blood cells was detected, and the potency of tested compounds was evaluated by comparing with the MIC value of standard compound. For example, standard compound L-fucose was able to inhibit hemagglutination produced by PA-IIL lectin at a concentration of 391 μmol , while compound **44** exerted the same effect at a concentration of 97.66 μmol , which in turn 4 times lower in value. Hence, compound **44** was 4 times stronger than standard L-fucose in term of potency [Figure 12]. Positive control (experiment without inhibitor) and negative control (experiment without lectin) were used to test activity of red blood cells and lectin under given experimental conditions.

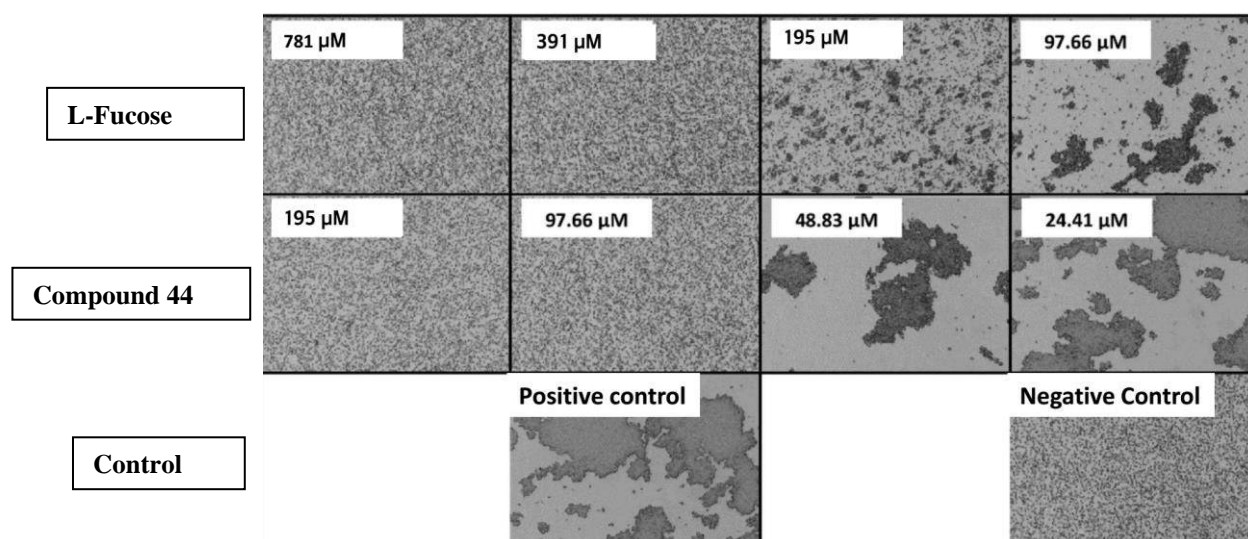


Figure 12. Influence of tested compound **44** and standard L-fucose on hemagglutination produced by PA-II lectin expressed in MIC [142].

Table 1a. Potencies of tested inhibitors against fucose-specific lectins determined by HIA

	AFL	RSL	AAL	AOL	PA-III	BC2L-C
L-fucose	1	1	1	1	1	1
2	4	8	4	4	4	1
5	8	32	8	8	4	2
6	4	8	4	4	4	2
7	4	128	8	4	8	2
11	0.5	0.5	0.5	0.5	0.25	ND
12	0.5	2	1	1	0.125	1
14	0.5	0.5	1	0.5	0.03125	0.5
15	1	2	2	1	0.0625	0.5
18	2	4	2	4	4	4
44	32	128	64	128	4	8

ND: Not detected

AFL: *Aspergillus fumigatus* lectin

RSL: *Ralstonia solanacearum* lectin

Aal: *Aleuria aurantia* lectin

AOL: *Aspergillus oryzae* lectin

PA-III: *Pseudomonas aeruginosa* lectin B

BC2L-C: *Burkholderia cenocepacia* lectin C

*Green color: effective

*Red color: ineffective

*Black color: moderate

*The result of Table 1a was measured by Lenka Malinovska et al, Masaryk University, Czech Republic

In general, all the synthetic α -O-L-fucopyranosides **2**, **5**, **6**, and **7** were better than standard L-fucose in all tested lectins as in **Table 1a**. Especially, compounds **5** and **7** were very effective inhibitors of RSL lectin with inhibitory potency up to 32 and 128 times stronger, respectively. This phenomenon could be explained by the higher affinity of RSL towards L-fucose and the avidity effect of divalent structure **7**. However, the β -S-L-fucose analogues **11**, **12**, **14** and **15** were poor inhibitors in general. Compound **12** was slightly better than standard L-fucose in RSL lectin binding, and compound **15** was slightly better in case of RSL and AAL. But all β -thio compounds showed a very poor binding potency in case of PA-III. This effect is opposite in case of compound **18**, which is an α -S analogue, this inhibitor is 2-4 times better than a normal L-fucose in binding affinity. The result of **2**, **5**, **6**, **7**, and **18** strongly confirmed that the poor performance of **11**, **12**, **14**, and **15** was mainly due to their β configuration, not because of the presence of sulfur atom. Therefore, α -S-L-fucopyranosides could be a highly potent inhibitor and used to achieve higher stability against hydrolase enzymes. Considering compound **44**, which is a trivalent α -L-fucocluster built from N-(t-

butyloxycarbonyl)-tris-(hydroxymethyl)-aminomethane scaffold and tetraethylene linker, displayed a very high binding potency toward most of the tested lectins. Particularly, this trivalent was 128 times stronger than standard L-fucose in case of RSL and AOL, 64 times in case of AAL, 32 times in case of AFL, and 8 times in case BC2L-C. Unfortunately, the binding potency was only 4 in case of PA-IIL, which is not differ from monovalent α -L-fucose-analogues **2**, **5**, **6**, and **18**. This result suggested that this type of trivalent structure was not able to bind multiple sites simultaneously and therefore could not exert a strong avidity effect against PA-IIL.

Table 1b. The MIC values and potency of tested trivalent inhibitors against fucose-specific lectin PA-IIL determined by HIA

Inhibitor	MIC	Potency	Valency	β
L-fucose	391 μ M	1	1	1
44	97.66 μ M	4	3	1.3
54	97.66 μ M	4	3	1.3
55	195 μ M	2	3	0.67
56	195 μ M	2	3	0.67
57	195 μ M	2	3	0.67

β : Potency/Valency

*Green color: effective

*Black color: moderate

*The result of Table 1b was measured by Lenka Malinovska et al, Masaryk University, Czech Republic

Table 1b shows the binding potency of all trivalent fucocluster compounds against fucose-specific PA-IIL. In general, the inhibitory potency of chimeric compounds **54**, **55**, **56**, and **57** was comparable to the potency of the precursor compound **44** that is without the antibiotic part, with compound **54** displaying exactly the same lectin inhibitory activity (4). On the other hand, the potency of compounds **55**, **56**, and **57** was somewhat decreased, as they are only 2 times stronger than standard trivalent compound **44**. This phenomenon was probably due to the longer/bigger antibiotic branch. However, even compounds with low potency proved to be able to inhibit lectin PA-IIL *in vitro* [142]. All the tested compounds were able to inhibit lectin PA-IIL, and no negative effect of the tested compounds on the red blood cells-hemolysis-was observed. Multivalent inhibitors were also reported to be able to highly cross-link bacterial cells via interactions with their surface lectins [158] which could be beneficial for guiding antibiotics to the bacterial cells. From this aspect, in order to find out the best universal multivalent glycocluster with higher binding potency, further optimization of scaffold, linker, and carbohydrate moiety is needed.

Table 2a. MIC and potency value of all tested inhibitors against galactose-specific lectin PA-IL determined by HIA

	MIC	Potency	Valency	β
D-Galactose	6250 μ M	1	1	1
24	48.33 μ M	128	3	42.7
27	97.66 μ M	64	3	21.3
30	24.41 μ M	256	4	64
33	48.84 μ M	128	4	32

β : potency/valency

**Green color: effective*

**The result of Table 2a was measured by Lenka Malinovska et al, Masaryk University, Czech Republic*

Table 2a shows the binding potency of all tested multivalent galactoclusters against their PA-IL galactose-specific lectin. In general, all multivalent inhibitors were able to suppress hemagglutination extensively better than the standard monovalent compound, and they easily exerted their lectin inhibitory effect in micromolar scale. Compound **30** was the best candidate which is 256 times stronger than the standard D-galactose, while compound **27** was the least effective candidate which was only 64 times stronger. On the other hand, both compounds **24** and **33** were equal in their binding potency (128-fold) although they have differences in valency (3 vs 4) and linker length (long vs short). When considering the effect of galactose-concentration in the multivalent compounds, we assigned β as the value of inhibitory potency divided by the number of valency in a given compound. We observed that compound **30** ($\beta=64$) is still the strongest candidate, and compound **27** ($\beta=21.3$) is still the weakest one. Comparing two compounds **24** and **33**, a difference in β value was observed. Compound **24** (a trivalent compound with longer linkers, $\beta=42.7$) was more effective than compound **33** (a tetravalent compound but with shorter linkers, $\beta=32$). This result suggested that a longer, more flexible linker is necessary for more efficient binding. Comparing the two best inhibitors **30** and **24**, they only differ in one carbohydrate unit and spatial arrangement but the inhibitory effect of compound **30** is two times higher than that of compound **24**. In brief, a compound with more valency units and longer linkers displayed a higher binding potency value.

Table 2b. The IC₅₀ values and potency of the tested inhibitors against galactose-specific lectin PA-IL obtained by SPR

	IC ₅₀	Potency	Valency	β
D-Galactose	187.1 μM	1	1	1
24	6.8 μM	27.5	3	9.2
27	7.4 μM	25.3	3	8.4
30	7.3 μM	25.6	4	6.4
33	4.3 μM	43.5	4	10.9

IC₅₀: concentration of inhibitor resulting in 50% inhibition of binding

β: potency/valency

**Green color: effective*

**The result of Table 2b was measured by Lenka Malinovska et al, Masaryk University, Czech Republic*

Table 2b shows a series of concentrations of inhibitors that resulted in 50% inhibition of binding of PA-IL to immobilized D-galactose by using SPR technique. All the multivalent compounds apparently illustrated a stronger inhibition effect compared to standard D-galactose, and the effect was obtained at relatively low concentrations. In this method, the most potent candidate is compound **33**, with almost 44 times stronger than D-galactose in potency and almost 11 times in β value when considering the effect per monomer unit. The inhibitory effects of the other three compounds **24**, **27**, and **30** were almost identical in term of potency.

In a short discussion, two techniques HIA and SPR were used to determine the ability of multivalent glycoclusters to inhibit bacterial lectin PA-IL. HIA is a fast and strong method that is widely employed for the investigation of lectin-carbohydrate interactions. This method mainly relies on eye detection and comparisons with positive and negative controls [159]. On the other hand, SPR inhibition assay could theoretically be a better tool as it mimics the real condition of lectin's binding. But this method is susceptible to precipitation and hidden artefacts such as cross-linking effect of lectin [160]. The disadvantages of these two models can be balanced when combined together, and the inhibitory potency of investigated compounds could be confirmed. In accordance with HIA results, compound **30** (a tetravalent with long linkers) was the best candidate, and compound **24** (a trivalent with long linkers) was the second-best candidate in term of potency and parameter β. This result suggested a greater interest for inhibitors with a longer and more flexible chain over a shorter one. Taking into consideration of SPR assay results, compound **33** was the best candidate but this technique did not display a clear relationship between valency and structure towards their inhibitory

ability, as the other three compounds **24**, **27**, and **30** were similar in potency. Due to the fact that SPR and HIA have distinct systems and detection principles, the differences in the results are not astonishing [161]. Nevertheless, both of the methods have strongly affirmed that all of the synthesized multivalent compounds can inhibit lectin PA-IL exceptionally stronger than standard D-galactose. Therefore, they could be used as potential agents for anti-adhesive therapies and antibacterial treatments.

4.2 Antibacterial results of chimeric antibiotics

Table 3. Antibacterial effect of synthetic fluoroquinolones and chimeric antibiotics expressed as minimum inhibitory concentration MIC ($\mu\text{g/ml}$)

	46	47	48	49	54	55	56	57	60	61
<i>Bacillus subtilis</i> ATCC 6633	0.5	0.5	0.5	2	16	16	8	32	4	16
<i>Staphylococcus aureus</i> MSSA ATCC 29213	0.5	0.5	0.5	4	64	16	16	32	16	16
<i>Staphylococcus aureus</i> MRSA ATCC 33591	0.5	0.5	0.5	4	64	8	32	32	8	16
<i>Staphylococcus epidermitis</i> ATCC 35984 biofilm	0.5	0.5	0.5	4	64	16	32	32	8	16
<i>Staphylococcus epidermitis</i> mecA	0.5	0.5	0.5	8	64	32	32	32	32	32
<i>Enterococcus faecalis</i> ATCC 29212	2	2	8	32	256	64	64	256	-	-
<i>Enterococcus faecalis</i> 15376 vanA	2	256	256	256	256	256	256	256	512	256
<i>Enterococcus faecalis</i> ATCC 51299 vanB	256	32	32	32	256	256	256	256	-	-
<i>Klebsiella pneumonia</i> ST258 clone K 160/09	256	256	256	256	256	256	256	256	512	512
<i>Pseudomonas aeruginosa</i> ATCC 27853	256	256	256	256	256	256	256	256	512	512
<i>Acinetobacter baumannii</i> ATCC BAA1605	256	64	256	256	256	256	256	256	512	512
<i>Escherichia coli</i> ATCC 25218	256	256	256	256	256	256	256	256	32	64

*Green color: effective

*Red color: ineffective

*Black color: moderate

*The result of Table 3 was measured by Eszter Ostorházi et al, Semmelweis University, Hungary

In general, all the compounds lost their antibacterial property against Gram-negative pathogens. Compounds **60** and **61** had moderate effect against *Escherichia coli* ATCC 25218, and compound **47** had low effect against *Acinetobacter baumannii* ATCC BAA1605. Whereas compounds **47**, **48**, and **49** had weak effect against *Enterococcus faecalis* ATCC 51299 *vanB*, compound **46** exhibited good activity against *Enterococcus faecalis* 15376 *vanA*. This result indicated that alkylated fluoroquinolones and their chimeric antibiotics were not good candidates for gram-negative pathogens. This phenomenon could probably be due to the alkyl side chain of fluoroquinolones and the large, bulky part of chimeric compounds. One interesting result is that for gram-positive *Enterococcus faecalis* ATCC 29212 only compounds **46**, **47**, and **48** were active, while compound **49** exhibited weak activity. Surprisingly, all three propargylated fluoroquinolones **46**, **47**, and **48** had enhanced activity against tested gram-positive pathogens, whereas the effect of compound **49** was slightly weaker. This can be explained by virtue of increased lipophilicity of fluoroquinolones that helps penetrate into bacterial cell membrane.

On the other hand, the anti-Gram-positive effect of all chimeric compounds was reduced to certain extent compared to their unglycosylated fluoroquinolones. Out of four fucoside-containing and two galactoside-containing chimeric antibiotics, compounds **55** and **60** exhibited the best antibacterial activity against *Bacillus subtilis* ATCC 6633, *Staphylococcus aureus* MSSA ATCC 29213, *Staphylococcus aureus* MRSA ATCC 33591, and *Staphylococcus epidermitis* ATCC 35984 biofilm. The reduced antibacterial incident can be explained by reason of large molecular weight and uncleavable bond between glycocluster and fluoroquinolone antibiotic. In short conclusion, in order to achieve a better antibacterial result in the future, a cleavable ester bond connecting antibiotic and glycocluster would be an ideal strategy.

4.3 Antibacterial results of pleuromutilin derivatives

Table 4. Antibacterial effect of synthetic pleuromutilin derivatives expressed as MIC ($\mu\text{g/ml}$)

	62	63	64	65	66	67	68	69	70	71	72	<u>73</u>	<u>74</u>	<u>76</u>	77	Pleuro mutilin
<i>Bacillus subtilis</i> ATCC 6633	512	512	256	32	512	512	512	128	512	64	256	4	32	32	256	16
<i>Staphylococcus aureus</i> MSSA ATCC 29213	512	512	512	512	512	512	512	128	256	512	128	8	16	16	256	4
<i>Staphylococcus aureus</i> MRSA ATCC 33591	512	512	512	256	512	512	512	16	32	128	128	4	4	4	256	2
<i>Staphylococcus epidermidis</i> ATCC 35984 biofilm	512	32	512	128	512	512	512	8	16	64	128	0.5	2	2	256	1
<i>Staphylococcus epidermidis</i> mecA	512	64	512	512	512	512	512	128	64	256	256	8	16	16	256	4
<i>Enterococcus faecalis</i> ATCC 29212	512	512	512	512	512	512	512	64	64	512	-	32	256	256	256	64
<i>Enterococcus faecalis</i> 15376 VanA	512	512	512	256	512	512	512	32	64	256	256	4	16	16	256	8
<i>Enterococcus faecalis</i> ATCC 51299 VanB	512	512	512	512	512	512	512	32	64	512	-	32	256	256	256	128
<i>Enterococcus faecium</i> VanA 38276 urine	-	-	-	-	-	-	-	-	-	-	-	-	128	128	256	128
<i>Enterococcus faecium</i> VanA 25192 blood culture	-	-	-	-	-	-	-	-	-	-	-	-	128	128	256	128
<i>Enterococcus faecium</i> VanA 3452 drain	-	-	-	-	-	-	-	-	-	-	-	-	2	2	256	2
<i>Enterococcus faecium</i> VanA 24581 wound	-	-	-	-	-	-	-	-	-	-	-	-	128	128	256	128

*Green color: effective

*Red color: ineffective

*Black color: moderate

*The result of Table 4 was measured by Eszter Ostorházi et al, Semmelweis University, Hungary

Generally, compounds **62-68**, which had sugar moieties or lipophilic side chains in their chemical structure, lost their antibacterial property compared to their parent pleuromutilin. Compounds **71**, **72**, and **77** were also quite ineffective. Compound **69** is almost two times stronger than compound **70** in every tested pathogen, especially it shows weak and moderate activity against *Staphylococcus aureus* MRSA ATCC 33591 and *Staphylococcus epidermidis* ATCC 35984 biofilm, respectively. The only exception is in the case of *Staphylococcus epidermidis* mecA where **70** is twice stronger than **69**, and in case of *Enterococcus faecalis* ATCC 29212 they had the same antibacterial effect. Surprisingly, compound **73**, in which the amino group of cysteine conjugate had been protected by acetyl group, displayed good antibacterial activity. This compound had better effect than pleuromutilin in case of *Bacillus subtilis* ATCC 6633, *Staphylococcus epidermidis* ATCC 35984 biofilm, *Enterococcus faecalis* ATCC 29212, *Enterococcus faecalis* 15376 VanA, and *Enterococcus faecalis* ATCC 51299 VanB pathogens. In case of *Staphylococcus aureus* MSSA ATCC 29213, *Staphylococcus aureus* MRSA ATCC 33591, and *Staphylococcus epidermidis* mecA its effect is just two times weaker than pleuromutilin. On the other hand, compounds **74** and **76**, with ethylenehydroxyl and N-acetyl neuraminic acid conjugate, respectively, expressed the same antibacterial effect in all cases, and their effect is slightly weaker than that of parent pleuromutilin. Out of fifteen tested compounds, compounds **73**, **74**, and **76** exhibited the best results, with compound **73** standing out as the best candidate. The above results together with the result of compound **69** implied that derivatives at C-19-20 double bond with a negative ionic charge could have an enhanced antibacterial effect compared to pleuromutilin. The negative charge could contribute to the binding of these compounds with their receptor by forming hydrogen bonds and/or ionic bond with surrounding amino acids of the bound enzyme.

4.4 Antibacterial results of lefamulin derivatives

Table 5. Antibacterial effect of synthetic lefamulin derivatives expressed as MIC ($\mu\text{g/ml}$)

	78	79	81	Lefamulin
<i>Bacillus subtilis</i> ATCC 6633	256	16	512	0.5
<i>Staphylococcus aureus</i> MSSA ATCC 29213	521	16	512	0.5
<i>Staphylococcus aureus</i> MRSA ATCC 33591	512	32	256	0.5
<i>Staphylococcus epidermidis</i> ATCC 35984 biofilm	512	16	128	0.5
<i>Staphylococcus epidermidis</i> mecA	512	16	256	0.5
<i>Enterococcus faecalis</i> 15376 VanA	512	32	256	1

*Green color: effective

*Red color: ineffective

*Black color: moderate

*The result of Table 5 was measured by Eszter Ostorházi et al, Semmelweis University, Hungary

Table 5 shows the antibacterial results of synthesized lefamulin derivatives. Compounds **78** and **81**, in which lefamulin was conjugated with *N*-acetylcysteine and *N*-acetylneuraminic acid, respectively, were inactive against all tested pathogen strains. Out of three new synthesized derivatives, compound **79**, with ethylenehydroxyl conjugate, was the best candidate which exhibited moderate and weak antibacterial activity, but the effect from this compound is still weaker than that of parent lefamulin. Results from these compounds indicated that a negative ionic charge at the C-19-20 position was not an ideal substituent. The binding of these compounds to their receptor could be prevented by this factor. This result also suggested that the binding mode of lefamulin could be different than that of pleuromutilin, although they share the same binding pocket. However, thiol-ene radical addition reaction carried out at this terminal double bond still holds an interest in synthesis as there are numerous thiols unexplored.

5. Discussion

Our *in vitro* results strongly confirmed that α -configuration of L-fucose-based compounds is crucial to the lectin-ligand binding. In opposite, the β -configuration ones provided very weak binding affinity or even non-binding, suggesting that the spatial position of the oxygen atom plays a decisive role in forming hydrogen bonding with amino acid constituents of lectin. Moreover, we can improve the binding efficacy of monovalent carbohydrate compounds by modifying the side chain at different positions, and we can enhance the durability by replacing oxygen with a sulfur atom. In addition, all multivalent compounds showed a much stronger lectin binding potency compared to standard L-fucose or D-galactose compound in HIA method, with the best candidates were compound **44** (a trivalent with long linkers) for fucose and **30** (a tetravalent with long linkers) for galactose. Controversy appeared when we used different biophysical methods to determine the compound's activity, in SPR method compound **33** (a tetravalent with short linkers) was better than **30**. Nevertheless, these results have firmly proved that multivalent compounds are strong potential candidates for inhibiting lectin-glycoconjugate binding. In order to optimize the multivalent candidates, we should take into account many factors such as scaffold structure, linker, configuration of carbohydrate units, and synthetic methods. Furthermore, lectin is an unarguable novel therapeutic target and can be utilized in tremendous biomedical applications, especially in antibacterial strategies. By inhibiting lectins with highly binding agents, we can inhibit bacterial adhesion, thus reducing bacterial invasion, infection, and propagation. More importantly, this antiadhesion therapy offers a new, safer method to eliminate bacteria as it employs the host's natural defence mechanisms to remove bacteria and does not result in bacterial resistance.

Compounds **55** and **60** exhibited a stronger antibacterial effect than the others. Although the antibacterial activity of these chimeric compounds was weaker than the effect of their fluoroquinolone parents, they could however target the gram-positive bacteria infection and reduce gram-negative bacteria binding, especially for cystic fibrosis patients who are usually infected by both *Staphylococcus aureus* and *Pseudomonas aeruginosa* bacteria. This type of new molecules and their results boded well for the future application of chimeric antibiotics. Deciphering from the *in vitro* results and chemical structure, a cleavable bond between glyocluster and fluoroquinolone is necessary in order to efficiently deliver antibiotic unit into a bacterial cell. Moreover, we could perform structural modifications to optimize the antibacterial effect. Despite the fact that there are still many hurdles to overcome before

chimeric antibiotics could make a success in antibiotic chemistry, it is worth considering this approach as a new tool to fight against bacterial infection and resistance in the near future.

From the pleuromutilin panel, compounds **73**, **74**, and **76** exhibited the best antibacterial activity. This result suggested that a thioether with a terminal negative charge that is capable of forming hydrogen bonds is important and worth further investigating as it could enhance the antibacterial effect of pleuromutilin, especially compound **73** was even better than parent pleuromutilin against some bacterial strains. This effect is opposite in the case of lefamulin, in which two derivatives (*N*-acetyl cysteine and *N*-acetyl-neuraminic acid) were inactive, and only compound **79** showed a weak antibacterial effect. From this point of view, we might come to conclusion that pleuromutilin and lefamulin have different binding modes; hence with the same conjugated moiety, they could exhibit distinct effect. Nonetheless, structural modification at terminal alkene position is a very promising tactic as many potential thiols or reactive agents are still unexplored. Pleuromutilin and lefamulin antibiotics with novel mode of action hold ideal characteristics to be future antibacterial therapy, and modifications of these compounds to find new active candidates are crucial and need further investigation.

6. Summary

During my doctoral research, I proposed three approaches to cope with bacterial infection and resistance issues through 1) anti-adhesion therapy, 2) synthesis of novel chimeric antibiotics, and 3) structural modification of mutilin antibiotics. In consequence, I have synthesized a series of 9 L-fucopyranoside analogues, 6 multivalent glycoclusters and 6 final chimeric antibiotics including fuco- and galacto-containing compounds, and 17 mutilin derivatives. All of the above-mentioned compounds were tested against their biological targets and showed enhanced outcomes. Our first goal is to produce a panel of anti-adhesive agents to find out the best candidates as well as to study the relationship between structure and binding activity. From the perspective of medicinal chemistry, anti-adhesive agents could be used in combination with antibacterial agents by joining these two agents into one single chimeric molecule. This invention could pave a new way to combat bacterial infection and resistance, especially we can target and eliminate bacteria in a two-pronged targeted therapy manner. In order to discover more potential antibiotics from the currently available ones, I performed structural modification of pleuromutilin and lefamulin antibiotics, especially with the terminal alkene C-19-20 which remains largely unexplored. During my synthetic work, I created 14 pleuromutilin and 3 lefamulin derivatives by conjugating these antibiotics with a wide range of thiol compounds.

New scientific results:

- Anti-adhesion therapy: 6 multivalent glycoclusters (4 fucoclusters and 2 galactoseclusters) were synthesized with greatly enhanced lectin inhibitory activity. I have found universal candidates for bacterial/fungal lectin.
- Chimeric strategy: 6 chimeric antibiotics were synthesized with potential anti-adhesive property and slight antimicrobial effect. This type of compound has the potential to detach and kill pathogens with a wide-spectrum effect.
- Structural modification: 17 mutilin derivatives were synthesized, I have found several analogues with improved antibacterial effect.

In conclusion, antibiotic resistance is a worldwide alarming issue that needs to be seriously aware of and dealt with a reasonable approach. Medicinal chemistry, with countless novel applications, will definitely continue to display its essential role in the future, especially in the field of antibiotic chemistry as well as in other areas. Thus, a good understanding and combination of chemistry and biology would pave the way for a feasible drug discovery project.

7. Methods and experimental data

7.1 Antibacterial measurement

For the in vitro minimal inhibitory concentration (MIC) measurements, we used 12 different bacterial strains. Some of these strains were purchased from the American Type Culture Collection (ATCC), whereas others were clinical isolates. Our bacterial collection contained wild-typed-sensitive and also multiresistant strains. According to the EUCAST (European Committee on Antimicrobial Susceptibility Testing) reading guide for broth microdilution, compounds were two-fold serially diluted from 256 to 0.5 mg/L in Müller–Hinton broth. Then, 100 μ L of each dilution was inoculated with 10 μ L of 0.5 McFarland bacterial suspension. Incubation was performed at 37°C for 24h without shaking, and determination of MIC was made with the naked eye.

7.2 Hemagglutination inhibition assay (HIA)

Lectins AFL, RSL, AAL, and AOL were dissolved in the PBS buffer to the concentration 0.1 mg/mL. Lectins were mixed with carbohydrate inhibitors serially diluted in PBS buffer in a 5 μ L:5 μ L ratio. The final (working) concentration of lectins was therefore 0.05 mg/mL. A total of 10 μ L of 20% papain-treated, acid-stabilized red blood cells O⁺ in PBS buffer was then added, and the mixture was thoroughly mixed and incubated for 5 min at room temperature. After incubation, the mixture was mixed again, transferred to a microscope slide, and examined. The examination was conducted using the Levenhuk D2L NG Digital Microscope (Levenhuk, Tampa, FL, USA). Images were obtained with a Levenhuk D2L digital camera (Levenhuk, Tampa, FL, USA) using the software ToupView for Windows (Levenhuk, Tampa, FL, USA). The positive (experiment without an inhibitor) and negative (experiment without a lectin) control were prepared and processed in the same way using an appropriate volume of dissolving buffer instead of the omitted components. The minimal inhibitory concentration (MIC) of the inhibitor able to inhibit hemagglutination was determined and compared with the standard (L-fucose), and the potency of the inhibitor was calculated (MIC of the standard/MIC of the inhibitor). MIC of the standard was determined every time a new batch of lectins or red blood cells were used for experiments to diminish the biological variability. The PA-III and BC2L C lectins were dissolved in the buffer containing calcium ions necessary for their activity (20 mM Tris/HCl, 150 mM NaCl, 5 mM CaCl₂, pH 7.5) to the concentration 2.5 mg/mL and 0.2 mg/mL, respectively. Lectins were mixed with carbohydrate inhibitors serially diluted in the Tris buffer in a 5 μ L:5 μ L ratio. The final (working) concentration of the lectins was therefore 1.25 mg/mL and 0.1 mg/mL. A total of

10 μL of 20% papain-treated, acid-stabilized red blood cells O^+ in the Tris buffer was then added, and the mixture was thoroughly mixed and incubated for 5 min at room temperature. The examination was conducted and evaluated as mentioned above.

PA-IL was dissolved in the buffer with calcium ions suitable for the activity of the lectin (20 mM Tris/HCl, 150 mM NaCl, 5 mM CaCl_2 , pH = 7.5) to the concentration 0.25 mg/mL. Lectin was mixed with carbohydrate inhibitors serially diluted in the buffer in a 5 μL :5 μL ratio. Therefore, the final (working) concentration of the lectin was 0.125 mg/mL. A total of 10 μL of 20% papain-treated, azid stabilized red blood cells B^+ in the buffer was then added, and the mixture was thoroughly mixed and incubated for 5 min at room temperature. The examination was conducted and evaluated as mentioned above. The minimal inhibitory concentration (MIC) of the inhibitor able to inhibit hemagglutination was determined and compared with the standard (D-galactose) and the potency of the inhibitor was calculated (MIC of the standard/MIC of the inhibitor).

7.3 Surface plasmon resonance (SPR)

Surface plasmon resonance (SPR) experiments were performed on a BIAcore T200 instrument (GE Healthcare, Chicago, IL, USA) at 25°C, using HBST running buffer (10 mM HEPES, 150 mM NaCl, 0.5 mM CaCl_2 , 0.05% Tween 20, pH = 7). A CM5 sensor chip (GE Healthcare, Chicago, IL, USA) covered with a carboxymethylated dextran matrix was used for ligand immobilization. The sensor chip surface was activated with *N*-ethyl-*N*-(3-dimethylaminopropyl)carbodiimide/*N*-hydroxysuccinimide solution and then coated with streptavidin (Sigma-Aldrich, St. Louis, MO, USA) in 10 mM acetate pH = 5.0 according to the manufacturer's standard protocol to a final response of 7000 RU. Unreacted groups were blocked with 1 M ethanolamine HCl, pH = 8.5. 0.5 mM biotinylated carbohydrate (1:1 mixture of biotin- α -D galactoside and biotin- β -D-galactoside for measuring channel and α -L-fucoside for blank channel, all Lectinity, Moskow, Russia) was injected into a particular channel at a flow rate of 5 $\mu\text{L}/\text{min}$.

In the experimental setup, SPR inhibition measurements were carried out simultaneously on both measuring and blank channels at a flow rate of 5 $\mu\text{L}/\text{min}$. Protein PA-IL at a concentration of 45 μM was mixed with various concentrations of inhibitors (0.1–125 μM for studied compounds or 5–5000 μM for D-galactose) and injected onto the sensor chip. The response of the blank channel was subtracted from the response of lectin bound to the galactose modified surface at equilibrium and plotted against the concentration of inhibitor in

order to determine IC₅₀ (concentration of inhibitor resulting in 50% inhibition of binding). As IC₅₀ is not a constant and depends on the experimental setup, a parameter called potency was used for characterization. The potency of a tested inhibitor is the ratio of IC₅₀ of a chosen standard inhibitor (in this case, D-galactose) and the inhibitor in question. Pure lectin PA-IL was used as a control (0% inhibition).

7.4 General methods for synthesis

Optical rotations were measured at room temperature with a Perkin-Elmer 241 automatic polarimeter. TLC analysis was performed on Kieselgel 60 F₂₅₄ (Merck) silica gel plates with visualization by immersing in a sulfuric-acid solution (5% in EtOH) followed by heating. Column chromatography was performed on silica gel 60 (Merck 0.063–0.200 mm), flash column chromatography was performed on silica gel 60 (Merck 0.040–0.063 mm). Gel filtration was performed on Sephadex G-25, using methanol or water as the eluent. Organic solutions were dried over MgSO₄ and concentrated under vacuum. The ¹H (400 and 500 MHz) and ¹³C NMR (100.28, 125.76 MHz) spectra were recorded with Bruker DRX-400 and Bruker Avance II 500 spectrometers. Chemical shifts are referenced to Me₄Si or DSS (0.00 ppm for ¹H) and to solvent signals (CDCl₃: 77.00 ppm, CD₃OD: 49.15 ppm, DMSO-d₆: 39.51 ppm for ¹³C). MS (MALDI-TOF) analysis was carried out in positive reflectron mode with a BIFLEX III mass spectrometer (Bruker, Germany) with delayed-ion extraction. The matrix solution was a saturated solution of 2,4,6-trihydroxy-acetophenone (THAP) in MeCN. ESI-QTOF MS measurements were carried out on a maXis II UHR ESI-QTOF MS instrument (Bruker), in positive ionization mode. The following parameters were applied for the electrospray ion source: capillary voltage: 3.6 kV; end plate offset: 500 V; nebulizer pressure: 0.5 bar; dry gas temperature: 200 °C and dry gas flow rate: 4.0 L/min. Constant background correction was applied for each spectrum; the background was recorded before each sample by injecting the blank sample matrix (solvent). Na-formate calibrant was injected after each sample, which enabled internal calibration during data evaluation. Mass spectra were recorded by OTOF Control version 4.1 (build: 3.5, Bruker) and processed by Compass DataAnalysis version 4.4 (build: 200.55.2969).

7.4.1 General method A for azide-alkyne click reaction (compounds 50, 51, 52, 58)

Ascorbic acid (1.0 equiv.) and CuSO₄ (0.2 equiv.) were added to a stirred solution of alkyne (1.5 equiv.) and azide (1.0 equiv.) in absolute DMF (3 mL) and stirred overnight at room

temperature. The reaction mixture was evaporated, and the crude product was purified by flash column chromatography to give the desired product.

7.4.2 General method B for azide-alkyne click reaction (compounds 5, 6, 7, 15, 23, 26, 29, 32, 38, 39, 53, 59)

Et₃N (1.0 equiv.) and CuI(I) (0.2 equiv.) were added to a stirred solution of alkyne (1.5 equiv.) and azide (1.0 equiv.) in absolute DMF (3 mL) or CH₃CN under argon gas and stirred overnight at room temperature. The reaction mixture was evaporated, and the crude product was purified by flash column chromatography to give the desired product.

7.4.3 General method C for Zemplén-deacetylation (compounds 11, 12, 14, 18, 24, 27, 30, 33, 44, 45, 54, 55, 56, 57, 60, 61)

The catalytic amount of NaOMe (pH ~ 9) was added to a stirred solution of compound (1.0 equiv.) in MeOH (3 mL) and stirred overnight at room temperature. The reaction mixture was neutralized with Amberlite IR-120 ion-exchange resin, filtered and evaporated, then the crude product was purified by Sephadex column or flash column chromatography to give the desired compound.

7.4.4 General method D for photoinitiated thiol-ene addition of pleuromutilin (compounds 17, 62-75)

To a solution of the pleuromutilin (1.0 equiv.) and thiol (1.0-3.0 equiv.) in the specified solvent (2-3 mL) 2,2-dimethoxy-2-phenylacetophenone (DPAP, 25 mg, 0.10 mmol) was added. The solution was irradiated at room temperature or under cooling temperature for 15 mins-60 mins. When the irradiation cycle was repeated 0.1 equiv. DPAP was added freshly. If the conversion of the starting material is satisfactory, the reaction mixture was concentrated and the residue was purified using flash column chromatography to obtain the desired product.

7.4.5 General methods E for photoinitiated thiol-ene addition of lefamulin (compounds 78-80)

To a solution of the lefamulin (1.0 equiv.) and trifluoroacetic acid (2.0 equiv.) in the specified solvent (1 mL), thiol (2.0 equiv.) and 2,2-dimethoxy-2-phenylacetophenone DPAP (0.10 mmol) were added. The solution was irradiated at -80°C for 15 mins-60 mins. Then the

solution was concentrated, co-evaporated with toluene 2-3 times, and the residue was purified using flash column chromatography to obtain the desired product.

7.4.6 General methods F for deprotection of *N*-acetylneuraminic acid derivatives (compounds 76 and 81)

To a stirred solution of the compound (1.0 equiv.) in 2ml Dioxane/H₂O 9:1, 0.2 M aqueous solution of KOH (5.0 equiv.) was added. The reaction mixture was stirred for half hour at 0°C, then allowed to stir at room temperature for 3h, pH=12. The reaction mixture was neutralized with Amberlite IR-120 H⁺ ion-exchange resin, filtered and evaporated. The crude product was purified by Sephadex column or flash column chromatography to obtain the desired compound.

7.5 Experimental data

Compound 5

Azide compound **3** (270 mg, 1.125 mmol 1.5 equiv.) and alkyne **2** (151 mg, 0.75 mmol, 1.0 equiv.) were reacted in CH₃CN according to general method **B**. The mixture was concentrated and purified by flash column chromatography (CH₂Cl₂/MeOH 9:1) to give the conjugated product (266 mg, 80%) as white powder. This product (222 mg, 0.5 mmol) was subsequently reacted with NaN₃ (48.8 mg, 0.75 mmol, 1.5 equiv.) in abs.DMF under an argon atmosphere and stirred overnight at room temperature. The reaction mixture was diluted with water dropwise, stirred for further 10 minutes and evaporated. The residue was dissolved in CH₂Cl₂ (200 mL) and extracted with water (2 x 50 mL) and brine (50 mL), dried over MgSO₄, filtered and evaporated. The crude product was purified by flash column chromatography (CH₂Cl₂/MeOH 9:1) to give compound **5** (77 mg, 49%) as a colourless syrup. *R*_f = 0.38 (CH₂Cl₂/MeOH 85:15), [α]²⁴_D -132.5 (c = 0.12, H₂O). ¹H NMR (400 MHz, CDCl₃+CD₃OD): δ 7.91 (s, 1H, *CH* triazole), 4.94 (s, 1H, *H*-1), 4.83 (d, *J* = 12.6 Hz, 1H, *CH*₂a propargyl), 4.67 (d, *J* = 12.5 Hz, 1H, *CH*₂b propargyl), 4.57-4.54 (m, 2H, *NCH*₂ ethylene glycol), 3.98 (q, *J* = 6.5 Hz, 1H, *H*-5), 3.86-3.83 (m, 2H, *N*₃*CH*₂ ethylene glycol), 3.78 (s, 2H, *H*-2, *H*-3), 3.71 (s, 1H, *H*-4), 1.26 (d, *J* = 6.6 Hz, 3H, *CH*₃). ¹³C NMR (100 MHz, CDCl₃+CD₃OD): δ 144.2 (1C, *C*_q triazole), 123.7 (1C, *CH* triazole), 98.2 (*C*-1), 71.6, 70.0, 68.4, 66.1 (4C, *C*-2, *C*-3, *C*-4, *C*-5), 60.2 (1C, *CH*₂ propargyl), 50.1, 49.1 (2C, 2 x *NCH*₂ ethylene glycol), 15.4 (1C, *CH*₃). MS (MALDI-TOF): *m/z* calcd for C₁₁H₁₈N₆NaO₅: 337.12 [*M* + Na]⁺; found: 337.26.

Compound 6 and 7

Diazide compound **4** (312 mg, 1.28 mmol) and alkyne **2** (72 mg, 0.36 mmol) were reacted in CH₃CN according to general method **B**. The crude product was purified by flash column chromatography (CH₂Cl₂/MeOH 9:1) to give compound **6** (56 mg, 35%) as a colourless syrup. (The dimer compound **7** was also observed, 28 mg, 12%).

Compound 6: R_f = 0.42 (CH₂Cl₂/MeOH 7:3), [α]²⁴_D -66.9 (c = 0.13, MeOH). ¹H NMR (400 MHz, CDCl₃): δ 7.83 (s, 1H, CH triazole), 4.94 (s, 1H, H-1), 4.79 (d, J = 12.3 Hz, 1H, CH₂a propargyl), 4.64 (d, J = 12.5 Hz, 1H, CH₂b propargyl), 4.54 (s, 2H, NCH₂ TEG), 3.96-3.94 (m, 1H, H-5), 3.88-3.84 (m, 4H, OCH₂TEG, H-2, H-3), 3.75 (s, 1H, H-4), 3.68-3.62 (m, 10H, 5 x OCH₂ TEG), 3.40-3.37 (m, 2H, N₃CH₂TEG), 1.23 (d J = 6.2 Hz, 3H, CH₃). ¹³C NMR (100 MHz, CDCl₃): δ 144.1 (1C, C_q triazole), 124.2 (1C, CH triazole), 98.5 (C-1), 72.1, 70.7, 68.9, 66.5 (4C, C-2, C-3, C-4, C-5), 70.6, 70.5, 70.1, 69.4 (6C, 6 x OCH₂TEG), 60.8 (1C, CH₂ propargyl), 50.7, 50.3 (2C, 2 x NCH₂TEG), 16.3 (CH₃). MS (MALDI-TOF): m/z calcd for C₁₇H₃₀N₆NaO₈: 469.20 [M + Na]⁺; found: 469.24.

Compound 7: R_f = 0.12 (CH₂Cl₂/MeOH 7:3), [α]²⁴_D -124.6 (c = 0.13, MeOH). ¹H NMR (400 MHz, CDCl₃) δ 7.90 (d, J = 6.0 Hz, 2H, 2 x CH triazole), 4.91 (t, J = 3.0 Hz, 2H, 2 x H-1), 4.80 (dd, J = 13.0, 4.5 Hz, 2H, 2 x H-2), 4.63 (dd, J = 12.0, 3.3 Hz, 2H, 2 x H-3), 3.96 (q, J = 6.6 Hz, 2H, 2 x H-4), 3.70 (m, 2H, 2 x H-5), 4.55, 4.30, 3.89, 3.76, 3.61 (20H, 8 x CH₂ TEG, 2 x CH₂ propargyl), 1.23 (m, 6H, 2 x CH₃). ¹³C NMR (101 MHz, CDCl₃) δ 148.0 (2C, 2 x C_q triazole), 128.2 (2C, 2 x CH triazole), 102.4 (2C, 2 x C-1), 75.9, 74.3, 72.7, 70.4 (8C, 2 x C-2, C-3, C-4, C-5), 74.3, 74.2, 73.1, 64.5 (8C, 4 x CH₂ TEG), 54.2 (2C, 2 x CH₂ propargyl), 19.8 (2C, 2 x C-6). MS (MALDI-TOF): m/z calcd for C₂₆H₄₄N₆NaO₁₃: 671.2864 [M + Na]⁺; found: 671.2408.

Compound 11

Compound **11** was synthesized from compound **10** (153.16 mg, 0.5 mmol) according to general method **C** under argon to obtain a product as white powder **11** (46 mg, 51%). R_f = 0.42 (CH₂Cl₂/MeOH 7:3), [α]²⁴_D +129.2 (c = 0.26, MeOH). ¹H NMR (400 MHz, MeOD) δ 4.53 – 4.39 (m, 1H, H-1), 3.82 – 3.65 (m, 1H, H-5), 3.69 – 3.57 (m, 1H, H-4), 3.52 (dd, J = 9.3, 3.4 Hz, 1H, H-2), 3.37 (s, 1H, H-3), 1.30 (d, J = 6.4 Hz, 3H). ¹³C NMR (101 MHz, MeOD) δ 91.3 (1C, C-1), 75.3, 75.0, 71.9, 68.7 (4C, C-2, C-3, C-4, C-5), 15.7 (1C, CH₃). HRMS: (ESI⁺-MS, m/z) calcd for C₆H₁₂NaO₄S: 203.0354 [M + Na]⁺; found: 203.0228.

Compound 12

Compound **12** was oxidized from compound **10** (153 mg, 0.5 mmol) using H₂O₂ (1.8 ml, 10%) and then deprotected according to general method **C** to obtain a product as white powder **12** (77 mg, 86%). R_f = 0.4 (CH₂Cl₂/MeOH 85:15), [α]²⁴_D +116.6 (c = 0.12, MeOH). ¹H NMR (400 MHz, D₂O) δ 4.50 (d, *J*=9.6 Hz, 2H, 2 x *H*-1), 3.81 (bq, *J*=6.4 Hz, 2H, 2 x *H*-5), 3.75 (bs, 2H, 2 x *H*-4), 3.71 (t, *J*=9.6 Hz, 2H, 2 x *H*-2), 3.64 (bd, *J*=9.6 Hz, 2H, 2 x *H*-3), 1.23 (*J*=6.0 Hz, 6H, 2 x CH₃). ¹³C NMR (100 MHz, D₂O) δ 90.0 (2C, 2 x C-1), 75.5, 73.8, 71.4, 68.3 (8C, 2 x C-2, C-3, C-4, C-5), 15.6 (2C, 2 x C-6). MALDI-MS: m/z calcd for C₁₂H₂₂NaO₈S₂: 381.0654 [M + Na]⁺; found: 381.0598.

Compound 13

To a stirring solution of compound **10** (765 mg, 2.5 mmol) in abs.DCM, propargyl bromide (270 μl, 2.5 mmol, 1.0 equiv.) and DIPEA (427 μl, 2.5 mmol, 1.0 equiv.) were added. The reaction was allowed to sitr at room temperature for 2h. EtOAc (20ml) was added and the precipitated salts were filtered off. The crude product was concentrated and purified by flash column chromatography (CH₂Cl₂/acetone 98:2) to give compound **13** (660 mg, 77%) as a white powder. R_f = 0.5 (CH₂Cl₂/acetone 98:2), [α]²⁴_D -71.6 (c = 1.0, CHCl₃). ¹H NMR (CDCl₃) δ 5.25 (mc, 1H, *H*-4), 5.18 (d, *J* = 10.1 Hz, 1H, *H*-2), 5.06 (dd, *J* = 9.9, 3.3 Hz, 1H, *H*-3), 4.68 (d, *J* = 9.8 Hz, 1H, *H*-1), 3.83 (q, *J* = 6.5 Hz, 1H, *H*-5), 3.54-3.27 (2 × d, *J* = 16.6 Hz, 2H, SCH₂), 2.23 (t, *J* = 2.6 Hz, 1H, CH propargyl), 2.14, 2.03, 1.95 (4 × s, 12 H, CH₃CO), 1.20 (m, 3H, CH₃). ¹³C NMR (CDCl₃) δ 170.7, 170.1, 169.8 (3 x CO), 82.3 (1C, C-1), 79.1 (1C, C_q propargyl), 73.8 (1C, C-3), 72.4 (1C, CH propargyl), 71.7 (1C, C-4), 70.5 (1C, C-2), 67.3 (1C, C-5), 20.8, 20.7, 20.6 (3C, 3 x CH₃), 17.5 (1C, SCH₂), 16.4 (1C, C-6). MALDI-MS: m/z calcd for C₁₅H₂₀NaO₇S: 367.0827 [M + Na]⁺; found: 367.0208.

Compound 14

Compound **14** was synthesized from compound **13** (120 mg, 0.35 mmol) according to general method **C** to obtain a product as white powder **14** (60 mg, 79%). R_f = 0.45 (CH₂Cl₂/MeOH 7:3), [α]²⁴_D +133.0 (c = 0.1, MeOH). ¹H NMR (400 MHz, MeOD) δ 4.85 (s, 2H, SCH₂), 4.51 (d, *J* = 9.5 Hz, 1H, *H*-4), 3.70 – 3.62 (m, 1H, *H*-2), 3.57 – 3.45 (m, 1H, *H*-3), 3.42 (d, *J* = 2.7 Hz, 1H, *H*-1), 3.38 (d, *J* = 2.7 Hz, 1H, *H*-5), 2.59 (t, *J* = 2.6 Hz, 1H, CH propargyl), 1.28 (d, *J* = 6.5 Hz, 3H, CH₃). ¹³C NMR (101 MHz, MeOD) δ 84.3 (1C, C-1), 75.1, 74.8, 71.8, 69.7 (4C, C-2, C-3, C-4, C-5), 70.9 (1C, C_q propargyl), 16.1 (1C, SCH₂), 15.5 (1C, C-6). MALDI-MS: m/z calcd for C₉H₁₄NaO₄S: 241.0510 [M + Na]⁺; found: 241.0190.

Compound 15

Azide **4** (293 mg, 1.2 mmol) and alkyne **14** (87.3 mg, 0.4 mmol) were reacted in CH₃CN according to general method **B**. The reaction mixture was concentrated and the crude product was purified by flash column chromatography (CH₂Cl₂/MeOH 95:5) and gel filtration to give compound **15** (98.05 mg, 53%) as a colorless syrup. R_f = 0.23 (CH₂Cl₂/MeOH 95:5), [α]²⁴_D +29.1 (c = 0.11, MeOH). ¹H NMR (400 MHz, MeOD) δ 7.77 (s, 1H, CH triazole), 4.50 (t, J = 5.0 Hz, 2H, SCH₂), 4.28 (d, J = 9.5 Hz, 1H, H-4), 4.20 (s, 1H, H-2), 3.95 (m, 1H, H-3), 3.86 (t, J = 5.1 Hz, 1H, H-1), 3.65 (dd, J = 16.2, 7.2 Hz, 12H, 6 x CH₂), 3.48 (dd, J = 9.0, 3.4 Hz, 1H, H-5), 3.37 (t, J = 5.0 Hz, 2H, CH₂), 3.33 (s, 2H, CH₂), 1.28 (d, J = 6.4 Hz, 3H, CH₃). ¹³C NMR (101 MHz, MeOD) δ 145.0 (1C, C_q triazole), 123.4 (1C, CH triazole), 84.8 (1C, C-1), 75.2, 74.6, 71.3, 69.7 (4C, C-2, C-3, C-4, C-5), 70.2, 70.2, 70.1, 70.1, 69.1, 68.9, 50.3, 50.0 (8C, 8 x CH₂), 22.7 (1C, SCH₂), 16.0 (1C, CH₃). MALDI-TOF MS: *m/z* calcd for C₁₇H₃₀N₆NaO₇S: 485.1794 [M + Na]⁺; found: 485.2601.

Compound 17

2-Acetoxy-3,4-di-*O*-acetyl-L-fucal **16** (272 mg, 1.0 mmol, 1.0 equiv.) and 2-mercaptoethanol (140 μL, 2 mmol, 2.0 equiv.) were reacted in toluene:methanol:water = 8:5:1 (5 mL) according to general method **D** at room temperature, irradiated for 3 times. Then, the solution was concentrated and the residue was purified using column chromatography (*n*-hexane: acetone 9:1) to give compound **17** (122 mg, 35%) as a colorless syrup. R_f = 0.50 (*n*-hexane: acetone 7:3), [α]²⁴_D -135.9 (c = 0.02, CH₃Cl). ¹H NMR (400 MHz, CDCl₃) δ 5.74 (d, J = 5.5 Hz, 1H, H-4), 5.37–5.13 (m, 2H, OCH₂), 4.48 (m, 1H, H-2), 3.86 (dt, J = 9.0, 4.6 Hz, 1H, H-3), 3.72 (2H, SCH₂), 2.85 (m, 1H, H-1), 2.67 (m, 1H, H-5), 2.14, 2.05, 1.96 (s, 9H, 3 x COCH₃), 1.14 (d, J = 6.5 Hz, 3H). ¹³C NMR (101 MHz, CDCl₃) δ 170.6, 170.3, 170.0 (3C, 3 x CO), 82.8 (1C, C-1), 70.8, 68.4, 67.9, 65.1 (4C, C-2, C-3, C-4, C-5), 61.8 (1C, OCH₂), 33.6 (1C, SCH₂), 20.8, 20.6, 20.6 (3C, 3 x COCH₃), 15.8 (1C, C-6). MALDI-TOF MS: *m/z* calcd for C₁₄H₂₂NaO₈S: 373.0933 [M + Na]⁺; found: 373.0854.

Compound 18

Compound **18** was synthesized from compound **17** (315.35 mg, 0.9 mmol) according to general method **C**. The crude product was then purified by flash column chromatography (CH₂Cl₂/MeOH 95:5) and gel filtration to give compound **18** (157 mg, 78%) as a colorless

syrup. $R_f = 0.23$ ($\text{CH}_2\text{Cl}_2/\text{MeOH}$ 95:5), $[\alpha]^{24}_{\text{D}} -331.9$ ($c = 0.16$, MeOH). ^1H NMR (400 MHz, MeOD) δ 5.36 (d, $J = 5.6$ Hz, 1H, $H-4$), 4.31 (qd, $J = 6.7, 1.1$ Hz, 1H, $H-2$), 4.06 (dd, $J = 10.1, 5.6$ Hz, 1H, $H-3$), 3.80–3.54 (m, 4H, 2 x CH_2), 2.78 (ddd, $J = 13.5, 7.3, 6.2$ Hz, 1H, $H-1$), 2.65 (ddd, $J = 13.6, 7.3, 6.5$ Hz, 1H, $H-5$), 1.25 (d, $J = 6.6$ Hz, 3H, CH_3). ^{13}C NMR (101 MHz, MeOD) δ 88.1 (1C, $C-1$), 73.4, 72.3, 69.5, 68.1 (4C, $C-2, C-3, C-4, C-5$), 62.7 (1C, HOCH_2), 33.7 (1C, SCH_2), 16.6 (1C, $C-6$). MALDI-TOF MS: m/z calcd for $\text{C}_8\text{H}_{16}\text{NaO}_5\text{S}$: 247.0616 $[\text{M} + \text{Na}]^+$; found: 247.0632.

Compound 19

To the mixture of propargyl α -L-fucospyranoside **2** (930 g, 4.6 mmol, 1.0 equiv.) in pyridine at 0°C , 5ml of acetic anhydride was added dropwise. The reaction mixture was allowed to stir overnight and monitored with TLC. The crude product was purified by flash column chromatography (n-hexane/Acetone 8:2) to give compound **19** (961 mg, 63%) as a white powder. $R_f = 0.5$ (n-hexane/Acetone 8:2), $[\alpha]^{24}_{\text{D}} -155.2$ ($c=1$, CHCl_3). ^1H NMR (400 MHz, CDCl_3) δ 5.35 (dd, $J_{2,3} = 11.0$ Hz, $J_{3,4} = 3.4$ Hz, 1H, $H-3$), 5.30 (d, $J_{3,4} = 3.4$ Hz, 1H, $H-4$), 5.24 (d, $J_{1,2} = 3.7$ Hz, 1H, $H-1$), 5.15 (dd, $J_{1,2} = 3.7$ Hz, 1H, $H-2$), 4.25 (d, $J = 2.3$ Hz, 2H, CH_2CCH), 4.19 (q, $J_{5,6} = 6.6$ Hz, 1H, $H-5$), 2.42 (t, $J = 2.3$ Hz, 1H, CH_2CCH), 2.16 (s, 3H, CH_3), 2.09 (s, 3H, CH_3), 1.99 (s, 3H, CH_3), 1.14 (d, $J_{5,6} = 6.6$ Hz, 3H, $H-6$). ^{13}C NMR (100 MHz, CDCl_3) δ 170.7, 170.6, 170.1 (3C, 3 x CO), 95.1 (1C, $C-1$), 78.7 (1C, CH_2CCH), 74.9 (1C, CH_2CCH), 71.7, 67.9, 67.9, 65.1 (4C, $C-2, C-3, C-4, C-5$), 55.3 (CH_2CCH), 20.9, 20.8, 20.8 (3C, 3 x CH_3), 15.9 (1C, $C-6$). HRMS: (ESI⁺-MS) m/z calcd for $\text{C}_{15}\text{H}_{20}\text{NaO}_8$: 351.1056 $[\text{M} + \text{Na}]^+$; found: 351.1493.

Compound 21

To stirring solution of per-O-acetylated D-galactose **20** (3.9 g, 10 mmol, 1.0 equiv.) and propargyl alcohol (0.87 ml, 15 mmol, 1.5 equiv.) in 30 ml absolute CH_2Cl_2 at 0°C , $\text{BF}_3\cdot\text{Et}_2\text{O}$ (2.47ml, 20 mmol, 2.0 equiv.) was added dropwise. The reaction mixture was allowed to stir overnight and monitored with TLC. After full conversion, the reaction mixture was diluted with CH_2Cl_2 (300ml), washed with H_2O (100ml), then washed with saturated aqueous solution of NaHCO_3 (20ml) and H_2O (80ml), and finally extracted with H_2O (100ml), dried over MgSO_4 , filtered and concentrated. The crude product was purified by flash column chromatography (n-hexane/Acetone 8:2) to give compound **21** (2 g, 52%) as a white powder. $R_f = 0.27$ (n-hexane/Acetone 8:2), $[\alpha]^{24}_{\text{D}} -46.7$ ($c=0.12$, CHCl_3). ^1H NMR (400 MHz, CDCl_3) δ 5.39 (dd, $J = 1.2$ Hz, $J = 3.6$ Hz, 1H, $H-4$), 5.21 (dd, $J = 8.0$ Hz, $J = 10.4$ Hz, 1H, $H-2$), 5.05

(dd, $J = 3.6$ Hz, $J = 10.4$ Hz, 1H, $H-3$), 4.73 (d, $J = 8.0$ Hz, 1H, $H-1$), 4.38 (d, $J = 2.4$ Hz, 2H, CH_2OCCH), 4.15 (m, 2H, $H-6a$, $H-6b$), 3.93 (dt, $J = 1.2$ Hz, $J = 6.8$ Hz, 1H, $H-5$), 2.46 (t, $J = 2.4$ Hz, 1H, CH_2OCCH), 2.15, 2.07, 2.05, 1.98 (12H, 4 x CH_3). ^{13}C NMR (100 MHz, $CDCl_3$) δ 170.5, 170.4, 170.3, 169.7 (4C, 4 x CO), 98.7 (1C, $C-1$), 78.3 (CH_2CCH), 75.5 (CH_2CCH), 70.9, 70.9, 68.5, 67.0, 61.3 (5C, $C-2$, $C-3$, $C-4$, $C-5$, $C-6$), 56.0 (CH_2CCH), 20.9–20.7 (4C, 4 x CH_3). HRMS: (ESI+-MS) m/z calcd for $C_{17}H_{22}NaO_{10}$: 409.1112 [$M + Na$] $^+$; found: 409.1111.

Compound 23

Azide compound **22** (100 mg, 0.10 mmol) and alkyne **21** (169 mg, 0.44 mmol) were reacted in CH_3CN according to the general method **B**. The crude product was purified by flash column chromatography ($CH_2Cl_2/MeOH$ 95:5) to give compound **23** (118 mg, 55%) as a colourless syrup. R_f 0.33 ($CH_2Cl_2/MeOH$ 95:5), $[\alpha]^{24}_D -21.96$ (c 0.46, $CHCl_3$). 1H NMR (400 MHz, $CDCl_3$): δ 7.94, 7.90, 7.72 (3 x s, 6H, 6 x CH triazole), 7.44 (s, 2H, arom), 5.40 (d, $J = 2.9$ Hz, 3H, skeleton proton), 5.23 (s, 6H, 3 x CH_2), 5.20–5.18 (m, 3H, 3 x skeleton protons), 5.02 (dd, $J = 3.4$ Hz, $J = 10.4$ Hz, 3H, 3 x skeleton protons), 4.94 (d, $J = 12.5$ Hz, 3H, 3 x $H-6a$), 4.80 (d, $J = 12.5$ Hz, 3H, 3 x $H-6b$), 4.68 (d, $J = 7.9$ Hz, 3H, 3 x $H-1$), 4.59–4.50 (m, 11H, 3 x $H-5$, 4 x CH_2), 4.18–4.15 (m, 6H, 3 x CH_2), 3.99–3.84 (m, 19H, 8 x CH_2 , $COOCH_3$), 3.61–3.55 (m, 24H, 12 x CH_2), 2.15, 2.06, 1.97 (3 x s, 36H, 12 x CH_3 acetyl). ^{13}C NMR (100 MHz, $CDCl_3$) δ 170.4, 170.2, 170.1, 169.5 (12C, 12 x CO acetyl), 166.3 (1C, $COOCH_3$), 152.0 (2C, 2 x C_q arom), 144.0, 148.8, 143.1, 141.6 (6C, 6 x C_q triazole), 125.7 (2C, 2 x C_q arom), 124.9, 124.5, 124.0 (6C, 6 x CH triazole), 109.2 (2C, arom), 100.3, 100.2 (3C, 3 x $C-1$), 70.9, 70.8, 68.8, 67.1 (12C, 3 x skeleton carbons), 70.5, 70.4, 69.3 (18C, 18 x CH_2 TEG), 63.0, 62.8, 62.7 (3C, 3 x $C-6$), 61.3 (6C, 6 x CH_2 propargyl), 52.4 (1C, $COOCH_3$), 50.3, 50.2, 50.1 (6C, 6 x NCH_2 TEG), 20.7, 20.6 (12C, 12 x CH_3 acetyl). MALDI-TOF: m/z calcd for $C_{92}H_{128}N_{18}NaO_{44}$: 2211.82 [$M + Na$] $^+$; found: 2211.78.

Compound 24

Compound **23** (86 mg, 0.04 mmol) was deacetylated according to general method **C**. The crude product was purified by flash column chromatography (CH_3CN/H_2O 7:3) to give compound **24** (48 mg, 73%) as a colourless syrup. R_f 0.34 (CH_3CN/H_2O 7:3), $[\alpha]^{24}_D -6.4$ (c 0.14, MeOH). 1H NMR (400 MHz, D_2O): δ 8.00, 7.92, 7.73 (3 x s, 6H, 6 x CH triazole), 7.29 (s, 2H, arom), 5.08 (s, 4H, 2 x CH_2 propargyl), 5.01 (s, 2H, CH_2 propargyl), 4.84–4.65 (m, 6H, 3 x CH_2 propargyl), 4.51–4.38 (m, 12H, 6 x NCH_2 TEG), 4.34 (d, $J = 7.7$ Hz, 3H, 3 x $H-1$), 3.81–3.70 (m, 22H, 3 x $H-4$, $COOCH_3$, 8 x OCH_2 TEG), 3.69–3.61 (m, 6H, 3 x $H-6a,b$), 3.56

(dd, $J = 4.4$ Hz, $J = 7.5$ Hz, 3H, 3 x $H-5$), 3.50 (dd, $J = 3.4$ Hz, $J = 9.9$ Hz, 3H, 3 x $H-3$), 3.44–3.32 (m, 23H, 3 x $H-2$, 10 x OCH₂ TEG). ¹³C NMR (100 MHz, D₂O) δ 168.7 (1C, COOCH₃), 152.4 (2C, 2 x C_q arom), 144.6, 143.8, 141.3 (6C, 6 x C_q triazole), 126.7, 126.4 (6C, 6 x CH triazole), 126.5 (2C, 2 x C_q arom), 110.1 (2C, arom), 103.0 (3C, 3 x $C-1$), 76.2 (3C, 3 x $C-5$), 73.8 (3C, 3 x $C-3$), 71.6 (3C, 3 x $C-2$), 70.7, 70.6, 70.4, 70.0, 69.6 (18C, 18 x CH₂ TEG), 69.5 (3C, 3 x $C-4$), 66.0, 62.9 61.7 (6C, 6 x CH₂ propargyl), 61.9 (3C, 3 x $C-6$), 53.9 (1C, COOCH₃), 51.1, 51.0, 50.9 (6C, 6 x NCH₂ TEG). MALDI-TOF: m/z calcd for C₆₈H₁₀₄N₁₈NaO₃₂: 1707.70 [M + Na]⁺; found: 1707.65.

Compound 26

Azide compound **25** (50 mg, 0.08 mmol) and alkyne **21** (139 mg, 0.36 mmol) were reacted in CH₃CN according to general method **B**. The crude product was purified by flash column chromatography (CH₂Cl₂/MeOH 97:3) to give compound **26** (125 mg, 89%) as a colourless syrup. R_f 0.11 (CH₂Cl₂/ MeOH 97:3), $[\alpha]^{24}_D$ -22.9 (c 0.17, CHCl₃). ¹H NMR (400 MHz, CDCl₃) δ 7.84, 7.76, 7.51, 7.50 (4 x s, 6H, 6 x CH triazole), 7.40 (s, 2H, arom), 5.39 (s, 3H, 3 x skeleton protons), 5.20 4.94 (m, 24H, 6 x CH₂ propargyl, 6 x CH₂ ethylene glycol), 4.91–4.88 (m, 3H, 3 x skeleton protons), 4.76–4.71 (m, 3H, 3 x skeleton protons), 4.63–4.60 (m, 3H, 3 x $H-1$), 4.19–4.09 (m, 6H, 3 x $H-6a,b$), 3.98–3.97 (m, 3H, 3 x $H-5$), 3.90 (s, 3H, COOCH₃), 2.14, 2.04, 1.99, 1.97 (4 x s, 36H, 12 x CH₃ acetyl). ¹³C NMR (100 MHz, CDCl₃) δ 170.5, 170.3, 170.1, 170.0, 169.6 (12C, 12 x CO acetyl), 166.2 (1C, COOCH₃), 151.8 (2C, 2 x C_q arom), 143.7, 141.4 (6C, 6 x C_q triazole), 124.2 (2C, 2 x C_q arom), 124.1 (6C, 6 x CH triazole), 109.1 (2C, arom), 100.4 (3C, 3 x $C-1$), 70.9, 70.8, 68.8, 67.1 (12C, 3 x skeleton carbons), 62.8, 62.7 (3C, 3 x $C-6$), 61.3 (6C, 6 x CH₂ propargyl), 52.5 (1C, COOCH₃), 49.6, 49.5 (6C, 6 x NCH₂ ethylene glycol), 20.8, 20.7, 20.6 (12C, 12 x CH₃ acetyl). MALDI-TOF: m/z calcd for C₇₄H₉₂N₁₈NaO₃₅: 1815.59 [M + Na]⁺; found: 1815.46.

Compound 27

Compound **26** (62 mg, 0.03 mmol) was deacetylated according to general method **C**. The crude product was purified by flash column chromatography (CH₃CN/H₂O 7:3) to give compound **27** (42 mg, 94%) as a colourless syrup. R_f 0.34 (CH₃CN/H₂O 7:3), $[\alpha]^{24}_D$ -8.0 (c 0.10, H₂O). ¹H NMR (400 MHz, D₂O) δ 7.97, 7.90, 7.83 (3 x s, 6H, 6 x CH triazole), 7.32 (s, 2H, arom), 5.13 4.73 (m, 24H, 6 x CH₂ propargyl, 6 x CH₂ ethylene glycol), 4.39 (d, $J = 7.2$ Hz, 3H, 3 x $H-1$), 3.91–3.90 (m, 6H, 3 x $H-4$, COOCH₃), 3.80–3.75 (m, 6H, 3 x $H-6a,b$), 3.56–3.60 (m, 6H, 3 x $H-5$, 3 x $H-3$), 3.54–3.50 (m, 3H, 3 x $H-2$). ¹³C NMR (100 MHz, D₂O) δ

168.8 (1C, COOCH₃), 152.1 (2C, 2 x *Cq* arom), 141.0 (6C, 6 x *Cq* triazole), 126.6 (2C, 2 x *Cq* arom), 125.5 (6C, 6 x CH triazole), 110.1 (2C, arom), 102.8 (3C, 3 x C-1), 76.2 (3C, 3 x C-5), 73.7 (3C, 3 x C-3), 71.6 (3C, 3 x C-2), 69.5 (3C, 3 x C-4), 62.5 (6C, 6 x CH₂ propargyl), 61.9 (3C, 3 x C-6), 53.8 (1C, COOCH₃), 50.9, 50.7 (6C, 6 x NCH₂ ethylene glycol). MALDI-TOF: *m/z* calcd for C₅₀H₆₈N₁₈NaO₂₃: 1311.46 [M + Na]⁺; found: 1311.45.

Compound 29

Azide compound **28** (85 mg, 0.05 mmol) and alkyne **21** (111 mg, 0.29 mmol) were reacted in CH₃CN according to general method **B**. The crude product was purified by flash column chromatography (CH₂Cl₂/MeOH 95:5) to give compound **29** (79 mg, 42%) as a colourless syrup. R_f 0.38 (CH₂Cl₂/MeOH 95:5), [α]²⁴_D -16.9 (*c* 0.13, CHCl₃). ¹H NMR (400 MHz, CDCl₃) δ 7.73, 7.72 (2 x s, 8H, 8 x CH triazole), 5.40 (d, *J* = 2.8 Hz, 4H, 4 x *H*-4), 5.20 (dd, *J* = 8.0 Hz, *J* = 10.4 Hz, 4H, 4 x *H*-2), 5.02 (dd, *J* = 3.4 Hz, *J* = 10.4 Hz, 4H, 4 x *H*-3), 4.95 (d, *J* = 12.5 Hz, 4H, 4 x CH₂a), 4.80 (d, *J* = 12.5 Hz, 4H, 4 x CH₂b), 4.68 (d, *J* = 8.0 Hz, 4H, 4 x *H*-1), 4.58–4.53 (m, 20H, 8 x CH₂ propargyl, 2 x CH₂ TEG), 4.19–4.15 (m, 8H, 4 x *H*-6a,b), 3.99–3.94 (m, 4H, 4 x *H*-5), 3.90–3.86 (m, 20H, 10 x CH₂ TEG), 3.62–3.58 (m, 32H, 16 x CH₂ TEG), 3.46 (s, 8H, 4 x CH₂ pentaerythritol), 2.15, 2.06, 1.98, 1.97 (4 x s, 48H, 16 x CH₃ acetyl). ¹³C NMR (100 MHz, CDCl₃) δ 170.4, 170.2, 170.1, 169.5 (16C, 16 x CO acetyl), 145.0, 143.9 (8C, *Cq* triazole), 124.0, 123.7 (8C, CH triazole), 100.3 (4C, 4 x C-1), 70.9, 70.8, 68.8, 67.1 (16C, 4 x skeleton carbons), 70.5, 70.4, 69.4, 69.3, 69.1 (28C, 24 x OCH₂ TEG, 4 x CH₂ pentaerythritol), 64.9 (4C, 4 x CH₂ propargyl), 62.8 (4C, 4 x C-6), 61.3 (4C, 4 x CH₂ propargyl), 50.3, 50.1 (8C, 8 x NCH₂ TEG), 45.3 (1C, *Cq* pentaerythritol), 20.7, 20.6, 20.5 (16C, 16 x CH₃ acetyl). MALDI-TOF: *m/z* calcd for C₁₁₇H₁₇₂N₂₄NaO₅₆: 2832.12 [M + Na]⁺; found: 2832.15.

Compound 30

Compound **29** (78 mg, 0.28 mmol) was deacetylated according to general method **C**. The crude product was purified by flash column chromatography (CH₃CN/H₂O 7:3) to give compound **30** (44 mg, 73%) as a colourless syrup. R_f 0.15 (CH₃CN/H₂O 7:3), [α]²⁴_D -2.5 (*c* 0.12, MeOH). ¹H NMR (400 MHz, D₂O) δ 7.95, 7.89 (2 x s, 8H, 8 x CH triazole), 4.85–4.66 (m, 16H, 8 x CH₂ propargyl), 4.45–4.44 (m, 16H, 4 x NCH₂ TEG), 4.32 (d, *J* = 7.6 Hz, 4H, 4 x *H*-1), 3.80–3.77 (m, 20H, 4 x C-4, 8 x CH₂ TEG), 3.68–3.59 (m, 8H, 4 x *H*-6a,b), 3.55–3.53 (m, 4H, 4 x *H*-5), 3.47 (dd, *J* = 3.3 Hz, *J* = 9.9 Hz, 4H, 4 x *H*-3), 3.43–3.37 (m, 36H, 4 x *H*-2, 16 x CH₂ TEG), 3.30–3.27 (m, 8H, 4 x CH₂ pentaerythritol). ¹³C NMR (100 MHz, D₂O) δ

125.7 (8C, CH triazole), 103.1 (4C, 4 x C-1), 76.2 (4C, 4 x C-5), 73.9 (4C, 4 x C-3), 71.7 (4C, 4 x C-2), 70.7, 70.6, 70.5, 69.7 (24C, 24 x OCH₂ TEG), 69.6 (4C, 4 x C-4), 69.3 (4C, 4 x CH₂ pentaerythritol), 62.7 (8C, 8 x CH₂ propargyl), 62.0 (4C, 4 x C-6), 51.0 (8C, 8 x NCH₂ TEG), 45.8 (1C, C_q pentaerythritol). MALDI-TOF: *m/z* calcd for C₈₅H₁₄₀N₂₄NaO₄₀: 2159.96 [M + Na]⁺; found: 2159.95.

Compound 32

Azide compound **31** (96 mg, 0.14 mmol) and alkyne **21** (315 mg, 0.82 mmol) were reacted in CH₃CN according to general method **B**. The crude product was purified by flash column chromatography (CH₂Cl₂/MeOH 95:5) to give compound **32** (150 mg, 51%) as a colourless syrup. R_f 0.27 (CH₂Cl₂/MeOH 95:5), [α]²⁴_D -16.1 (*c* 0.23, CHCl₃). ¹H NMR (400 MHz, CDCl₃) δ 7.59, 7.52 (2 x s, 8H, 8 x CH triazole), 5.41 (d, *J* = 2.1 Hz, 4H, 4 x H-4), 5.18 (dd, *J* = 8.1 Hz, *J* = 10.2 Hz, 4H, 4 x H-2), 5.04 (dd, *J* = 3.2 Hz, *J* = 10.4 Hz, 4H, 4 x H-3), 4.95-4.73 (m, 24H, 12 x CH₂), 4.65 (d, *J* = 7.9 Hz, 4H, 4 x H-1), 4.51 (s, 8H, 4 x CH₂), 4.21-4.11 (m, 8H, 4 x H-6a,b), 4.01-3.97 (m, 4H, 4 x H-5), 3.37 (s, 8H, 4 x CH₂ pentaerythritol), 2.14, 2.05, 1.99, 1.98 (4 x s, 48H, 16 x CH₃ acetyl). ¹³C NMR (100 MHz, CDCl₃) δ 170.4, 170.2, 170.0, 169.6 (16C, 16 x CO acetyl), 145.4, 144.2 (8C, 8 x C_q triazole), 124.0, 123.7 (8C, 8 x CH triazole), 100.3 (4C, 4 x C-1), 70.8, 70.7, 68.7, 67.1 (16C, 4 x skeleton carbons), 68.9 (4C, 4 x CH₂ pentaerythritol), 64.6 (4C, 4 x CH₂ propargyl), 62.6 (4C, 4 x C-6), 61.2 (4C, 4 x CH₂ propargyl), 49.5, 49.3 (8C, 8 x NCH₂ ethylene glycol), 45.1 (1C, C_q pentaerythritol), 20.8, 20.7, 20.6, 20.5 (16C, 16 x CH₃ acetyl). MALDI-TOF: *m/z* calcd for C₉₃H₁₂₄N₂₄NaO₄₄: 2303.81 [M + Na]⁺; found: 2304.49.

Compound 33

Compound **32** (148 mg, 0.06 mmol) was deacetylated according to general method **C**. The crude product was purified by flash column chromatography (CH₃CN/H₂O 7:3) to give compound **33** (70 mg, 66%) as a colourless syrup. R_f 0.20 (CH₃CN/H₂O 7:3), [α]²⁴_D + 44.8 (*c* 0.31, H₂O). ¹H NMR (400 MHz, D₂O) δ 7.94 (s, 8H, 8 x CH triazole), 4.97 (s, 16H, 8 x NCH₂ ethylene glycol), 4.93-4.78 (m, 16H, 8 x CH₂ propargyl), 4.44 (d, *J* = 7.6 Hz, 4H, 4 x H-1), 3.94 (d, *J* = 2.8 Hz, 4H, 4 x H-4), 3.83-3.74 (m, 8H, 4 x H-6a,b), 3.71-3.68 (m, 4H, 4 x H-5), 3.65 (dd, *J* = 3.0 Hz, *J* = 9.8 Hz, 4H, 4 x H-3), 3.57-3.53 (m, 4H, 4 x H-2), 3.34 (s, 8H, 4 x CH₂ pentaerythritol). ¹³C NMR (100 MHz, D₂O) δ 125.4 (8C, 8 x CH triazole), 102.9 (4C, 4 x C-1), 76.2 (4C, 4 x C-5), 73.7 (4C, 4 x C-3), 71.6 (4C, 4 x C-2), 69.6 (4C, 4 x C-4), 69.2 (4C, 4 x CH₂ pentaerythritol), 62.5 (8C, 8 x CH₂ propargyl), 61.9 (4C, 4 x C-6), 50.9 (8C, 8 x

NCH₂ ethylene glycol), 45.5 (1C, *C_q* pentaerythritol). MALDI-TOF: *m/z* calcd for C₆₁H₉₂N₂₄NaO₂₈: 1631.64 [M + Na]⁺; found: 1631.59.

Compound 38

Azide **37** (1.6g, 1.5 mmol, 1.0 equiv.) and alkyne **19** (2.0 g, 6.0 mmol, 4.0 equiv.) were reacted in CH₃CN according to general method **B**. The solution was evaporated and crude product was purified by flash column chromatography (CH₂Cl₂/MeOH 97:3) to give compound **38** (3.0 g, 97%) as whitish-yellow crystal. R_f 0.38 (CH₂Cl₂/MeOH 95:5), [α]²⁴_D -68.18 (c 0.22, CHCl₃). ¹H NMR (360 MHz, CDCl₃) δ 7.73 (s, 6H, 6 x *CH* triazole), 5.37-4.10 (m, 15H, 3 x *H*-1, *H*-2, *H*-3, *H*-4), 4.82 (d, *J* = 12.4 Hz, 3H), 4.66 (d, *J* = 12.4 Hz, 3H), 4.60-4.53 (m, 15H), 4.25-4.19 (m, 3H), 3.89 (t, *J* = 5.2 Hz, 14H), 3.75 (s, 7H), 3.60 (d, *J* = 4.0 Hz, 20H, 10 x *CH*₂), 2.14, 2.04, 1.9 (s, 27H, 9 x *CH*₃ acetyl), 2.10-2.01 (m, 2H), 1.40 (s, 9H, 3 x *CH*₃ Boc), 1.1 (d, *J* = 6.4 Hz, 9H, 3 x *CH*₃). ¹³C NMR (91 MHz, CDCl₃) δ 196.7 (1C, CO Boc) 170.4, 170.2, 169.8 (9C, 9 x CO acetyl), 144.3 (6C, 6 x *C_q* triazol) 123.8, (6C, 6 x *CH* triazol), 95.4 (3C, *C*-1), 70.9, 67.8, 67.7, 64.5 (12C, 3 x *C*-2, *C*-3, *C*-4, *C*-5), 70.3, 70.2 (18C, 18 x OCH₂ TEG), 69.2 (6C, 6 x OCH₂ propargyl), 64.5 (1C, *C_q* scaffold), 61.0 (3C, 3 x OCH₂ scaffold), 50.0, 50.1 (6C, 6 x NCH₂ TEG), 28.2 (3C, 3 x *CH*₃ Boc), 20.6, 20.5 (9C, 9 x *CH*₃ acetyl), 15.7 (3C, 3 x *C*-6). HRMS (ESI): *m/z* calcd for C₈₇H₁₃₃N₁₉NaO₃₈: 2075.8990 [M + Na]⁺; found: 2075.9005.

Compound 39

Azide **37** (1.4 g, 1.3 mmol, 1.0 equiv.) and alkyne **21** (2.0 g, 5.0 mmol, 4.0 equiv.) were reacted in CH₃CN according to general method **B**. The solution was evaporated and crude product was purified by flash column chromatography (CH₂Cl₂/MeOH 97:3) to give compound **39** (960 mg, 56%) as yellow-whitish crystal. R_f 0.42 (CH₂Cl₂/MeOH 95:5), [α]²⁴_D -19.2 (c 0.12, CHCl₃). ¹H NMR (400 MHz, CDCl₃) δ 7.73 (s, 6H, 6 x *CH* triazole), 5.40 (dd, *J* = 3.5, 1.2 Hz, 3H, 3 x *H*-4), 5.21 (dd, *J* = 10.5, 8.0 Hz, 3H, 3 x *H*-2), 5.02 (dd, *J* = 10.4, 3.4 Hz, 3H, 3 x *H*-3), 4.99 – 4.78 (m, 6H, 3 x OCH₂ propargyl), 4.68 (d, *J* = 8.0 Hz, 3H, 3 x *H*-1), 4.60 (s, 6H, 3 x OCH₂ scaffold), 4.58 – 4.49 (m, 12H, 6 x NCH₂), 4.16 (dd, *J* = 6.7, 3.3 Hz, 6H, 3 x *CH*_{2a,b}), 3.97 (td, *J* = 6.6, 1.2 Hz, 3H, 3 x *H*-5), 3.92 – 3.82 (m, 12H, 6 x OCH₂), 3.75 (s, 6H, 3 x OCH₂ propargyl), 3.64 – 3.52 (m, 24H, 12 x *CH*₂ TEG), 2.15, 2.06, 1.98 (36H, 12 x *CH*₃ acetyl), 1.39 (s, 9H, 3 x *CH*₃ Boc). ¹³C NMR (101 MHz, CDCl₃) δ 170.4, 170.2, 170.0, 169.5 (12C, 12 x CO acetyl), 154.7 (1C, CO Boc), 144.6, 143.9 (6C, 6 x *C_q* triazole), 124.0, 123.8 (6C, 6 x *CH* triazole), 100.3 (3C, 3 x *C*-1), 70.8, 70.8, 68.8, 67.1, 61.2

(15C, 3 x C-2, C-3, C-4, C-5, C-6), 70.5, 70.4, 69.3 (24C, 18 x CH₂ TEG, 6 x OCH₂ propargyl), 64.7 (1C, C_q scaffold), 62.8, (3C, 3 x OCH₂ scaffold), 58.5 (1C, C_q Boc), 50.3, 50.2 (6C, 6 x NCH₂ TEG), 28.4 (3C, 3 x CH₃ Boc), 20.7, 20.7, 20.6, 20.5 (12C, 12 x CH₃ acetyl). HRMS (ESI): *m/z* calcd for C₉₃H₁₃₉N₁₉NaO₄₄: 2249.91255 [M + Na]⁺; found: 2249.9148.

Compound 40

To the stirred solution of compound **38** (3g, 1.46 mmol) in CH₂Cl₂ (3mL), 1ml of TFA:DCM 1:1 solution was added slowly and the mixture was allowed to stir at room temperature for 2-3 hours. Triethylamine was added dropwise to neutralize the reaction mixture. Solution was diluted with DCM (100mL) and extracted two times with saturated NaCl solution (50mL), then washed with water (100mL). The organic phase was dried over MgSO₄, filtered and evaporated. The obtained crude product was purified by flash column chromatography (CH₂Cl₂/MeOH 95:5) to give compound **40** (1.8g, 64%) as yellow-whitish crystal. R_f 0.36 (CH₂Cl₂/MeOH 9:1), [α]²⁴_D -14.29 (c 0.14, CHCl₃). ¹H NMR (360 MHz, CDCl₃) δ 7.8-7.3 (s, 6H, 6 x CH triazol), 5.2, 4.8, 4.2 (15H, 3 x H-1, H-2, H-3, H-4, H-5), 4.6, 3.9 (s, 12H, 6 x CH₂ propargyl), 3.6 (s, 24H, 6 x NCH₂CH₂TEG), 3.5 (s, 30H, 3 x CH₂ Tris, 12 x CH₂ TEG), 2.2 – 1.9 (m, 27H, 9 x CH₃ acetyl), 1.2 (t, J = 24.7 Hz, 9H, 3 x CH₃). ¹³C NMR (91 MHz, CDCl₃) δ 170.6 (9C, 9 x CO acetyl), 143.8 (6C, 6 x C_q triazol), 121.3 (6C, 6 x CH triazol), 95.6, 71.1, 67.9, 67.9, 64.6 (15C, 3 x C-1, C-2, C-3, C-4, C-5), 70.3, 70.2 (18C, 18 x CH₂ TEG), 69.3, 69.2 (6C, 6 x OCH₂ propargyl), 61.1 (3C, 3 x OCH₂ scaffold), 50.2 (6C, 6 x NCH₂ TEG), 20.6 (9C, 9 x CH₃ acetyl), 15.8 (3C, 3 x CH₃). HRMS (ESI): *m/z* calcd for C₈₂H₁₂₅N₁₉NaO₃₆: 1975.8466 [M + Na]⁺; found: 1975.8420.

Compound 41

To the stirred solution of compound **39** (960 mg, 0.43 mmol) in CH₂Cl₂ (3 ml), 2 ml of TFA/DCM 1:1 solution was added slowly and the mixture was allowed to stir at room temperature for 2-3 hours. Triethylamine was added dropwise to neutralize the reaction mixture. Solution was diluted with DCM (100mL) and extracted two times with saturated NaCl solution (50mL), then washed with water (100 mL). The organic phase was dried over MgSO₄, filtered and evaporated. The obtained crude product was purified by flash column chromatography (CH₂Cl₂/MeOH 95:5) to give compound **41** (500 mg, 55%) as yellow-whitish crystal. R_f 0.3 (CH₂Cl₂/MeOH 9:1), [α]²⁴_D -21 (c 0.1, CHCl₃). ¹H NMR (400 MHz, CDCl₃) δ 7.73 (d, J = 8.4 Hz, 6H, 6 x CH triazole), 5.40 (dd, J = 3.4, 1.1 Hz, 3H, 3 x H-4),

5.20 (dd, $J = 10.4, 7.9$ Hz, 3H, 3 x $H-2$), 5.02 (dd, $J = 10.5, 3.4$ Hz, 3H, 3 x $H-3$), 4.87 (m, 6H, 3 x OCH_2 propargyl), 4.67 (d, $J = 7.9$ Hz, 3H, 3 x $H-1$), 4.58 (s, 6H, 3 x OCH_2 scaffold), 4.54 (12H, 6 x NCH_2), 4.16 (m, 6H, 3 x $CH_{2a,b}$), 4.01 – 3.91 (m, 3H, 3 x $H-5$), 3.87 (q, $J = 4.9$ Hz, 12H, 6 x OCH_2), 3.65 – 3.53 (m, 24H, 12 x CH_2 TEG), 3.47 (s, 6H, 3 x OCH_2 propargyl), 2.15, 2.06, 1.98, 1.97 (36H, 12 x CH_3 acetyl). ^{13}C NMR (101 MHz, $CDCl_3$) δ 170.4, 170.2, 170.1, 169.5 (12C, 12 x CO acetyl), 144.6, 143.9 (6C, 6 x C_q triazole), 124.0, 123.8 (6C, 6 x CH triazole), 100.3 (3C, x $C-1$), 70.8, 70.8, 68.7, 67.0, 61.2 (15C, 3 x $C-2, C-3, C-4, C-5, C-6$), 70.5, 70.4, 69.4 (24C, 18 x CH_2 TEG, 6 x OCH_2 propargyl), 64.8 (1C, C_q scaffold), 62.8 (3C, 3 x OCH_2 scaffold), 50.3, 50.1 (6C, 6 x NCH_2 TEG), 20.8, 20.7, 20.7, 20.6 (12C, 12 x CH_3 acetyl). HRMS (ESI): m/z calcd for $C_{88}H_{131}N_{19}NaO_{42}$: 2148.8597 [$M + Na$] $^+$; found: 2148.8591.

Compound 42

To a stirred solution of compound **40** (1g, 0.5 mmol, 1.0 equiv.) and imidazole sulfonylazide hydrochloride (161 mg, 1.5 mmol, 1.5 equiv.) in pyridine (3 mL), triethylamine (144 μ L, 2.0 equiv.) and $CuSO_4$ (25.6mg, 0.2 equiv.) were added and allowed to stir overnight at room temperature. The reaction mixture was evaporated and the residue was purified by flash chromatography ($CH_2Cl_2/MeOH$ 95:5) to give compound **42** (648 mg, 64%) as a yellowish syrup. R_f 0.9 ($CH_2Cl_2/MeOH$ 85:15), $[\alpha]^{24}_D$ -57.1 (c 0.14, MeOH). 1H NMR (400 MHz, MeOD) δ 8.05 (d, $J = 20.2$ Hz, 6H, 6 x CH triazol), 5.51-5.05 (12H, $H-1, H-2, H-3, H-4$), 4.84 (s, 6H, 3 x CH_2 propargyl), 4.79-4.67 (3H, 3 x $H-5$), 4.59 (6H, 3 x CH_2 propargyl), 3.9-3.6 (48H, 24 x CH_2 TEG), 3.37 (s, 6H, 3 x CH_2 Tris), 2.16-1.97 (d, $J = 13.3$ Hz, 27H, 9 x CH_3 Acetyl), 1.12 (d, $J = 6.5$ Hz, 9H, 3 x CH_3). ^{13}C NMR (101 MHz, MeOD) δ 170.9, 170.5, 170.2 (9C, 9 x CO acetyl), 143.5 (6C, 6 x C_q triazol), 124.8 (6C, 6 x CH triazol), 95.4 (3C, $C-1$), 71.1, 67.9, 64.6 (12C, 3 x $C-2, C-3, C-4, C-5$), 70.1, 68.9 (18C, 18 x CH_2 TEG), 69.6, 64.1 (6C, 6 x OCH_2 propargyl), 65.6 (1C, C_q scaffold), 60.3 (3C, OCH_2 scaffold), 50.0 (6C, 6 x NCH_2 TEG), 19.3, 19.2 (9C, 9 x CH_3 acetyl), 14.8 (3C, 3 x CH_3). HRMS (ESI): m/z calcd for $C_{82}H_{123}N_{21}NaO_{36}$: 2000.8371 [$M + Na$] $^+$; found: 2000.8332.

Compound 43

To a stirred solution of compound **41** (500 mg, 0.235 mmol, 1.0 equiv.) and imidazole sulfonylazide hydrochloride (98.54 mg, 0.47 mmol, 2.0 equiv.) in pyridine (3 mL), triethylamine (66 μ L, 2.0 equiv.) and $CuSO_4$ (12 mg, 0.2 equiv.) were added and allowed to stir overnight at room temperature. The reaction mixture was evaporated and the residue was

purified by flash chromatography (CH₂Cl₂/MeOH 9:1) to give compound **43** (268 mg, 53%) as a yellowish powder. R_f 0.67 (CH₂Cl₂/MeOH 9:1), [α]²⁴_D -12.5 (c 0.12, CHCl₃). ¹H NMR (400 MHz, CDCl₃) δ 7.73 (d, *J* = 9.6 Hz, 6H, 6 x CH triazole), 5.40 (d, *J* = 3.4 Hz, 3H, 3 x H-4), 5.21 (dd, *J* = 10.4, 7.9 Hz, 3H, 3 x H-2), 5.02 (dd, *J* = 10.5, 3.4 Hz, 3H, 3 x H-3), 4.88 (m, 6H, 3 x OCH₂ propargyl), 4.68 (m, 9H, 3 x H-1, 3 x OCH₂ propargyl), 4.62 (s, 6H, 3 x OCH₂ scaffold), 4.54 (q, *J* = 4.7 Hz, 12H, 6 x NCH₂), 4.16 (m, 6H, 3 x CH_{2a,b}), 3.96 (t, *J* = 6.7 Hz, 3H, 3 x H-5), 3.88 (t, *J* = 5.1 Hz, 12H, 6 x OCH₂), 3.60 (dt, *J* = 9.8, 4.6 Hz, 24H, 12 x CH₂ TEG), 2.15, 2.06, 1.98 (36H, 12 x CH₃ acetyl). ¹³C NMR (101 MHz, CDCl₃) δ 170.4, 170.2, 170.1, 169.5 (12C, 12 x CO acetyl), 144.4, 143.9 (6C, 6 x C_q triazole), 129.7, 124.0, 123.9 (6C, 6 x CH triazole), 100.3 (3C, x C-1), 70.8, 70.8, 68.7, 67.0, 61.2 (15C, 3 x C-2, C-3, C-4, C-5, C-6), 70.5, 70.4, 69.4, (24C, 18 x CH₂ TEG, 6 x OCH₂ propargyl), 70.0 (1C, C_q scaffold), 64.9, 62.8 (3C, 3 x OCH₂ scaffold), 50.3, 50.2 (6C, 6 x NCH₂ TEG), 20.8, 20.7, 20.6 (12C, 4 x CH₃ acetyl). HRMS (ESI): *m/z* calcd for C₈₈H₁₂₉N₂₁NaO₄₂: 2174.8502 [M + Na]⁺; found: 2174.8486.

Compound 44

Compound **44** was prepared from compound **38** (100 mg, 0.05 mmol) according to **general method C**. The solution was evaporated and crude product was purified by flash column chromatography (CH₃CN/H₂O 7:3) to give compound **44** (73 mg, 90%) as yellow-whitish crystal. R_f 0.37 (CH₃CN/H₂O 8:2), [α]²⁴_D -27.3 (c 0.22, MeOH). ¹H NMR (360 MHz, D₂O) δ 8.03 (s, 3H, 3 x CH), 7.98 (s, 3H, 3 x CH), 4.95 (bs, 2H), 4.84–4.73 (m, 8H), 4.73–4.63 (m, 8H, 4 x CH₂), 4.62–4.74 (m, 12H, 3 x H-2, H-3, H-4, H-5), 3.89 (d, *J* = 6.4 Hz, 18H), 3.82–3.69 (m, 12H), 3.52 (dt, *J* = 24.8, 5.0 Hz, 31H), 1.26 (s, 9H, 3 x CH₃ Boc), 1.07 (d, *J* = 6.5 Hz, 9H, 3 x CH₃). ¹³C NMR (91 MHz, D₂O) δ 197.2 (1C, CO Boc), 143.8 (6C, 6 x C_q triazol), 125.1 (6C, 6 x CH triazol), 98.5 (3C, C-1), 71.7, 69.5, 67.9, 66.7 (12C, 3 x C-2, C-3, C-4, C-5), 69.6, 69.4 (18C, 18 x OCH₂), 68.6 (6C, 6 x OCH₂ propargyl) 63.4 (1C, C_q scaffold), 60.5 (3C, 6 x CH₂ scaffold), 49.9 (6C, 6 x NCH₂), 27.5 (3C, 3 x CH₃ Boc), 15.2 (3C, 3 x C-6). HRMS (ESI): *m/z* calcd for C₆₉H₁₁₅N₁₉NaO₂₉: 1697.8039 [M + Na]⁺; found: 1697.8029.

Compound 45

Compound **45** was prepared from compound **41** (50 mg, 0.235mmol) according to **general method C**. The solution was concentrated to give compound **45** (38 mg, 99%) as yellow syrup. R_f 0.1 (CH₃CN/H₂O 6:4), [α]²⁴_D -6.25 (c 0.08, MeOH). ¹H NMR (400 MHz, MeOD) δ 8.05 (d, *J* = 11.6 Hz, 6H, 6 x CH triazole), 4.98 (d, *J* = 12.2 Hz, 3H, 3 x H-4), 4.76 (d, *J* =

12.3 Hz, 3H, 3 x *H*-2), 4.58 (dt, *J* = 9.8, 2.9 Hz, 18H), 4.38 (d, *J* = 7.5 Hz, 3H, 3 x *H*-3), 3.98 – 3.85 (m, 18H), 3.79 (qd, *J* = 11.3, 6.1 Hz, 6H, 3 x *CH*_{2a,b}), 3.68 – 3.45 (m, 42H), 3.37 (s, 3H, 3 x *H*-1), 1.32 (m, 3H, 3 x *H*-5). ¹³C NMR (101 MHz, MeOD) δ 143.8 (6C, 6 x *C*_q triazole), 124.6 (6C, 6 x CH triazole), 102.9 (3C, 3 x *C*-1), 75.4, 73.5, 71.1, 68.9, 61.2, (15C, 3 x *C*-2, *C*-3, *C*-4, *C*-5, *C*-6), 70.0, 70.0, 68.9 (24C, 18 x *CH*₂ TEG, 6 x *OCH*₂ propargyl), 63.9 (1C, *C*_q scaffold), 61.7 (3C 3 x *OCH*₂ scaffold), 50.0 (6C, 6 x *NCH*₂ TEG). HRMS (ESI): *m/z* calcd for C₆₄H₁₀₇N₁₉O₃₀: 1622.7509 [M + H]⁺; found: 1622.7504.

Compound 48

To a stirred solution of ciprofloxacin (100 mg, 0.3 mmol) in abs. DMF (3 mL), NaHCO₃ (25 mg, 0.3 mmol, 1.0 equiv.) and 1-bromo-3,6,9,12-tetraoxapentadec-14-yne (89 mg, 1.0 equiv.) were added under vigorous stirring. The mixture was allowed to react at 80°C overnight. After cooling and evaporation, the residue was purified by flash column chromatography (CH₂Cl₂/MeOH 97:3) to give compound **48** (141 mg, 86%) as a yellowish syrup. *R*_f 0.78 (CH₂Cl₂/MeOH 9:1). ¹H NMR (400 MHz, MeOD) δ 8.63, 7.63, 7.48 (3H, 3 x *CH* aromatic), 5.51 (s, 1H, *CH* cyclopropane), 4.91 (m, 4H, 2 x *CH*₂), 4.19 (d, *J* = 2.4 Hz, 2H, *CH*₂CCH), 3.74, 3.71 – 3.64 (m, 12H, 6 x *CH*₂ TEG), 3.42 (t, *J* = 4.8 Hz, 4H, 2 x *CH*₂ piperazine ring), 2.86 (4H, 2 x *CH*₂ piperazine ring), 2.77 (1H, *CH*₂CCH propargyl), 1.47 – 1.38, 1.27 – 1.14 (4H, 2 x *CH*₂ cyclopropane). ¹³C NMR (101 MHz, MeOD) δ 177.2, 168.5, 155.4, 152.9, 148.3, 146.30, 146.2, 139.9, 119.6, 107.3, 70.9, 70.8, 70.7, 69.5, 68.8, 58.4, 57.4, 53.6, 49.7, 49.7, 36.3, 7.9. HRMS (ESI): *m/z* calcd for C₂₈H₃₆FN₃NaO₇: 568.2435 [M + Na]⁺; found: 568.2429.

Compound 49

To a stirred solution of moxifloxacin (100 mg, 0.25 mmol) in abs. DMF (3 mL) NaHCO₃ (21 mg, 0.25mmol, 1.0 equiv.) and 1-bromo-3,6,9,12-tetraoxapentadec-14-yne (73.8 mg, 1.0 equiv.) were added under vigorous stirring. The mixture was allowed to react at 80°C overnight. After cooling and evaporation, the residue was purified by flash column chromatography (CH₂Cl₂/MeOH 95:5) to give compound **49** (113 mg, 73.6%) as a yellowish syrup, *R*_f: 0.54 (CH₂Cl₂/MeOH 9:1). ¹H NMR (360 MHz, MeOD) δ 8.79, 7.98, 7.67 (3H, 3 x *CH*), 4.18 (4H, *CH*₂, *CH*₂CCH), 3.93 – 3.34 (m, 16H, 8 x *CH*₂ TEG), 3.00, 2.93 – 2.70 (m, 8H, 4 x *CH*₂), 2.54 (m, 2H, 2 x *CH*), 2.24 – 1.97 (m, 1H, *CH*₂CCH), 1.93 – 1.45, 1.10 – 0.69 (4H, 2 x *CH*₂ cyclopropane). 1.44 – 1.09 (m, 3H, *CH*₃). ¹³C NMR (91 MHz, MeOD) δ 177.2,

168.5, 155.4, 152.9, 148.3, 146.30, 146.2, 139.9, 119.6, 107.3, 74.7, 71.3, 71.2, 70.4, 70.3, 68.9, 62.0, 60.8, 57.9, 55.2, 54.2, 52.0, 50.4, 42.6, 37.4, 35.9, 30.2, 22.4, 9.0, 8.9. HRMS (ESI): m/z calcd for $C_{32}H_{42}FN_3NaO_8$: 638.2854 $[M + Na]^+$; found: 638.2848.

Compound 54

Compound **42** (100 mg, 0.05 mmol) and **46** (27.7 mg, 0.075 mmol, 1.5 equiv.) were reacted according to **general method A**. The crude product was purified by flash column chromatography (CH_3CN/H_2O 9:1) to give compound **50** (72 mg, 61%) as yellow powder. R_f 0.1 (CH_3CN/H_2O 95:5), $[\alpha]_D^{24}$ -42.3 (c 0.13, MeOH). The obtained product **50** (70 mg, 0.03 mmol) was directly deacetylated according to **general method C**. The crude product was purified by Sephadex column (H_2O) to give compound **54** (53 mg, 90%) as yellow powder. R_f 0.25 (CH_3CN/H_2O 7:3), $[\alpha]_D^{24}$ -42 (c 0.15, H_2O). 1H NMR (500 MHz, MeOD) δ 7.35 (10H, 3 x *CH* aromatic, 7 x *CH* triazole), 4.16 3.86, 3.18, 2.85, 2.61 (77H, 38 x CH_2 , *CH* cyclopropane), 3.04, 2.95, 2.90, 1.93, 1.61 (15H, 3 x *H*-1, *H*-2, *H*-3, *H*-4, *H*-5), 1.45-1.34 (9H, 3 x CH_3), 1.26, 0.93 (4H, 2 x CH_2 cyclopropane). ^{13}C NMR (126 MHz, MeOD) δ 142.5, 123.2, 97.3, 70.7, 68.5, 67.7, 67.4, 67.1, 65.0, 62.5, 61.41, 58.8, 48.5, 30.1, 27.8, 20.8, 13.8, 11.5. HRMS (ESI): m/z calcd for $C_{84}H_{125}FN_{24}NaO_{30}$: 1991.8875 $[M + Na]^+$; found: 1991.8870.

Compound 55

Compound **42** (100 mg, 0.05 mmol) and **47** (33 mg, 0.075 mmol, 1.5 equiv.) were reacted according to **general method A**. The crude product was purified by flash column chromatography (CH_3CN/H_2O 9:1) to give compound (95 mg, 78%) as yellow-whittish powder. R_f 0.19 (CH_3CN/H_2O 95:5), $[\alpha]_D^{24}$ -5.0 (c 0.14, H_2O). The obtained product **51** (82 mg, 0.034 mmol) was directly deacetylated according to **general method C**. The crude product was purified by sephadex column (H_2O) to give compound **55** (68 mg, 90 %) as yellow-orange powder. R_f 0.33 (CH_3CN/H_2O 7:3), $[\alpha]_D^{24}$ -14.2 (c 0.19, MeOH). 1H NMR (500 MHz, MeOD) δ 8.59 (s, 2H, 2 x *CH* aromatic), 8.31 – 7.64 (m, 7H, 7 x *CH* triazole), 4.89, 4.57, 4.00, 3.69, 3.55 (78H, 39 x CH_2), 3.88, (2H, 2 x *CH*), 3.77 (s, 1H, *CH* cyclopropane), 3.88, 3.62, 3.43, 3.37, 3.33 (15H, 3 x *H*-1, *H*-2, *H*-3, *H*-4, *H*-5), 1.31 (s, 3H, OCH_3), 1.20 (t, $J = 6.9$ Hz, 9H, 3 x CH_3), 1.63, 0.91 (4H, 2 x CH_2 cyclopropane). ^{13}C NMR (126 MHz, MeOD) δ 169.0, 144.2, 143.8, 124.6, 98.7, 87.5, 82.4, 72.2, 70.2, 70.0, 69.9, 69.6, 69.2, 68.9, 68.5, 67.6, 66.5, 64.0, 60.3, 56.9, 50.4, 50.0, 48.5, 29.4, 17.1, 15.4. HRMS (ESI): m/z calcd for $C_{88}H_{131}FN_{24}NaO_{31}$: 2061.9294 $[M + Na]^+$; found: 2061.9288.

Compound 56

Compound **42** (100 mg, 0.05 mmol) and **48** (41 mg, 0.075 mmol, 1.5 equiv.) were reacted according to **general method A**. The crude product was purified by flash column chromatography (CH₃CN/H₂O 9:1) to give compound **52** (34 mg, 27%) as yellow powder. R_f 0.1 (CH₃CN/H₂O 95:5), [α]²⁴_D -9.2 (c 0.12, H₂O). The obtained product **52** (25 mg, 0.01 mmol) was directly deacetylated according to **general method C**. The crude product was purified by sephadex column (H₂O) to give compound **56** (20 mg, 92 %) as yellow powder. R_f 0.1 (CH₃CN/H₂O 7:3), [α]²⁴_D -10.6 (c 0.17, MeOH). ¹H NMR (500 MHz, MeOD) δ 8.21 – 7.88 (m, 10H, 3 x CH aromatic, 7 x CH triazole), 4.83, 4.55, 3.61, 3.35, 3.31 (92H, 46 x CH₂), 3.94 (d, *J* = 3.6 Hz, 1H, CH cyclopropane), 4.04, 3.87, 3.74, 3.65, 3.54 (15H, 3 x H-1, H-2, H-3, H-4, H-5), 1.33 (m, 9H, 3 x CH₃), 1.20, 0.91 (4H, 2 x CH₂ cyclopropane). ¹³C NMR (126 MHz, MeOD) δ 168.7, 144.2, 132.4, 131.9, 127.7, 122.6, 97.3, 70.7, 67.7, 67.4, 67.1, 65.0, 50.1, 48.6, 34.4, 30.2, 28.0, 27.9, 27.6. HRMS (ESI): *m/z* calcd for C₉₂H₁₄₁FN₂₄NaO₃₄: 2167.9924 [M + Na]⁺; found: 2167.9918.

Compound 57

Compound **42** (100 mg, 0.05 mmol) and **49** (46.2 mg, 0.075 mmol, 1.5 equiv.) were reacted according to **general method B**. The crude product was purified by flash column chromatography (CH₃CN/H₂O 9:1) to give compound **53** (33mg, 18%) as yellow powder. R_f 0.1 (CH₃CN/H₂O 9:1), [α]²⁴_D -20.7 (c 0.15, MeOH). The obtained product **53** (30 mg, 0.011 mmol) was directly deacetylated according to **general method C**. The crude product was purified by sephadex column to give compound **57** (25 mg, 98 %) as yellow-orange powder. R_f 0.1 (CH₃CN/H₂O 7:3), [α]²⁴_D -25.0 (c 0.12, MeOH). ¹H NMR (500 MHz, MeOD) δ 8.69 (s, 2H, 2 x CH aromatic), 8.36 – 7.81 (m, 7H, 7 x CH triazole), 4.90, 4.61, 4.14, 3.80, 3.59 (94H, 47x CH₂), 3.72, 3.70 (2H, 2 x CH), 3.65 (1H, CH cyclopropane), 3.92, 3.62, 3.40, 3.36, 3.31 (15H, 3 x H-1, H-2, H-3, H-4, H-5), 1.48 – 1.39 (m, 3H, OCH₃), 1.34 (s, 9H, 3 x CH₃), 1.23, 0.94 (4H, 2 x CH₂ cyclopropane). ¹³C NMR (126 MHz, MeOD) δ 172.5, 169.2, 145.7, 121.9, 104.4, 96.5, 81.1, 80.9, 70.0, 69.2, 68.6, 67.0, 66.7, 66.3, 64.2, 60.7, 58.1, 47.8, 46.4, 27.3, 27.1, 13.1, 10.8. HRMS (ESI): *m/z* calcd for C₉₆H₁₄₇FN₂₄NaO₃₅: 2239.0376 [M + Na]⁺; found: 2239.0344

Compound 60

Compound **43** (300 mg, 0.14 mmol, 1.0 equiv.) and **48** (91 mg, 0.16 mmol, 1.2 equiv) were reacted according to **general method A**. The reaction mixture was evaporated, and the crude product was purified by flash column chromatography (CH₃CN/H₂O 95:5) to give compound **58** (95 mg, 25 %) as yellow powder. R_f 0.22 (CH₃CN/H₂O 9:1), [α]²⁴_D -3.75 (c 0.08, MeOH). The obtained product **58** (90 mg, 0.033 mmol) was directly deacetylated according to **general method C**. The crude product was purified by Sephadex column (H₂O) to give compound **60** (62 mg, 84 %) as yellow powder. R_f 0.06 (CH₃CN/H₂O 7:3), [α]²⁴_D +29.2 (c 0.19, H₂O). ¹H NMR (500 MHz, MeOD) δ 8.62, 8.04, 7.95, 7.46 (10H, 7 x CH triazole, 3 x CH aromatic), 4.96 (d, *J* = 12.2 Hz, 3H, 3 x *H*-4), 4.75 (d, *J* = 12.2 Hz, 3H, 3 x *H*-2), 4.37 (d, *J* = 7.5 Hz, 3H, 3 x *H*-3), 4.01 (s, 3H, 3 x *H*-1), 3.76 (td, *J* = 12.7, 5.9 Hz, 6H, 3 x CH₂a,b), 4.6 (1H, CH cyclopropane), 4.54, 4.18, 3.86, 3.65, 3.53, 3.43, 3.36, 2.89, 1.32 (95H, 3 x *H*-5, 46 x CH₂), 1.32, 0.90 (4H, 2 x CH₂ cyclopropane). ¹³C NMR (126 MHz, MeOD) δ 168.7, 144.2, 143.7, 124.7, 102.9, 75.4, 73.5, 71.1, 70.0, 69.4, 69.2, 68.9, 67.7, 64.0, 61.7, 61.2, 52.7, 50.9, 50.0, 48.8, 48.5, 29.1. HRMS (ESI): *m/z* calcd for (C₉₂H₁₄₁FN₂₄Na₂O₃₇)/2: 1119.4936 [M + 2Na]⁺²; found: 1119.4829.

Compound 61

Compound **43** (300 mg, 0.14 mmol, 1.0 equiv.) and **49** (103 mg, 0.16 mmol, 1.2 equiv.) were reacted according to **general method B**. The reaction mixture was evaporated, and the crude product was purified by flash column chromatography (CH₃CN/H₂O 95:5) to give compound **59** (93mg, 24%) as yellow powder. R_f 0.1 (CH₃CN/H₂O 9:1), [α]²⁴_D -11.2 (c 0.17, MeOH). The obtained product **59** (93 mg, 0.034 mmol) was directly deacetylated according to **general method C**. The crude product was purified by sephadex column (H₂O) to give compound **61** (74 mg, 97 %) as yellow powder. R_f 0.06 (CH₃CN/H₂O 7:3), [α]²⁴_D -5.83 (c 0.1, MeOH). ¹H NMR (500 MHz, MeOD) δ 7.98(m, 9H, 7 x CH triazole, 2 x CH aromatic), 4.96 (d, *J* = 12.3 Hz, 3H, 3 x *H*-4), 4.75 (d, *J* = 12.3 Hz, 3H, 3 x *H*-2), 4.37 (d, *J* = 7.5 Hz, 3H, 3 x *H*-3), 4.16 (m, 3H, 3 x *H*-1), 3.86 (6H, 3 x CH₂a,b), 3.78 (qd, *J* = 11.5, 6.0 Hz, 3H, 3 x *H*-5), 4.59 (1H, CH cyclopropane), 3.64 (2H, 2 x CH), 4.55, 4.00, 3.86, 3.71, 3.57, 3.51, 3.36 (94H, 47 x CH₂), 1.32 (3H, OCH₃), 1.32, 0.9 (4H, 2 x CH₂ cyclopropane). ¹³C NMR (126 MHz, MeOD) δ 168.9, 144.2, 143.8, 124.7, 102.4, 75.4, 73.5, 71.1, 70.0, 69.9, 69.3, 69.2, 68.9, 67.7, 64.0, 61.7, 61.2, 55.0, 54.9, 48.5, 29.3. HRMS (ESI): *m/z* calcd for (C₉₆H₁₄₇FN₂₄Na₂O₃₈)/2: 1155.0163 [M + 2Na]⁺²; found: 1155.0053.

Compound 62

Pleuromutilin (95 mg, 0.25 mmol) and **2,3,4-tri-*O*-acetyl-1-thio- β -L-fucopyranoside** (153 mg, 0.5 mol, 2x1 equiv.) were reacted in CH₃CN at room temperature according to the general method **D**, using two irradiation cycles (2x15 mins). The crude product was purified by flash column chromatography (CH₂Cl₂/acetone 99:1) to result in compound **62** as white powder (140 mg, 81%). R_f 0.31 (CH₂Cl₂/acetone 9:1), [α]²⁴_D +43.0 (c 0.1, MeOH), m.p. 192-193°C. ¹H NMR (400 MHz, CDCl₃) δ 5.62 (d, *J* = 8.2 Hz, 1H), 5.24 – 5.20 (m, 1H), 5.12 (t, *J* = 9.9 Hz, 1H), 5.03 (dd, *J* = 10.0, 3.3 Hz, 1H), 4.55 (d, *J* = 9.7 Hz, 1H), 4.12 – 3.97 (m, 2H), 3.96 – 3.86 (m, 1H), 3.38 (d, *J* = 5.7 Hz, 1H), 3.20 (s, 1H), 2.60 (dt, *J* = 11.9, 6.0 Hz, 1H), 2.45 (td, *J* = 12.0, 5.0 Hz, 1H), 2.30 (t, *J* = 6.7 Hz, 1H), 2.11 (d, *J* = 1.4 Hz, 9H), 2.03 (s, 4H), 1.92 (s, 3H), 1.86 – 1.67 (m, 2H), 1.65 – 1.39 (m, 3H), 1.35 (s, 4H), 1.21 (d, *J* = 5.2 Hz, 1H), 1.16 (d, *J* = 6.4 Hz, 3H), 1.14 – 1.01 (m, 1H), 0.99 (s, 3H), 0.90 (d, *J* = 7.0 Hz, 3H), 0.63 (d, *J* = 6.9 Hz, 3H). ¹³C NMR (101 MHz, CDCl₃) δ 216.9, 172.2, 170.6, 170.2, 170.1, 82.9, 75.9, 72.8, 72.3, 70.6, 69.5, 67.7, 61.3, 58.2, 45.5, 42.0, 41.8, 41.2, 36.5, 34.5, 34.4, 30.9, 30.1, 29.6, 26.8, 26.6, 24.9, 24.8, 20.9, 20.6, 16.5, 16.4, 14.7, 11. HRMS (ESI): m/z calcd for C₃₄H₅₂NaO₁₂S: 707.3077 [M + Na]⁺; found: 707.3070.

Compound 63

Pleuromutilin (125 mg, 0.33 mmol) and **1-thio- β -L-fucopyranoside** (119 mg, 0.66 mmol, 2x1 equiv.) were reacted in ethanol at room temperature according to the general method **D**, using two irradiation cycles (2x15 mins). The crude product was purified by flash column chromatography (CH₂Cl₂/MeOH 95:5) to result in compound **63** as white crystal (121 mg, 66%). R_f 0.31 (CH₂Cl₂/MeOH 9:1), [α]²⁴_D +12.22 (c 0.09, MeOH), m.p. 91-93°C. ¹H NMR (400 MHz, MeOD) δ 5.78 (d, *J* = 8.2 Hz, 1H), 4.57 – 4.43 (m, 1H), 4.14 (d, *J* = 17.3 Hz, 1H), 4.02 (d, *J* = 17.1 Hz, 1H), 3.88 – 3.77 (m, 1H), 3.69 (d, *J* = 3.2 Hz, 1H), 3.62 – 3.51 (m, 2H), 3.47 (d, *J* = 5.8 Hz, 1H), 3.33 (t, *J* = 1.7 Hz, 1H), 2.65 (td, *J* = 12.3, 4.2 Hz, 1H), 2.52 (td, *J* = 12.6, 4.9 Hz, 1H), 2.38 (dd, *J* = 14.6, 4.6 Hz, 2H), 2.33 – 2.23 (m, 1H), 2.19 (t, *J* = 9.4 Hz, 2H), 2.10 (ddd, *J* = 17.7, 11.4, 5.3 Hz, 2H), 2.00 – 1.80 (m, 4H), 1.77 – 1.54 (m, 4H), 1.45 (s, 3H), 1.38 (d, *J* = 21.9 Hz, 1H), 1.30 (t, *J* = 5.9 Hz, 4H), 1.23 – 1.11 (m, 1H), 1.04 (d, *J* = 2.9 Hz, 3H), 0.97 (d, *J* = 6.9 Hz, 3H), 0.74 (d, *J* = 6.1 Hz, 3H). ¹³C NMR (101 MHz, MeOD) δ 217.0, 172.5, 85.3, 75.1, 74.9, 74.3, 71.9, 69.6, 69.0, 60.5, 57.9, 45.4, 41.7, 41.4, 41.0, 36.7, 34.8, 33.9, 30.1, 30.0, 26.7, 25.9, 24.7, 24.3, 15.8, 15.6, 13.9, 10.4. HRMS (ESI): m/z calcd for C₂₈H₄₆NaO₉S: 581.2760 [M + Na]⁺; found: 581.2754.

Compound 64

Pleuromutilin (190 mg, 0.5 mmol) and **2,3,4,6-tetra-*O*-acetyl-1-thio- α -D-mannopyranoside** (365 mg, 1.0 mmol, 2x1 equiv.) were reacted in CH₃CN at room temperature according to

general method **D**, using two irradiation cycles (2x15 mins). The crude product was purified by flash column chromatography (CH₂Cl₂/acetone 95:5) to result in compound **64** as white crystal (219 mg, 59%). R_f 0.38 (CH₂Cl₂/acetone 9:1), [α]²⁴_D+107.0 (c 0.1, CHCl₃), m.p. 127-130°C. ¹H NMR (400 MHz, MeOD) δ 5.71 (d, *J* = 8.3 Hz, 1H), 5.48 (d, *J* = 1.5 Hz, 1H), 5.36 (dd, *J* = 3.2, 1.5 Hz, 1H), 5.31 (t, *J* = 9.9 Hz, 1H), 5.25 (dd, *J* = 10.1, 3.3 Hz, 1H), 4.46 (ddd, *J* = 9.6, 4.8, 2.4 Hz, 1H), 4.31 (dd, *J* = 12.3, 4.8 Hz, 1H), 4.15 (dd, *J* = 12.3, 2.5 Hz, 1H), 4.11 – 3.97 (m, 2H), 3.48 (d, *J* = 5.8 Hz, 1H), 2.72 – 2.48 (m, 2H), 2.36 (d, *J* = 7.1 Hz, 2H), 2.31 – 2.19 (m, 1H), 2.18 (d, *J* = 1.6 Hz, 5H), 2.08 (d, *J* = 5.8 Hz, 6H), 2.03 (dd, *J* = 9.9, 7.3 Hz, 2H), 1.99 (s, 1H), 1.97 – 1.79 (m, 4H), 1.76 – 1.54 (m, 4H), 1.45 (s, 3H), 1.30 (dd, *J* = 16.0, 6.9 Hz, 2H), 1.23 – 1.11 (m, 1H), 1.05 (s, 3H), 0.97 (d, *J* = 7.0 Hz, 3H), 0.75 (d, *J* = 6.3 Hz, 3H). ¹³C NMR (101 MHz, MeOD) δ 217.0, 172.1, 171.0, 170.3, 170.2, 170.1, 81.5, 74.9, 70.9, 69.8, 69.0, 68.7, 66.1, 62.4, 60.6, 57.8, 45.4, 41.8, 41.7, 41.0, 36.6, 34.8, 33.9, 30.0, 29.7, 26.7, 26.0, 25.9, 24.3, 19.4, 19.4, 19.3, 19.2, 15.8, 13.9, 10.4. HRMS (ESI): *m/z* calcd for C₃₆H₅₄NaO₁₄S: 765.3132 [M + Na]⁺; found: 765.3125.

Compound 65

Pleuromutilin (190 mg, 0.5 mmol) and **3,4,6-tri-*O*-acetyl-2-deoxy-2-*N*-acetyl-1-thio- β -D-glucopyranoside** (364 mg, 1.0 mmol, 2x1 equiv.) were reacted in CH₃CN at room temperature according to general method **D**, using two irradiation cycles (2x15 mins). The crude product was purified by flash column chromatography (CH₂Cl₂/acetone 95:5) resulted in compound **65** as white crystal (255 mg, 69%). R_f: 0.11 (CH₂Cl₂/acetone 9:1), [α]²⁴_D+13 (c 0.1, CHCl₃), m.p. 97-98°C. ¹H NMR (400 MHz, CDCl₃) δ 6.79 (d, *J* = 9.3 Hz, 1H), 5.70 (d, *J* = 8.2 Hz, 1H), 5.41 – 5.24 (m, 1H), 5.13 (t, *J* = 9.7 Hz, 1H), 4.68 (d, *J* = 10.4 Hz, 1H), 4.25 (dd, *J* = 12.3, 4.7 Hz, 1H), 4.19 – 4.10 (m, 3H), 4.10 – 3.97 (m, 1H), 3.76 (ddd, *J* = 9.9, 4.6, 2.4 Hz, 1H), 3.42 (d, *J* = 5.7 Hz, 1H), 2.80 (td, *J* = 12.3, 4.3 Hz, 1H), 2.37 (tq, *J* = 12.8, 7.8, 6.2 Hz, 3H), 2.29 – 2.21 (m, 1H), 2.18 (s, 1H), 2.14 – 2.06 (m, 4H), 2.08 – 1.95 (m, 10H), 1.95 – 1.74 (m, 3H), 1.73 – 1.52 (m, 2H), 1.53 – 1.44 (m, 2H), 1.42 (s, 4H), 1.33 – 1.20 (m, 2H), 1.14 (td, *J* = 14.0, 4.5 Hz, 1H), 1.03 (s, 3H), 0.96 (d, *J* = 6.9 Hz, 3H), 0.70 (d, *J* = 7.0 Hz, 3H). ¹³C NMR (101 MHz, CDCl₃) δ 217.0, 172.7, 171.1, 171.1, 170.9, 169.4, 86.1, 76.0, 75.8, 73.8, 69.6, 68.4, 62.5, 61.4, 58.2, 53.5, 45.5, 42.3, 41.8, 41.3, 36.5, 34.7, 34.4, 30.8, 30.2, 27.7, 26.9, 26.7, 24.8, 23.2, 20.8, 20.8, 20.7, 16.6, 14.7, 11.1. HRMS (ESI): *m/z* calcd for C₃₆H₅₅NNaO₁₃S: 764.3292 [M + Na]⁺; found: 764.3287.

Compound 66

Pleuromutilin (95 mg, 0.25 mmol) and ***n*-butyl mercaptan** (45 mg, 60 μ l, 0.5 mmol, 2x1 equiv.) were reacted in CH₃CN/MeOH 2:1 at -40°C according to general method **D**, using two

irradiation cycles (2x15 mins). The crude product was purified by flash column chromatography (CH₂Cl₂/acetone 95:5) resulted in compound **66** as white crystal (97 mg, 82%). R_f 0.56 (CH₂Cl₂/acetone 9:1), [α]²⁴_D +52.2 (c 0.18, CHCl₃), m.p. 177-180°C. ¹H NMR (400 MHz, CDCl₃) δ 5.65 (d, *J* = 8.3 Hz, 1H), 4.01 (q, *J* = 17.1 Hz, 2H), 3.38 (d, *J* = 5.8 Hz, 1H), 2.51 (dd, *J* = 7.9, 6.8 Hz, 2H), 2.41 (t, *J* = 8.3 Hz, 2H), 2.37 – 2.27 (m, 2H), 2.24 – 2.15 (m, 1H), 2.13 (s, 2H), 1.91 (t, *J* = 8.4 Hz, 2H), 1.83 – 1.68 (m, 2H), 1.62 – 1.41 (m, 7H), 1.36 (s, 5H), 1.30 – 1.18 (m, 2H), 1.08 (td, *J* = 13.8, 4.3 Hz, 1H), 0.99 (s, 3H), 0.92 (d, *J* = 7.0 Hz, 3H), 0.88 (t, *J* = 7.3 Hz, 3H), 0.64 (d, *J* = 6.8 Hz, 3H). ¹³C NMR (101 MHz, CDCl₃) δ 217.1, 172.3, 76.0, 69.9, 61.3, 58.3, 45.5, 42.4, 41.8, 41.2, 36.5, 34.5, 34.4, 31.9, 31.8, 30.1, 30.1, 27.4, 26.8, 26.8, 24.8, 22.0, 16.5, 14.7, 13.7, 11.1. HRMS (ESI): *m/z* calcd for C₂₆H₄₄NaO₅S: 491.2807 [M + Na]⁺; found: 491.2801.

Compound 67

Pleuromutilin (95 mg, 0.25 mmol) and *n*-octyl mercaptan (73 mg, 87 μl, 0.5 mmol, 2 equiv.) were reacted in CH₃CN/MeOH 2:1 at -40°C according to general method **D**, using one irradiation cycles (15 mins). The crude product was purified by flash column chromatography (CH₂Cl₂/acetone 95:5) resulted in compound **67** as white crystal (96 mg, 73%). R_f 0.66 (CH₂Cl₂/acetone 9:1), [α]²⁴_D +20.0 (c 0.04, CHCl₃). ¹H NMR (400 MHz, CDCl₃) δ 5.68 (d, *J* = 8.3 Hz, 1H), 4.04 (qd, *J* = 17.0, 4.1 Hz, 2H), 3.41 (d, *J* = 5.8 Hz, 1H), 2.54 (t, *J* = 7.4 Hz, 2H), 2.45 (dt, *J* = 9.3, 3.0 Hz, 2H), 2.41 – 2.28 (m, 2H), 2.28 – 2.14 (m, 2H), 2.09 (d, *J* = 2.7 Hz, 1H), 1.94 (ddd, *J* = 9.9, 6.2, 2.4 Hz, 2H), 1.81 – 1.74 (m, 2H), 1.68 – 1.43 (m, 7H), 1.40 (s, 5H), 1.28 (dt, *J* = 10.0, 5.1 Hz, 10H), 1.11 (td, *J* = 13.8, 4.4 Hz, 1H), 1.03 (s, 3H), 0.96 (d, *J* = 7.0 Hz, 3H), 0.91 – 0.82 (m, 3H), 0.67 (d, *J* = 6.9 Hz, 3H). ¹³C NMR (101 MHz, CDCl₃) δ 216.7, 172.3, 76.1, 70.0, 61.3, 58.3, 45.5, 42.4, 41.8, 41.2, 36.5, 34.5, 34.4, 32.3, 31.8, 30.1, 30.1, 29.8, 29.3, 29.2, 29.0, 27.4, 26.8, 26.8, 24.9, 22.6, 16.6, 14.7, 14.1, 11.1. HRMS (ESI): *m/z* calcd for C₃₀H₅₂NaO₅S: 547.3433 [M + Na]⁺; found: 547.3427.

Compound 68

Pleuromutilin (95 mg, 0.25 mmol) and *n*-dodecyl mercaptan (202 mg, 240 μl, 1.0 mmol, 2x2 equiv.) were reacted in EtOH at 0°C according to general method **D**, using two irradiation cycles (2x15 mins). The crude product was purified by flash column chromatography (CH₂Cl₂/acetone 95:5) resulted in compound **68** as white crystal (61 mg, 42%). R_f 0.66 (CH₂Cl₂/acetone 9:1), [α]²⁴_D +47.4 (c 0.19, CHCl₃). ¹H NMR (400 MHz, CDCl₃) δ 5.72 (d, *J* = 8.3 Hz, 1H), 4.06 (q, *J* = 17.0 Hz, 2H), 3.43 (d, *J* = 6.0 Hz, 1H), 2.57 (t, *J* = 7.4 Hz, 2H), 2.48 (td, *J* = 10.6, 9.7, 6.1 Hz, 2H), 2.40 (dd, *J* = 13.8, 6.1 Hz, 2H), 2.31 – 2.16 (m, 2H), 2.11 (s, 1H), 1.97 (dt, *J* = 10.8, 4.8 Hz, 2H), 1.82 (td, *J* = 15.5, 14.2, 5.8 Hz, 2H), 1.73 – 1.48 (m,

7H), 1.42 (d, $J = 9.2$ Hz, 5H), 1.28 (d, $J = 5.3$ Hz, 18H), 1.14 (td, $J = 13.8, 4.3$ Hz, 1H), 1.06 (s, 3H), 0.99 (d, $J = 7.0$ Hz, 3H), 0.89 (t, $J = 6.6$ Hz, 3H), 0.70 (d, $J = 6.9$ Hz, 3H). ^{13}C NMR (101 MHz, CDCl_3) δ 216.7, 172.3, 76.2, 70.1, 61.3, 58.3, 45.5, 42.5, 41.9, 41.2, 36.5, 34.5, 34.4, 32.4, 31.9, 30.1, 30.1, 29.8, 29.7, 29.6, 29.6, 29.3, 29.3, 29.0, 27.4, 26.8, 26.8, 24.9, 22.7, 16.5, 14.7, 14.1, 11.0. HRMS (ESI): m/z calcd for $\text{C}_{34}\text{H}_{60}\text{NaO}_5\text{S}$: 603.4059 $[\text{M} + \text{Na}]^+$; found: 603.4052.

Compound 69

Pleuromutilin (95 mg, 0.25 mmol) and **sodium 2-mercaptoethanesulfonate** (165 mg, 1.0 mmol, 2x2 equiv.) were reacted in MeOH at 0°C according to general method **D**, using two irradiation cycles (2x15 mins). The crude product was purified by flash column chromatography ($\text{CH}_2\text{Cl}_2/\text{MeOH}$ 95:5) resulted in compound **69** as white powder (58 mg, 42%). R_f 0.69 ($\text{CH}_2\text{Cl}_2/\text{MeOH}$ 7:3), $[\alpha]^{24}_{\text{D}} +25.0$ (c 0.12, MeOH), m.p. 113-114 $^\circ\text{C}$. ^1H NMR (400 MHz, MeOD) δ 5.77 (d, $J = 8.3$ Hz, 1H), 4.19 – 3.93 (m, 2H), 3.47 (d, $J = 5.9$ Hz, 1H), 3.33 (p, $J = 1.6$ Hz, 1H), 3.09 (ddd, $J = 9.1, 7.0, 2.2$ Hz, 2H), 3.02 – 2.84 (m, 2H), 2.58 (td, $J = 12.0, 4.7$ Hz, 1H), 2.50 – 2.32 (m, 3H), 2.33 – 2.23 (m, 1H), 2.18 (d, $J = 2.5$ Hz, 1H), 1.91 (tdd, $J = 25.3, 12.9, 4.1$ Hz, 4H), 1.78 – 1.54 (m, 4H), 1.44 (s, 4H), 1.33 (d, $J = 16.5$ Hz, 2H), 1.27 – 1.08 (m, 1H), 1.05 (s, 3H), 0.97 (d, $J = 7.0$ Hz, 3H), 0.74 (d, $J = 6.1$ Hz, 3H). ^{13}C NMR (101 MHz, MeOD) δ 217.0, 172.0, 75.0, 69.0, 60.5, 57.9, 51.9, 45.5, 42.3, 41.7, 40.9, 36.7, 34.8, 33.9, 30.1, 30.0, 27.2, 26.7, 26.5, 25.9, 24.3, 15.6, 13.9, 10.4. HRMS (ESI): m/z calcd for $\text{C}_{24}\text{H}_{39}\text{Na}_2\text{O}_8\text{S}_2$: 565.1882 $[\text{M} + \text{Na}]^+$; found: 565.1876.

Compound 70

Pleuromutilin (95 mg, 0.25 mmol) and **benzylmercaptan** (186 mg, 177 μl , 1.5 mmol, 3x2 equiv.) were reacted in toluene at -40°C according to general method **D**, using three irradiation cycles (3x15 mins). The crude product was purified by flash column chromatography ($\text{CH}_2\text{Cl}_2/\text{acetone}$ 97:3) resulted in compound **70** as white crystal (100 mg, 79%). R_f 0.60 ($\text{CH}_2\text{Cl}_2/\text{acetone}$ 9:1), $[\alpha]^{24}_{\text{D}} +67.1$ (c 0.21, CHCl_3), m.p. 150-151 $^\circ\text{C}$. ^1H NMR (400 MHz, MeOD) δ 7.45 – 7.40 (m, 2H), 7.30 (td, $J = 7.1, 6.1, 1.3$ Hz, 2H), 7.25 – 7.19 (m, 1H), 5.74 (d, $J = 8.3$ Hz, 1H), 4.13 – 3.95 (m, 2H), 3.88 (d, $J = 13.5$ Hz, 1H), 3.74 (d, $J = 13.5$ Hz, 1H), 3.41 (d, $J = 6.0$ Hz, 1H), 2.37 (ddd, $J = 9.7, 5.8, 2.5$ Hz, 2H), 2.33 – 2.29 (m, 1H), 2.29 – 2.21 (m, 1H), 2.17 (s, 2H), 2.04 (ddd, $J = 13.7, 10.3, 6.5$ Hz, 1H), 1.95 – 1.77 (m, 4H), 1.64 (dt, $J = 11.4, 6.7$ Hz, 4H), 1.44 (s, 4H), 1.23 (d, $J = 16.2$ Hz, 1H), 1.15 (td, $J = 13.4, 4.3$ Hz, 1H), 0.98 (s, 3H), 0.83 (d, $J = 6.9$ Hz, 3H), 0.75 (d, $J = 6.0$ Hz, 3H). ^{13}C NMR (101 MHz, MeOD) δ 217.0, 171.9, 139.2, 128.7, 128.0, 126.4, 74.9, 68.9, 60.6, 57.9, 45.5, 42.5, 41.7,

40.8, 36.7, 35.1, 34.8, 33.9, 30.8, 30.0, 26.8, 26.3, 26.1, 24.4, 15.7, 14.0, 10.5. HRMS (ESI): m/z calcd for $C_{29}H_{42}NaO_5S$: 525.2651 $[M + Na]^+$; found: 525.2643.

Compound 71

To the mixture of pleuromutilin (95 mg, 0.25 mmol) and **thioacetic acid** (57 mg, 54 μ l, 0.75 mmol, 3.0 equiv.) in EtOAc at room temperature, 0.1 equiv. of 2,2-dimethoxy-2-phenylacetophenone **DPAP** (0.025mmol, 6 mg) and 0.1 equiv. of 4-methoxyacetophenone **MAP** (0.025mmol, 3.8mg) were added, using one irradiation cycle for one hour. The crude product was purified by flash column chromatography (*n*-hexane/acetone 8:2) resulted in compound **71** as white crystal (91 mg, 80%). R_f 0.36 (*n*-hexane/acetone 6:4), $[\alpha]^{24}_D +54.7$ (c 0.15, MeOH), m.p. 188-189°C. 1H NMR (400 MHz, MeOD) δ 5.69 (d, $J = 8.2$ Hz, 1H), 4.14 – 3.87 (m, 2H), 3.44 (d, $J = 6.1$ Hz, 1H), 3.03 – 2.89 (m, 1H), 2.66 (td, $J = 12.4, 5.0$ Hz, 1H), 2.33 (d, $J = 3.1$ Hz, 2H), 2.30 (s, 4H), 2.28 – 2.17 (m, 1H), 2.18 – 2.05 (m, 1H), 1.97 – 1.77 (m, 5H), 1.73 – 1.51 (m, 3H), 1.42 (s, 4H), 1.31 (d, $J = 16.4$ Hz, 1H), 1.14 (td, $J = 13.7, 4.4$ Hz, 1H), 1.07 (s, 3H), 0.94 (d, $J = 7.0$ Hz, 3H), 0.71 (d, $J = 6.6$ Hz, 3H). ^{13}C NMR (101 MHz, MeOD) δ 217.0, 194.0, 168.0, 73.3, 67.3, 59.0, 56.4, 43.9, 40.2, 40.2, 39.6, 35.1, 33.4, 32.4, 28.6, 28.2, 27.6, 25.2, 24.2, 22.8, 14.1, 12.4, 8.9. HRMS (ESI): m/z calcd for $C_{24}H_{38}NaO_6S$: 477.2287 $[M + Na]^+$; found: 477.2281.

Compound 72

Pleuromutilin (95 mg, 0.25 mmol) and **N-Fmoc-L-cystein** (172 mg, 0.5 mmol, 2x1 equiv.) were reacted in toluene/MeOH 1:1 at -40°C according to general method **D**, using two irradiation cycles (2x15 mins). The crude product was purified by flash column chromatography (toluene/MeOH 95:5) resulted in compound **72** as yellow crystal (169 mg, 93%). R_f 0.11 (toluene/MeOH 8:2), $[\alpha]^{24}_D +15.3$ (c 0.15, MeOH), m.p. 143-147°C. 1H NMR (500 MHz, DMSO) δ 7.89 (d, $J = 7.6$ Hz, 2H), 7.74 (t, $J = 6.9$ Hz, 2H), 7.42 (t, $J = 7.5$ Hz, 2H), 7.34 (t, $J = 7.5$ Hz, 2H), 5.60 (d, $J = 8.0$ Hz, 1H), 4.32 – 4.23 (m, 2H), 4.22 (q, $J = 6.7, 6.1$ Hz, 2H), 4.06 (d, $J = 17.1$ Hz, 1H), 3.82 (d, $J = 17.1$ Hz, 1H), 3.00 (dd, $J = 13.9, 4.5$ Hz, 1H), 2.79 (dd, $J = 13.5, 6.8$ Hz, 1H), 2.37 (d, $J = 21.5$ Hz, 3H), 2.24 – 2.14 (m, 2H), 2.12 – 1.96 (m, 1H), 1.83 (dd, $J = 16.2, 8.0$ Hz, 1H), 1.67 (ddt, $J = 37.8, 21.7, 10.0$ Hz, 4H), 1.49 (d, $J = 7.9$ Hz, 2H), 1.40 – 1.28 (m, 5H), 1.30 – 1.21 (m, 5H), 1.11 (d, $J = 15.8$ Hz, 2H), 0.92 (s, 3H), 0.89 – 0.80 (m, 3H), 0.63 (d, $J = 5.7$ Hz, 3H). ^{13}C NMR (126 MHz, DMSO) δ 217.2, 172.20, 155.5, 143.9, 140.7, 127.6, 127.1, 125.4, 125.3, 120.1, 73.6, 67.5, 65.6, 60.3, 57.3, 46.7, 45.0, 41.3, 40.6, 36.3, 34.6, 33.9, 31.1, 30.2, 29.8, 29.0, 27.6, 26.9, 26.6, 24.4, 16.1, 14.5, 11.5. HRMS (ESI): m/z calcd for $C_{40}H_{51}NNaO_9S$: 744.3182 $[M + Na]^+$; found: 744.3163.

Compound 73

Pleuromutilin (95 mg, 0.25 mmol) and *N*-acetyl-L-cystein (82 mg, 0.5 mmol, 2x1 equiv.) were reacted in MeOH at -80°C according to general method **D**, using two irradiation cycles (2x15 mins). The crude product was purified by flash column chromatography (CH₂Cl₂/MeOH 9:1) resulted in compound **73** as white-yellow crystal (124.7 mg, 92%). R_f: 0.31 (CH₂Cl₂/MeOH 7:3), [α]²⁴_D +34.3 (*c* 0.14, MeOH), m.p. 73-74°C. ¹H NMR (360 MHz, MeOD) δ 5.93 (d, *J* = 8.1 Hz, 1H), 4.66 (q, *J* = 5.4 Hz, 2H), 4.39 (d, *J* = 17.2 Hz, 1H), 4.20 (d, *J* = 17.2 Hz, 1H), 3.67 – 3.55 (m, 1H), 3.40 (q, *J* = 7.3 Hz, 1H), 3.30 (dd, *J* = 13.8, 5.1 Hz, 1H), 3.13 (td, *J* = 9.8, 8.2, 5.0 Hz, 2H), 2.73 – 2.27 (m, 6H), 2.23 (dd, *J* = 8.0, 4.0 Hz, 5H), 2.18 – 1.65 (m, 6H), 1.60 (d, *J* = 9.4 Hz, 3H), 1.57 – 1.43 (m, 4H), 1.20 (s, 3H), 1.13 (d, *J* = 6.9 Hz, 3H), 0.92 (d, *J* = 6.3 Hz, 3H). ¹³C NMR (91 MHz, MeOD) δ 219.5, 185.1, 174.0, 76.2, 70.3, 61.8, 59.2, 47.6, 46.6, 42.8, 42.6, 42.1, 37.8, 35.8, 35.7, 35.2, 31.2, 30.5, 30.2, 28.7, 27.9, 27.3, 25.5, 22.8, 16.9, 15.2, 11.7. HRMS (ESI): *m/z* calcd for C₂₇H₄₃NNaO₈S: 564.2607 [M + Na]⁺; found: 564.2616.

Compound 74

Pleuromutilin (95 mg, 0.25 mmol) and **2-hydroxyethylmercaptan** (39 mg, 35μl, 0.5 mmol, 2 equiv.) were reacted in CH₃CN/MeOH 2:1 at -40°C according to general method **D**, using one irradiation cycle (15 mins). The crude product was purified by flash column chromatography (*n*-hexane/acetone 8:2) resulted in compound **74** as white crystal (89 mg, 78%). R_f 0.10 (*n*-hexane/acetone 7:3), [α]²⁴_D +10.3 (*c* 0.35, MeOH), m.p. 189°C. ¹H NMR (400 MHz, MeOD) δ 5.70 (d, *J* = 8.3 Hz, 1H), 4.00 (q, *J* = 17.1 Hz, 2H), 3.65 (td, *J* = 6.9, 1.7 Hz, 2H), 3.37 (d, *J* = 5.9 Hz, 1H), 2.73 (dt, *J* = 13.8, 6.8 Hz, 1H), 2.63 (dt, *J* = 13.6, 6.9 Hz, 1H), 2.44 (td, *J* = 12.1, 4.7 Hz, 1H), 2.40 – 2.31 (m, 2H), 2.28 – 2.18 (m, 3H), 2.19 – 2.05 (m, 2H), 1.98 (ddd, *J* = 13.6, 12.0, 5.2 Hz, 1H), 1.81 (dtd, *J* = 15.5, 8.9, 8.5, 3.8 Hz, 3H), 1.69 – 1.48 (m, 4H), 1.48 – 1.40 (m, 1H), 1.38 (s, 4H), 1.25 (d, *J* = 16.2 Hz, 1H), 1.18 – 1.04 (m, 1H), 0.98 (s, 3H), 0.91 (d, *J* = 7.0 Hz, 3H), 0.68 (d, *J* = 6.3 Hz, 3H). ¹³C NMR (101 MHz, MeOD) 217.0, 169.0, 73.7, 67.6, 59.9, 59.3, 56.7, 44.1, 40.4, 40.3, 39.5, 35.2, 33.3, 32.7, 32.2, 28.7, 28.6, 25.5, 25.3, 24.8, 23.0, 14.4, 12.8, 9.2. HRMS (ESI): *m/z* calcd for C₂₀H₄₀NaO₆S: 479.2443 [M + Na]⁺; found: 479.2438.

Compound 75

Pleuromutilin (47.5 mg, 0.125 mmol) and **2-thio-N-acetylneuraminic acid peracetate** (191 mg, 0.375 mmol, 3x1 equiv.) were reacted in toluene/MeOH 1:1 at -40°C according to general method **D**, using three irradiation cycles (3x15 mins). The crude product was purified by flash

column chromatography (CH₂Cl₂/acetone 9:1) resulted in compound **75** as white powder (69 mg, 62%). R_f 0.20 (CH₂Cl₂/acetone 8:2), [α]²⁴_D +46.7 (c 0.12, MeOH). ¹H NMR (400 MHz, CDCl₃) δ 5.59 (d, *J* = 8.1 Hz, 1H), 5.46 (d, *J* = 10.1 Hz, 1H), 5.31 (q, *J* = 4.9, 3.6 Hz, 2H), 4.95 – 4.76 (m, 1H), 4.37 – 4.22 (m, 1H), 4.16 – 3.94 (m, 4H), 3.94 – 3.66 (m, 4H), 3.38 (d, *J* = 5.5 Hz, 1H), 2.71 (dd, *J* = 12.7, 4.6 Hz, 1H), 2.62 (s, 1H), 2.57 (dd, *J* = 12.2, 4.1 Hz, 1H), 2.43 (td, *J* = 11.7, 5.2 Hz, 1H), 2.30 (dt, *J* = 10.0, 4.8 Hz, 1H), 2.22 – 2.06 (m, 6H), 2.02 (d, *J* = 1.8 Hz, 8H), 1.86 (s, 4H), 1.75 (dt, *J* = 9.8, 5.8 Hz, 2H), 1.68 – 1.50 (m, 2H), 1.50 – 1.42 (m, 1H), 1.41 (s, 4H), 1.38 – 1.29 (m, 1H), 1.24 (s, 5H), 1.10 (td, *J* = 14.1, 3.0 Hz, 1H), 1.03 (s, 3H), 0.91 (d, *J* = 6.8 Hz, 3H), 0.67 (d, *J* = 6.9 Hz, 3H). ¹³C NMR (101 MHz, CDCl₃) δ 218.0, 172.4, 170.9, 170.8, 170.3, 170.2, 168.4, 83.3, 76.0, 73.9, 69.8, 69.7, 68.3, 67.2, 62.4, 61.3, 58.3, 53.8, 52.9, 49.3, 45.4, 41.7, 41.7, 41.4, 38.0, 36.5, 34.4, 30.1, 29.6, 29.3, 28.0, 26.8, 26.1, 24.8, 24.5, 23.1, 21.2, 20.9, 20.8, 16.6, 14.8, 11.0. HRMS (ESI): *m/z* calcd for C₄₂H₆₃NNaO₁₇S: 908.3714 [M + Na]⁺; found: 908.3709.

Compound 76

Compound **76** was prepared from compound **75** (65mg, 0.073 mmol) according to **general method F**. The crude product was purified by Sephadex column (H₂O) to obtain **80** as yellow powder (50 mg, 97%). R_f 0.56 (CH₃CN/H₂O 9:1), [α]²⁴_D +28.9 (c 0.09, MeOH). ¹H NMR (400 MHz, DMSO-*d*₆) δ 5.55 (d, *J* = 7.6 Hz, 1H, H-14), 4.09 (d, *J* = 5.7 Hz, 2H, H-22ab), 3.75 (dd, *J* = 19.5, 10.4 Hz, 4H), 3.63 – 3.56 (m, 2H), 3.51 (d, *J* = 9.7 Hz, 2H), 3.43 (d, *J* = 4.9 Hz, 1H, H-11), 3.27 (d, *J* = 1.2 Hz, 14H), 2.73 (dd, *J* = 12.4, 4.0 Hz, 1H), 2.65 – 2.56 (m, 1H), 2.47 (dd, *J* = 11.5, 3.7 Hz, 1H, H-19*a), 2.41 (s, 1H, H-19*b), 2.29 – 2.10 (m, 4H), 1.95 (s, 1H, H-20*a), 1.85 (s, 5H, H-20*b), 1.75 (d, *J* = 14.4 Hz, 1H, H-1a), 1.66 (d, *J* = 11.9 Hz, 2H), 1.59 – 1.50 (m, 1H), 1.49 – 1.39 (m, 4H, H-1b), 1.30 (s, 5H), 1.21 (dd, *J* = 29.0, 9.0 Hz, 6H), 1.09 – 0.97 (m, 2H), 0.91 (s, 3H, H18abc), 0.83 (d, *J* = 6.2 Hz, 3H, H-17abc), 0.60 (d, *J* = 5.3 Hz, 3H, H-16abc). * Interchangeable signals. ¹³C NMR (101 MHz, DMSO-*d*₆) δ 174.3, 172.6, 171.1 (3C, C-1', C-21, AcCO), 85.1 (1C, C-2'), 75.2, 73.9, 71.1, 69.2, 67.4, 66.9 53.6, 51.9 (8C, skeletal carbons, C-11, C-14), 63.4, 60.4, (2C, C-22, C-9'), 57.5 (1C, C-4), 45.0, 41.3, 40.8 (4C, C-12, C-13, C-5, C-9), 36.4 (1C, C-6), 34.0, 29.0, 27.4 (3C, C-19, C-20, C-8), 26.9 (1C, C-18), 25.5 (1C, C-1), 24.5 (1C, C-7), 22.3 (1C, AcCH₃), 16.1 (1C, C-16), 14.6 (1C, C-15), 11.6 (1C, C-17). HRMS (MALDI): *m/z* calcd for C₃₃H₅₃NNaO₁₃S: 726.3135 [M + Na]⁺; found: 726.3159.

Compound 77

Compound **72** (100 mg, 0.138 mmol) was dissolved in 20% piperidine solution in DMF (5 ml) and allowed to stir at room temperature for two hours. The reaction mixture was

evaporated, and the crude product was purified by flash column chromatography (CH₃CN/H₂O 9:1) to obtain compound **77** as yellow crystal (46 mg, 66%), R_f 0.1 (CH₃CN/H₂O 9:1), [α]²⁴_D +41.7 (*c* 0.06, MeOH), m.p. 197-199°C. ¹H NMR (400 MHz, MeOD) δ 5.69 (t, *J* = 8.6 Hz, 1H), 4.22 (dd, *J* = 25.1, 17.2 Hz, 1H), 4.04 (dd, *J* = 17.2, 13.4 Hz, 1H), 3.79 (dt, *J* = 10.9, 5.2 Hz, 1H), 3.47 (t, *J* = 5.0 Hz, 1H), 3.37 (s, 2H), 3.33 (p, *J* = 1.7 Hz, 1H), 3.22 (dd, *J* = 15.2, 4.8 Hz, 1H), 3.19 – 3.07 (m, 1H), 2.52 (tq, *J* = 10.8, 5.2, 4.8 Hz, 2H), 2.41 – 2.31 (m, 2H), 2.31 – 2.24 (m, 1H), 2.17 (q, *J* = 9.6 Hz, 1H), 2.13 – 1.98 (m, 1H), 1.98 – 1.48 (m, 5H), 1.45 (d, *J* = 3.7 Hz, 5H), 1.39 – 1.27 (m, 2H), 1.17 (td, *J* = 13.8, 4.3 Hz, 1H), 1.03 (d, *J* = 5.0 Hz, 3H), 0.95 (dd, *J* = 7.1, 1.8 Hz, 3H), 0.74 (dd, *J* = 7.0, 2.0 Hz, 3H). ¹³C NMR (101 MHz, MeOD) δ 217.0, 190.0, 173.3, 74.9, 69.3, 60.5, 57.8, 53.8, 45.4, 41.6, 41.0, 36.6, 34.6, 33.9, 32.8, 30.0, 28.4, 28.1, 27.2, 26.8, 25.8, 24.2, 15.8, 13.9, 10.3. HRMS (ESI): *m/z* calcd for C₂₅H₄₁NNaO₇S: 522.2501 [M + Na]⁺; found: 522.2496.

Compound 78

Lefamulin (50.8 mg, 0.1 mmol) and *N*-acetyl-L-cystein (33 mg, 0.2 mmol, 2x1.0 equiv.) were reacted in methanol at -80°C according to **general method E**, using two irradiation cycles (2x15 mins). The crude product was purified by flash column chromatography (CH₃CN/H₂O 9:1) resulted in compound **78** as yellow-white crystal (57.4 mg, 86%). R_f 0.46 (CH₃CN/H₂O 85:15), [α]²⁴_D +36.0 (*c* 0.2, H₂O). ¹H NMR (400 MHz, DMSO-*d*₆) δ 7.42 (d, *J* = 7.1 Hz, 1H, *NH*), 5.50 (d, *J* = 8.0 Hz, 1H, *H*-14), 4.57 (d, *J* = 4.4 Hz, 1H, *OH*), 4.08 (dd, *J* = 12.1, 5.4 Hz, 1H, *H*-24), 3.68 (d, *J* = 16.2 Hz, 2H, *H*-22a), 3.35 (dd, *J* = 21.8, 11.0 Hz, 2H, *H*-2', *H*-11), 3.19 – 3.13 (m, 2H, *H*-22b), 2.95 (dt, *J* = 19.3, 9.7 Hz, 2H, *H*-23a, *H*-4'), 2.74 – 2.60 (m, 2H, *H*-23b, *H*-1'), 2.53 – 2.49 (m, 2H), 2.42 – 2.32 (m, 2H, *H*-4), 2.32 – 2.22 (m, 1H), 2.18 (dd, *J* = 12.1, 6.1 Hz, 2H, *H*-10, *H*-5'a), 2.03 (ddd, *J* = 21.3, 17.6, 5.7 Hz, 4H, *H*-5'b), 1.84 (s, 3H, CH₃ acetyl), 1.79 (dd, *J* = 13.9, 9.4 Hz, 3H, *H*-13a), 1.72 – 1.60 (m, 6H, *H*-7a, *H*-8a), 1.48 (dd, *J* = 11.9, 9.0 Hz, 1H, *H*-6), 1.41 (d, *J* = 13.3 Hz, 1H, *H*-6'a), 1.33 (s, 3H, *H*-15abc), 1.31 – 1.23 (m, 3H, *H*-7b), 1.18 (dd, *J* = 9.7, 6.4 Hz, 2H, *H*-13b), 1.07 – 0.97 (m, 1H, *H*-8b), 0.91 (s, 3H, *H*-18abc), 0.83 (d, *J* = 6.8 Hz, 3H, *H*-17abc), 0.60 (d, *J* = 6.6 Hz, 3H, *H*-16abc). ¹³C NMR (101 MHz, DMSO-*d*₆) δ 217.3 (1C, C-3), 173.0 (1C, C-21), 169.0, 168.4 (2C, AcCO, COOH), 73.6 (2C, C-2', C-11), 72.8, 68.5 (1C, C-14), 57.2 (1C, C-4), 53.9 (1C, C-24), 47.4, 47.2 (2C, C-4', C-1'), 41.2 (1C, C-13), 45.0, 40.7 (3C, C-5, C-12, C-9), 36.4 (1C, C-6), 35.9 (1C, C-23), 34.5 (1C, C-10), 34.0 (1C, C-5'), 33.0 (1C, C-22), 30.1 (1C, C-8), 31.1, 29.2, 28.2, 27.7 (4C, C-19, C-20, C-3', C-6'), 26.8 (1C, C-18), 24.3 (1C, C-7), 22.9 (1C, CH₃ acetyl), 16.4 (1C, C-16), 14.6 (1C, C-15), 11.5 (1C, C-17). HRMS (MALDI): *m/z* calcd for C₃₃H₅₄N₂NaO₈S₂: 693.3219 [M + Na]⁺; found: 693.3219.

Compound 79

Lefamulin (50.8 mg, 0.1 mmol) and **2-mercaptoethanol** (31 mg, 28 μ l, 0.4 mmol, 2x2 equiv.) were reacted in methanol at -80°C according to **general method E**, using two irradiation cycles (2x15 mins). The crude product was purified by flash column chromatography ($\text{CH}_3\text{CN}/\text{H}_2\text{O}$ 9:1) resulted in compound **79** as whitish-yellow crystal (35 mg, 60%). R_f 0.19 ($\text{CH}_3\text{CN}/\text{H}_2\text{O}$ 9:1), $[\alpha]_D^{24} +50.0$ (c 0.07, H_2O). ^1H NMR (400 MHz, $\text{DMSO}-d_6$) δ 5.51 (d, J = 7.6 Hz, 1H, H -14), 4.61 (s, 1H, OH), 3.63 – 3.46 (m, 3H, H -24ab), 3.40 – 3.29 (m, 3H, H -11, H -2'), 2.98 (s, 1H, H -4'), 2.57 (t, J = 7.0 Hz, 2H, H -23ab), 2.51 (s, 2H), 2.37 (t, J = 13.0 Hz, 3H, H -4), 2.23 – 2.02 (m, 3H, H -10, H -3'a), 1.96 (s, 3H), 1.91 – 1.78 (m, 2H, H -13a, H -5'a), 1.67 (t, J = 16.9 Hz, 3H, H -7a, H -8a), 1.49 (d, J = 5.9 Hz, 1H, H -6), 1.42 (d, J = 15.5 Hz, 1H), 1.37 (s, 3H, H -15abc), 1.33 – 1.18 (m, 7H, H -7b, H -3'a, H -5'b, H -6'ab), 1.12 (d, J = 16.0 Hz, 1H, H -13b), 1.07 – 0.98 (m, 1H, H -8b), 0.93 (s, 3H, H -18abc), 0.83 (d, J = 6.3 Hz, 3H, H -17abc), 0.64 (d, J = 6.2 Hz, 3H, H -16abc). ^{13}C NMR (101 MHz, $\text{DMSO}-d_6$) δ 217.1 (1C, C -3), 169.3 (1C, C -21), 73.5, 72.3 (2C, C -11, C -2'), 68.7 (1C, C -14), 61.0 (1C, C -24), 57.2 (1C, C -4), 49.5 (1C, C -1'), 47.3 (1C, C -4'), 45.0, 41.3, 40.6, 40.3 (4C, C -5, C -13, C -12, C -9), 36.4 (1C, C -6), 34.6 (1C, C -10), 33.9, 33.5, 30.5, 30.1, 28.3, 27.0, 26.7 (8C, C -3', C -5', C -6', C -1, C -2, C -19, C -20, C -23), 26.9 (1C, C -18), 24.3 (1C, C -7), 16.5 (1C, C -16), 14.6 (1C, C -15), 11.5 (1C, C -17). HRMS (ESI): m/z calcd for $\text{C}_{30}\text{H}_{52}\text{NO}_6\text{S}_2$: 586.3236 $[\text{M} + \text{H}]^+$; found: 586.3230.

Compound 80

Lefamulin (51 mg, 0.1 mmol) and **2-thio-*N*-acetylneuraminic acid per-*O*-acetate** ((203 mg, 0.4 mmol, 2x2 equiv.) were reacted in methanol at -80°C according to **general method E**, using two irradiation cycles (2x60 mins). The crude product was purified by flash column chromatography ($\text{CH}_2\text{Cl}_2/\text{MeOH}$ 85:15) resulted in compound **80** as yellow-white crystal (79 mg, 78%). R_f 0.56 ($\text{CH}_2\text{Cl}_2/\text{MeOH}$ 7:3), $[\alpha]_D^{24} +24.4$ (c 0.09, DMSO). ^1H NMR (400 MHz, $\text{DMSO}-d_6$) δ 7.77 (d, J = 6.5 Hz, 1H, NH), 5.42 (d, J = 6.8 Hz, 1H, H -14), 5.20 (d, J = 2.3 Hz, 1H, H -8''), 5.16 (d, J = 7.1 Hz, 1H), 4.69 (s, 1H, H -4''), 4.65 (s, 1H, OH), 4.21 (d, J = 12.1 Hz, 1H, H -9''a), 4.04 (dd, J = 11.6, 4.5 Hz, 1H, H -9''b), 3.84 (s, 1H, H -5''), 3.80 (d, J = 1.6 Hz, 1H), 3.54 (d, J = 14.5 Hz, 1H), 3.42 (s, 5H), 3.33 (d, J = 12.8 Hz, 3H, H -11, H -2'), 3.02 (s, 1H, H -4'), 2.64 (d, J = 8.7 Hz, 1H, H -3''a), 2.56 (s, 1H, H -1'), 2.51 (d, J = 1.4 Hz, 2H), 2.35 (s, 1H, H -4), 2.16 (d, J = 10.9 Hz, 2H, H -5'a, H -10), 2.07 (d, J = 1.7 Hz, 3H, CH_3 acetyl), 2.01 (s, 3H, CH_3 acetyl), 1.96 (s, 3H, CH_3 acetyl), 1.92 (d, J = 1.7 Hz, 3H, CH_3 acetyl), 1.83 (d, J = 16.5 Hz, 1H, H -13a), 1.75 (d, J = 12.3 Hz, 1H, H -3''b), 1.65 (s, 5H, CH_3 acetyl, H -7a, H -8a), 1.49 (s, 2H, H -6), 1.37 (s, 3H, H -15abc), 1.23 (s, 6H, H -7b), 1.13 (d, J =

16.1 Hz, 2H, *H*-13b), 1.08 – 0.95 (m, 2H, *H*-8b), 0.90 (s, 3H, *H*-18abc), 0.80 (d, *J* = 5.4 Hz, 3H, *H*-17abc), 0.64 (d, *J* = 5.7 Hz, 3H, *H*-16abc). ¹³C NMR (101 MHz, DMSO-*d*₆) δ 217.1 (1C, *C*-3), 170.1, 169.7, 169.4, 169.3, 169.3, 169.1, 168.4 (7C, 7xCO), 83.1 (1C, *C*-2''), 73.7, 73.3, 72.3, 67.3 (4C, *C*-11, *C*-2', *C*-7'', *C*-6''), 69.6 (1C, *C*-4'), 68.9 (1C, *C*-14), 68.4 (1C, *C*-8''), 61.8 (1C, *C*-9''), 57.2 (1C, *C*-4), 54.9, 53.0 (1C, COOCH₃), 49.7 (1C, *C*-1'), 47.8 (1C, *C*-5''), 47.2 (1C, *C*-4'), 44.9 (1C, *C*-9), 41.2, 40.6 (3C, *C*-13, *C*-12, *C*-5), 36.4 (1C, *C*-6), 34.4 (1C, *C*-10), 33.9 (1C, *C*-5'), 33.7 (1C, *C*-22), 30.1 (1C, *C*-8), 29.8, 29.6, 28.2, 26.8, 23.7 (6C, *C*-19, *C*-20, *C*-3', *C*-6', *C*-1, *C*-2), 26.2 (1C, *C*-18), 24.3 (1C, *C*-7), 22.6 (1C, NAcCH₃), 20.9, 20.7, 20.6, 20.6 (4C, 4xOAcCH₃), 16.8 (1C, *C*-16), 14.6 (1C, *C*-15), 11.5 (1C, *C*-17). HRMS (ESI): *m/z* calcd for C₄₈H₇₅N₂O₁₇S₂: 1015.4507 [M + H]⁺; found: 1015.4502.

Compound 81

Compound **81** was prepared from compound **80** (58mg, 0.057mmol) according to **general method F**. The crude product was purified by flash column chromatography (CH₃CN/H₂O 9:1) to obtain **81** as white powder (25 mg, 53%). *R*_f 0.4 (CH₃CN/H₂O 8:2), [α]²⁴_D -3.33 (c 0.06, DMSO). ¹H NMR (400 MHz, DMSO-*d*₆) δ 8.05 (d, *J* = 7.9 Hz, 1H, NH), 5.49 (d, *J* = 7.8 Hz, 1H, *H*-14), 5.17 (s, 1H, *H*-8''), 4.87 (s, 1H), 4.69 (s, 1H, *H*-4''), 4.48 (d, *J* = 5.5 Hz, 1H), 4.08 (s, 1H), 3.60 (t, *J* = 14.9 Hz, 4H, *H*-5'', *H*-9''a, *H*-11, *H*-2'), 3.26 (s, 1H, *H*-9''b), 3.16 (s, 2H), 2.98 (s, 1H, *H*-4'), 2.89 (s, 1H), 2.74 (s, 2H), 2.69 (dd, *J* = 8.6, 3.6 Hz, 1H, *H*-22a), 2.63 (d, *J* = 12.8 Hz, 1H, *H*-1'), 2.56 (d, *J* = 6.7 Hz, 1H, *H*-22b), 2.35 (s, 1H, *H*-4), 2.21 – 2.08 (m, 3H, *H*-5'a, *H*-10), 2.03 (d, *J* = 9.2 Hz, 3H, *H*-5'b), 1.89 (s, 3H), 1.77 (t, *J* = 16.3 Hz, 4H, *H*-13a), 1.63 (dd, *J* = 21.1, 9.8 Hz, 3H, *H*-7a, *H*-8a), 1.48 (dd, *J* = 21.3, 10.7 Hz, 5H, *H*-6), 1.33 (s, 3H), 1.24 (s, 3H, *H*-7b), 1.19 (s, 3H, *H*-13b), 1.03 (dd, *J* = 16.5, 4.5 Hz, 2H, *H*-8b), 0.94 (s, 3H, *H*-18abc), 0.83 (d, *J* = 6.5 Hz, 3H, *H*-17abc), 0.61 (d, *J* = 6.3 Hz, 3H, *H*-16abc). ¹³C NMR (101 MHz, DMSO-*d*₆) δ 217.2 (1C, *C*-3), 172.4, 172.2, 168.5 (3C, CO acetyl, *C*-1'', *C*-21), 84.8 (1C, *C*-2''), 75.2, 73.5, 72.0, 71.2 (4C, *C*-11, *C*-2'), 68.8, 68.6 (2C, *C*-8'', *C*-14), 67.7, 63.2 (2C, *C*-9''), 57.2 (1C, *C*-4), 54.9, 52.8, 49.8 (3C, *C*-1'), 47.3, 47.1 (2C, *C*-4'), 44.9 (1C, *C*-9), 42.3, 41.2, 40.9 (3C, *C*-12, *C*-13, *C*-5), 36.4 (1C, *C*-6), 35.8, 34.4 (2C, *C*-10), 34.0 (1C, *C*-5'), 33.0 (1C, *C*-22), 31.1, 28.9, 30.1 (3C, *C*-8), 26.8 (1C, *C*-18), 24.4 (1C, *C*-7), 24.2 (1C, *C*-22), 22.5 (1C, CH₃ acetyl), 16.4 (1C, *C*-6), 14.6 (1C, *C*-15), 11.4 (1C, *C*-17). HRMS (ESI): *m/z* calcd for C₃₉H₆₄N₂NaO₁₃S₂: 855.3748 [M + Na]⁺; found: 855.3746.

8. References

8.1 References

1. Shallcross, L.J., Howard, S.J., Fowler, T., Davies, S.C. Tackling the threat of antimicrobial resistance: from policy to sustainable action. *Phil. Trans. R. Soc.*, **2015**, B 370: 20140082.
2. McArthur, A.G., Waglechner, N., Nizam, F., Yan, A., Azad, M.A., Baylay, A.J., Bhullar, K., Canova, M.J., De Pascale, G., Ejim, L., Kalan, L., King, A.M., Koteva, K., Morar, M., Mulvey, M.R., O'Brien, J.S., Pawlowski, A.C., Piddock, L.J., Spanogiannopoulos, P., Sutherland, A.D., Tang, I., Taylor, P.L., Thaker, M., Wang, W., Yan, M., Yu, T., Wright, G.D. The comprehensive antibiotic resistance database. *Antimicrob. Agents Chemother.*, **2013**, 57(7):3348-57.
3. Ventola, C.L. The antibiotic resistance crisis: Part 1: causes and threats. *PandT.*, **2015**, 40(4):277-83.
4. Ventola, C.L. The antibiotic resistance crisis: Part 2: management strategies and new agents. *PandT.*, **2015**, 40(5):344-52.
5. Watkins, R.R., Bonomo, R.A. Overview: The Ongoing Threat of Antimicrobial Resistance. *Infect. Dis. Clin. North Am.*, **2020**, 34(4):649-58.
6. Global antimicrobial resistance surveillance system (GLASS) report: early implementation 2020. Geneva: World Health Organization, **2020**. Licence: CC BY-NC—SA 3.0 IGO.
7. EFSA and ECDC (European Food Safety Authority and European Centre for Disease Prevention and Control). The European Union Summary Report on Antimicrobial Resistance in zoonotic and indicator bacteria from humans, animals and food in 2018/2019. *EFSA Journal.*, **2021**, 19(4):6490, 179.
8. CDC. Antibiotic Resistance Threats in the United States. Atlanta, GA: U.S. Department of Health and Human Services. *CDC*, **2019**.
9. Ahmad, M., Khan, A.U. Global economic impact of antibiotic resistance: A review. *J. Glob. Antimicrob. Resist.*, **2019**, 19:313-16.
10. Cosgrove, S.E., Carmeli, Y. The impact of antimicrobial resistance on health and economic outcomes. *Clin. Infect. Dis.*, **2003**, 36:1433-37.
11. Bonnet, V., Dupont, H., Glorion, S., Aupée, M., Kipnis, E., Gérard, J.L., Hanouz, J.L., Fischer, M. O. Influence of bacterial resistance on mortality in intensive care units: A registry study from 2000 to 2013 (IICU Study). *J. Hosp. Infect.*, **2019**, 102(3):317-24.

12. Hay, S.I., Rao, P.C., Dolecek, C., Day, N.P.J., Stergachis, A., Lopez, A.D., Murray, C.J.L. Measuring and mapping the global burden of antimicrobial resistance. *BMC Medicine.*, **2018**, 16(1):78.
13. Hawkey, P.M. The growing burden of antimicrobial resistance. *J. Antimicrob. Chemother.*, **2008**, 62(1):1-9.
14. Livermore, D.M. Has the era of untreatable infections arrived? *J. Antimicrob. Chemother.*, **2009**, 64(1):29-36.
15. Wester, A.L., Gopinathan, U., Gjefle, K., Solberg, S.Ø., Røttingen, J.-A. Antimicrobial Resistance in a One Health and One World Perspective-Mechanisms and Solutions. *International Encyclopedia of Public Health*, **2017**, 140-153.
16. Morrison, L., Zembower, T.R. Antimicrobial Resistance. *Gastrointest. Endosc. Clin. N Am.*, **2020**, 30(4):619-35.
17. Martínez, J.L., Baquero, F. Emergence and spread of antibiotic resistance: setting a parameter space. *Ups. J. Med. Sci.*, **2014**, 119(2):68-77.
18. Munita, J.M., Arias, C.A. Virulence Mechanisms of bacterial pathogens (5th edition), chapter 17: Mechanisms of antibiotic resistance. *Microbiol. Spectr.*, **2016**, 4(2):10.
19. Walsh, C. Molecular mechanisms that confer antibacterial drug resistance. *Nature*, **2000**, 406(6797):775-81.
20. Botelho, J., Grosso, F., Peixe, L. Antibiotic resistance in *Pseudomonas aeruginosa*-mechanisms, epidemiology and evolution. *Drug Resist. Updat.*, **2019**, 44:26-47.
21. Kanagaratnam, R., Sheikh, R., Alharbi, F., Kwon, D.H. An efflux pump (MexAB-OprM) of *Pseudomonas aeruginosa* is associated with antibacterial activity of Epigallocatechin-3-gallate (EGCG). *Phytomedicine*, **2017**, 36:194-200.
22. Aloush, V., Navon-Venezia, S., Seigman-Igra, Y., Cabili, S., Carmeli, Y. Multidrug-resistant *Pseudomonas aeruginosa*: risk factors and clinical impact. *Antimicrob. Agents. Chemother.*, **2006**, 50(1):43-8.
23. Kariminik, A., Baseri-Salehi, M., Kheirkhah, B. *Pseudomonas aeruginosa* quorum sensing modulates immune responses: An updated review article. *Immunol. Lett.*, **2017**, 190:1-6.
24. Driscoll, J.A., Brody, S.L., Kollef, M.H. The epidemiology, pathogenesis and treatment of *Pseudomonas aeruginosa* infections. *Drugs*, **2007**, 67(3):351-68.
25. Gonçalves-de-Albuquerque, C. F., Silva, A. R., Burth, P., Rocco, P. R. M., Castro-Faria, M.V., Castro-Faria-Neto, H.C. Possible mechanisms of *Pseudomonas aeruginosa*-associated lung disease. *Int. J. Med. Microbiol.*, **2016**, 306(1): 20-28.

26. Osmon, S., Ward, S., Fraser, V.J., Kollef, M.H. Hospital mortality for patients with bacteremia due to *Staphylococcus aureus* or *Pseudomonas aeruginosa*. *Chest.*, **2004**, 125(2):607-16.
27. Liener, I.E., Sharon, N., Goldstein, I.J. The Lectins: Properties, Functions and Applications in Biology and Medicine, chapter 5: Applications of lectins. *Academic Press, Inc.*, **1986**, 293-370.
28. Sharon, N., Lis, H. Lectins: Carbohydrate-specific proteins that mediate cellular recognition. *Chem. Rev.*, **1998**, 98:637-74.
29. Bianchet, M.A., Ahmed, H., Vasta, G.R., Amzel, L.M. Animal lectins: A functional view, chapter 2: Structural aspects of lectin-ligand interactions. *CRC Press*, **2009**, 13-31.
30. Shanmugham, L.N., Castellani, M.L., Salini, V., Falasca, K., Vecchiet, J., Conti, P., Petrarca, C. Relevance of plant lectins in human cell biology and immunology. *Riv Biol.*, **2006**, 99(2):227-49.
31. Imberty, A., Varrot, A. Microbial recognition of human cell surface glycoconjugates. *Curr. Opin. Struct. Biol.*, **2008**, 18(5):567-76.
32. Pieters, R.J. Carbohydrate mediated bacterial adhesion. *Bacterial Adhesion*, **2011**, 715:227-40.
33. Esko, J.D., Sharon, N. Essentials of Glycobiology (2nd edition), chapter 34: Microbial Lectins: Hemagglutinins, Adhesins, and Toxins. *Cold Spring Harbor Laboratory Press*, **2009**.
34. Karlsson, K.A. Pathogen-host protein-carbohydrate interactions as the basis of important infections. *Adv. Exp Med Biol.*, **2001**, 491:431-43.
35. Sharon, N. Carbohydrate-lectin interactions in infectious disease. *Adv Exp Med Biol.*, **1996**, 408:1-8.
36. Zeng, H., Goldsmith, C.S., Maines, T.R., Belser, J.A., Gustin, K.M., Pekosz, A., Zaki, S.R., Katz, J.M., Tumpey, T.M. Tropism and infectivity of influenza virus, including highly pathogenic avian *H5N1* virus, in ferret tracheal differentiated primary epithelial cell cultures. *J. Virol.*, **2013**, 87(5):2597-607.
37. Van Riel, D., Munster, V.J., de Wit, E., Rimmelzwaan, G.F., Fouchier, R.A., Osterhaus, A.D., Kuiken, T. Human and avian influenza viruses target different cells in the lower respiratory tract of humans and other mammals. *Am. J. Pathol.*, **2007**, 171(4):1215-23.
38. Van Riel, D., Kuiken, T. The role of cell tropism for the pathogenesis of influenza in humans. *Future Virol.*, **2012**, 7(3):295-307.

39. Lan, J., Ge, J., Yu, J., Shan, S., Zhou, H., Fan, S., Zhang, Q., Shi, X., Wang, Q., Zhang, L., Wang, X. Structure of the SARS-CoV-2 spike receptor-binding domain bound to the ACE2 receptor. *Nature*, **2020**, 581(7807):215-20.
40. Liu, J., Li, Y., Liu, Q., Yao, Q., Wang, X., Zhang, H., Chen, R., Ren, L., Min, J., Deng, F., Yan, B., Liu, L., Hu, Z., Wang, M., Zhou, Y. SARS-CoV-2 cell tropism and multiorgan infection. *Cell Discov.*, **2021**, 7(1):17.
41. Li, W., Zhang, C., Sui, J., Kuhn, J.H., Moore, M.J., Luo, S., Wong, S.K., Huang, I.C., Xu, K., Vasilieva, N., Murakami, A., He, Y., Marasco, W.A., Guan, Y., Choe, H., Farzan, M. Receptor and viral determinants of SARS-coronavirus adaptation to human ACE2. *EMBO J.*, **2005**, 24(8):1634-43.
42. Ofek, I. Doyle, R.J. Bacterial Adhesion to Cells and Tissues, chap 1: Principle of bacterial adhesion. *Chapman & Hall*, **1994**, 1-15.
43. Ofek, I., Bayer, E.A., Abraham, S.N. Bacterial Adhesion. *The Prokaryotes*, **2013**, 107-123.
44. Vestby, L.K., Grønseth, T., Simm, R., Nesse, L.L. Bacterial Biofilm and its Role in the Pathogenesis of Disease. *Antibiotics*, **2020**, 9, 59.
45. Singh, R.S., Walia, A.K., Kennedy, J.F. Structural aspects and biomedical applications of microfungus lectins. *Int. J. Biol. Macromol.*, **2019**, 134:1097-107.
46. Kotecha, H., Poduval, P.B. Microbial lectins. *Adv. Biol Res.*, **2019**, 135-47.
47. Lavín de Juan, L., García Recio, V., Jiménez López, P., Gírbés Juan, T., Córdoba-Díaz, M., Córdoba-Díaz, D. Pharmaceutical applications of lectins. *J. Drug. Deliv. Sci. Tech.*, **2017**, 42:126-33.
48. Disney, M.D., Seeberger, P.H. The Use of Carbohydrate Microarrays to Study Carbohydrate-Cell Interactions and to Detect Pathogens. *Chem. Biol.*, **2004**, 11(12):1701-07.
49. Schumacher, U. Lectins: Biomedical Perspectives (1st ed.), chapter11: Lectins and Cancer-An Old Field Revisited. *CRC Press*, **1995**, 178-89.
50. Wdowiak, K., Francuz, T., Gallego-Colon, E., Ruiz-Agamez, N., Kubeczko, M., Grochoła, I., Wojnar, J. Galectin Targeted Therapy in Oncology: Current Knowledge and Perspectives. *Int. J. Mol. Sci.*, **2018**, 19(1):210.
51. Wizemann, T.M., Adamou, J.E., Langermann, S. Adhesins as targets for vaccine development. *Emerg.Infect.Dis.*, **1999**, 5:395-403.
52. Wang, L.-X. Glycobiology and Drug Design, chapter 6: Carbohydrate-Based Vaccines against HIV/AIDS. *Glycobiology and Drug Design*, **2012**, 157-86.
53. Klyosov, A.A. Glycobiology and Drug Design, chapter 2: Galectin-Targeted Drug Design. *Glycobiology and Drug Design*, **2012**, 25-66.

54. Ofek, I., Hasty, D.L., Sharon, N. Anti-adhesion therapy of bacterial diseases: prospects and problems. *FEMS Immunol.Med. Microbiol.*, **2003**, 38(3):181-91.
55. Krachler, A.M., Orth, K. Targeting the bacteria–host interface. *Virulence*, **2013**, 4(4):284-94.
56. Cozens, D., Read, R.C. Anti-adhesion methods as novel therapeutics for bacterial infections. *Expert. Rev. Anti. Infect. Ther.*, **2012**,10(12):1457-68.
57. Shoaf-Sweeney, K.D., Hutkins, R.W. Adherence, anti-adherence, and oligosaccharides preventing pathogens from sticking to the host. *Adv. Food. Nutr. Res.*, **2009**, 55:101-61.
58. Asadi, A., Razavi, S., Talebi, M., Gholami, M.A. A review on anti-adhesion therapies of bacterial diseases. *Infection*, **2019**, 47(1):13-23.
59. Aronson, M., Medalia, O., Schori, L., Mirelman, D., Sharon, N., Ofek, I. Prevention of colonization of the urinary tract of mice with *Escherichia coli* by blocking of bacterial adherence with methyl alpha-D-mannopyranoside. *J.Infect.Dis.*, **1979**, 139:329-32.
60. Lindhorst, T.K., Kieburg, C., Krallmann-Wenzel, U. Inhibition of the type 1 fimbriae-mediated adhesion of *Escherichia coli* to erythrocytes by multiantennary alpha-mannosyl clusters: the effect of multivalency. *Glycoconj J.*, **1998**,15(6):605-13.
61. Boukerb, A.M., Rousset, A., Galanos, N., Méar, J.-B., Thépaut, M., Grandjean, T., Gillon, E., Cecioni, S., Abderrahmen, C., Faure, K., Redelberger, D., Kipnis, E., Dessen, R., Havet, S., Darblade, B., Matthews, S. E., Bentzmann, S., Guéry, B., Cournoyer, B., Imbery, A., Vidal, S. Antiadhesive Properties of Glycoclusters against *Pseudomonas aeruginosa* Lung Infection. *J. Med. Chem.*, **2014**, 57(24):10275-89.
62. Jayaraman, N. Multivalent ligand presentation as a central concept to study intricate carbohydrate-protein interactions. *Chem. Soc. Rev.*, **2009**, 38(12):3463-83.
63. Pieters, R.J. Maximising multivalency effects in protein-carbohydrate interactions. *Org. Biomol. Chem.*, **2013**, 7(10):2013-25.
64. Dam, T.K., Brewer, C.F. Multivalent Lectin-Carbohydrate Interactions: Energetics and Mechanism of Binding. *Adv. Carbohydr. Chem. Biochem.*, **2010**, 139-64.
65. Cecioni, S., Imbery, A., Vidal, S. Glycomimetics versus Multivalent Glycoconjugates for the Design of High Affinity Lectin Ligands. *Chem. Rev.*, **2014**, 115(1):525-61.
66. Lahmann, M. Architectures of Multivalent Glycomimetics for Probing Carbohydrate-Lectin Interactions. *Top. Curr. Chem.*, **2009**, 288:17–65.
67. Deniaud, D., Julienne, K., Gouin, S.G. Insights in the rational design of synthetic multivalent glycoconjugates as lectin ligands. *Org. Biomol. Chem.*, **2011**, 9(4):966-79.
68. Kadam, R.U., Bergmann, M., Hurley, M., Garg, D., Cacciarini, M., Swiderska, M.A., Nativi, C., Sattler, M., Smyth, A.R., Williams, P., Cámara, M., Stocker, A., Darbre,

- T., Reymond, J.L. A glycopeptide dendrimer inhibitor of the galactose-specific lectin LecA and of *Pseudomonas aeruginosa* biofilms. *Angew. Chem. Int. Ed. Engl.*, **2011**, 50(45):10631-5.
69. Donnier-Maréchal, M., Galanos, N., Grandjean, T., Pascal, Y., Ji, D.-K., Dong, L., Gillon, E., He, X.-P., Imberty, A., Kipnis, E., Desseinc, R., Sébastien Vidal, S. Perylenediimide-based glycoclusters as high affinity ligands of bacterial lectins: synthesis, binding studies and anti-adhesive properties. *Org. Biomol Chem.*, **2017**, 15(47):10037-43.
70. Cecioni, S., Faure, S., Darbost, U., Bonnamour, I., Parrot-Lopez, H., Roy, O., Taillefumier, C., Wimmerova, M., Praly J.-P., Imberty, A., Vidal, S. Selectivity among Two Lectins: Probing the Effect of Topology, Multivalency and Flexibility of “Clicked” Multivalent Glycoclusters. *Chem. Eur. J.*, **2011**, 17(7):2146-59.
71. Bernardi, A., Jiménez-Barbero, J., Casnati, A., Castro, C. D., Darbre, T., Fieschi, F., Finne, J., Funken, H., Jaeger, K.-E., Lahmann, M., Lindhorst, T. K., Marradi, M., Messner, P., Molinaro, A., Murphy, P., Nativi, C., Oscarson, S., Penadés, S., Peri, F., Pieters, R.J., Renaudet, O., Reymond, J.-L., Richichi, B., Rojo, J., Sansone, F., Schäffer, C., Turnbull, W.B., Velasco-Torrijos, T., Vidal, S., Vincent, S., Wennekes, T., Zuilhof, H., Imberty, A. Multivalent glycoconjugates as antipathogenic agents. *Chem. Soc. Rev.*, **2013**, 42:4709-27.
72. Reymond, J.L., Bergmann, M., Darbre, T. Glycopeptide dendrimers as *Pseudomonas aeruginosa* biofilm inhibitors. *Chem. Soc. Rev.*, **2013**, 42:4814-22.
73. Jimenez Blanco, J.L., Ortiz Mellet, C., Garcia Fernandez, J.M. Multivalency in heterogeneous glycoenvironments: hetero-glycoclusters, -glycopolymers and -glycoassemblies. *Chem. Soc. Rev.*, **2013**, 42:4518-31.
74. Hatano, K., Matsuoka, K., Terunuma, D. Carbosilane glycodendrimers. *Chem. Soc. Rev.*, **2012**, 42:4574-98.
75. Galan, M.C., Dumy, P., Renaudet, O. Multivalent glyco(cyclo)peptides. *Chem. Soc. Rev.*, **2013**, 42:4599-612.
76. Sansone, F., Casnati, A. Multivalent glycoalexarenes for recognition of biological macromolecules: glycoalyx mimics capable of multitasking. *Chem. Soc. Rev.*, **2013**, 42:4623-39.
77. Martinez, A., Ortiz Mellet, C., Garcia Fernandez, J.M. Cyclodextrin-based multivalent glycodisplays: covalent and supramolecular conjugates to assess carbohydrate-protein interactions. *Chem. Soc. Rev.*, **2013**, 42:4746-73.
78. Kelsey, S.M., Collins, P.W., Delord, C., Weinhard, B., Newland, A.C. A randomized study of teicoplanin plus ciprofloxacin versus gentamicin plus piperacillin for the

- empirical treatment of fever in neutropenic patients. *Br. J. Haematol.*, **1990**, 76(2):10-3.
79. Wistrand-Yuen, P., Olsson, A., Skarp, K.-P., Friberg, L. E., Nielsen, E.I., Lagerbäck, P., Tängdén, T. Evaluation of polymyxin B in combination with 13 other antibiotics against carbapenemase-producing *Klebsiella pneumoniae* in time-lapse microscopy and time-kill experiments. *Clin. Microbiol.Infect.*, **2020**, 26:1214-21.
80. Paul, M., Carmeli, Y., Durante-Mangoni, E., Mouton, J.W., Tacconelli, E., Theuretzbacher, U., Mussini, C., Leibovici, L. Combination therapy for carbapenem-resistant Gram-negative bacteria. *J. Antimicrob. Chemother.*, **2014**, 69(9):2305-9.
81. Scudeller, L., Righi, E., Chiamenti, M., Bragantini, D., Menchinelli, G., Cattaneo, P., Giske, C., Lodise, T., Sanguinetti, M., Piddock, L.J., Franceschi, F., Ellis, S., Carrara, E., Savoldi, A., Tacconelli, E. Systematic review and meta-analysis of in vitro efficacy of antibiotic combination therapy against carbapenem-resistant Gram-negative bacilli. *Int. J. Antimicrob. Agents.*, **2021**, 57(5):106344.
82. Plotz, P.H., Davis, B.D. Synergism between streptomycin and penicillin: a proposed mechanism. *Science*, **1962**, 135:1067-68.
83. Ofek, I., Cohen, S., Rahmani, R., Kabha, K., Tamarkin, D., Herzig, Y., Rubinstein, E. Antibacterial synergism of polymyxin B nonapeptide and hydrophobic antibiotics in experimental Gram-negative infections in mice. *Antimicrob. Agents. Chemother.*, **1994**, 38:374-7.
84. Sullivan, G.J., Delgado, N.N., Maharjan, R., Cain, A.K. How antibiotics work together: molecular mechanisms behind combination therapy. *Curr. Opin. Microbiol.*, **2020**, 57:31-40.
85. Tschudin-Sutter, S., Fosse, N., Frei, R., Widmer, A.F. Combination therapy for treatment of *Pseudomonas aeruginosa* bloodstream infections. *PloS ONE*, **2018**, 13(9):e0203295.
86. Blaskovich, M.A.T., Hansford, K.A., Butler, M.S., Jia, Z., Mark, A.E., Cooper, M.A. Developments in Glycopeptide Antibiotics. *ACS Infect. Dis.*, **2018**, 4(5):715-35.
87. Cândido, E. de S., de Barros, E., Cardoso, M.H., Franco, O.L. Bacterial cross-resistance to anti-infective compounds. Is it a real problem? *Curr. Opin. Pharmacol.*, **2019**, 48:76-81.
88. Gorityala, B.K., Guchhait, G., Fernando, D.M., Deo, S., McKenna, S.A., Zhanel, G.G., Kumar, A., Schweizer, F. Adjuvants Based on Hybrid Antibiotics Overcome Resistance in *Pseudomonas aeruginosa* and Enhance Fluoroquinolone Efficacy. *Angew. Chem. Int. Ed. Engl.*, **2016**, 55(2):555-9.

89. Parkes, A.L., Yule, I.A. Hybrid Antibiotics-Clinical Progress and Novel Designs, *Expert Opin. Drug Discov.*, **2016**, 11(7):665-80.
90. Barbachyn, M. R. Recent Advances in the Discovery of Hybrid Antibacterial Agents. *Annu. Rep. Med. Chem.*, **2008**, 281-290.
91. Högberg, L.D., Heddini, A., Cars, O. The global need for effective antibiotics: challenges and recent advances. *Trends Pharmacol. Sci.*, **2010**, 31(11):509-15.
92. Fernandes, P., Martens, E. Antibiotics in Late Clinical Development. *Biochem Pharmacol.*, **2016**, 133:152-63.
93. Rios, A.C., Moutinho, C.G., Pinto, F.C., Del Fiol, F.S., Jozala, A., Chaud, M.V., Vila, M.M., Teixeira, J.A., Balcão, V.M. Alternatives to overcoming bacterial resistances: State-of-the-art. *Microbiol. Res.*, **2016**, 191:51-80.
94. Singh, S.B., Young, K., Silver, L.L. What is an “Ideal” Antibiotic? Discovery Challenges and Path forward. *Biochem.Pharmacol.*, **2017**,133:63-73.
95. Chemani, C., Imberty, A., de Bentzmann, S., Pierre, M., Wimmerová, M., Guery, B.P., Faure, K. Role of LecA and LecB lectins in *Pseudomonas aeruginosa*-induced lung injury and effect of carbohydrate ligands. *Infect Immun.*, **2009**, 77(5):2065-75.
96. Imberty, A., Wimmerová, M., Mitchell, E.P., Gilboa-Garber, N. Structures of the lectins from *Pseudomonas aeruginosa*: insight into the molecular basis for host glycan recognition. *Microbes Infect.*, **2004**, 6(2):221-8.
97. Grishin, A.V., Krivozubov, M.S., Karyagina, A.S., Gintsburg, A.L. *Pseudomonas aeruginosa* Lectins As Targets for Novel Antibacterials. *Acta Naturae.*, **2015**, 7(2):29-41.
98. Bucior, I., Abbott, J., Song, Y., Matthay, M.A., Engel, J.N. Sugar administration is an effective adjunctive therapy in the treatment of *Pseudomonas aeruginosa* pneumonia. *Am. J. Physiol. Lung Cell Mol. Physiol.*, **2013**, 305(5):352-63.
99. Hauber, H.P., Schulz, M., Pforte, A., Mack, D., Zabel, P., Schumacher, U. Inhalation with fucose and galactose for treatment of *Pseudomonas aeruginosa* in cystic fibrosis patients. *Int. J. Med. Sci.*, **2008**, 5(6):371-6.
100. Von Bismarck, P., Schneppenheim, R., Schumacher, U. Successful treatment of *Pseudomonas aeruginosa* respiratory tract infection with a sugar solution-a case report on a lectin based therapeutic principle. *Klin. Padiatr.*, **2001**, 213(5):285-7.
101. Park, J.W., Nam, S.J., Yoon, Y.J. Enabling techniques in the search for new antibiotics: Combinatorial biosynthesis of sugar-containing antibiotics. *Biochem. Pharmacol.*, **2017**, 134:56-73.

102. Karoli, T., Mamidyala, S.K., Zuegg, J., Fry, S.R., Tee, E.H., Bradford, T.A., Madala, P.K., Huang, J.X., Ramu, S., Butler, M.S., Cooper, M.A. Structure aided design of chimeric antibiotics. *Bioorg. Med. Chem. Lett.*, **2012**, 22(7):2428-33.
103. Otvos, L., Snyder, C., Condie, Bulet, P., Wade, J.D. Chimeric Antimicrobial Peptides Exhibit Multiple Modes of Action. *Int. J. Pept. Res. Ther.*, **2005**, 11:29-42.
104. Křen, V., Řezanka, T. Sweet antibiotics-the role of glycosidic residues in antibiotic and antitumor activity and their randomization, *FEMS Microbiol. Rev.*, **2008**, 32:858-889.
105. Andersson, M.I., MacGowan, A.P. Development of the quinolones. *J. Antimicrob Chemother.*, **2003**, 51(1):1-11.
106. Ball, P., Fernald, A., Tillotson, G. Therapeutic advances of new fluoroquinolones. *Expert Opin. Investig. Drugs*, **1998**, 7:761-83.
107. Gootz, T.D., Brighty, K.E. Fluoroquinolone antibacterials: SAR mechanism of action, resistance, and clinical aspects. *Med. Res. Rev.*, **1996**, 16:433-86.
108. Zhanel, G.G., Ennis, K., Vercaigne, L., Walkty, A., Gin, A.S., Embil, J., Smith, H., Hoban, D.J. A critical review of the fluoroquinolones: focus on respiratory infections. *Drugs*, **2002**, 62:13-59.
109. Blondeau, J.M. Fluoroquinolones: mechanism of action, classification, and development of resistance. *Surv. Ophthalmol.*, **2004**, 49(2):73-8.
110. Kavanagh, F., Hervey, A., Robbins, W.J. Antibiotic Substances From Basidiomycetes: VIII. *Pleurotus Multilus* (Fr.) Sacc. and *Pleurotus Passeckerianus* Pilat. *Proc. Natl. Acad. Sci. U.S.A.*, **1951**, 37(9):570-4.
111. Kavanagh, F., Hervey, A., Robbins, W.J. Antibiotic Substances from *Basidiomycetes*: IX. *Drosophila Subtarata*. (Batsch Ex Fr.) Quel. *Proc. Natl. Acad. Sci. U.S.A.*, **1952**, 38(7):555-60.
112. Davidovich, C., Bashan, A., Auerbach-Nevo, T., Yaggie, R.D., Gontarek, R.R., Yonath, A. Induced-fit tightens pleuromutilins binding to ribosomes and remote interactions enable their selectivity. *Proc. Natl. Acad. Sci. U.S.A.*, **2007**, 104(11):4291-6.
113. Fazakerley, N. J., Procter, D. J. Synthesis and synthetic chemistry of pleuromutilin. *Tetrahedron*, **2014**, 70(39):6911-30.
114. Goethe, O., Heuer, A., Ma, X., Wang, Z., Herzon, S.B. Antibacterial properties and clinical potential of pleuromutilins. *Nat. Prod. Rep.*, **2019**, 36(1):220-47.
115. Dong, Y.J., Meng, Z.H., Mi, Y.Q., Zhang, C., Cui, Z.H., Wang, P., Xu, Z.B. Synthesis of novel pleuromutilin derivatives. Part 1: preliminary studies of antituberculosis activity. *Bioorg. Med Chem Lett.*, **2015**, 25(8):1799-803.

116. Mu, S., Liu, H., Zhang, L., Wang, X., Xue, F., Zhang, Y. Synthesis and Biological Evaluation of Novel Thioether Pleuromutilin Derivatives. *Biol. Pharm. Bull.*, **2017**, 40(8):1165-73.
117. Lemieux, M.R., Siricilla, S., Mitachi, K., Eslamimehr, S., Wang, Y., Yang, D., Pressly, J.D., Kong, Y., Park, F., Franzblau, S.G., Kurosu, M. An antimycobacterial pleuromutilin analogue effective against dormant *bacilli*. *Bioorg. Med. Chem.*, **2018** 26(17):4787-96.
118. Zhang, Z., Li, K., Zhang, G.-Y., Tang, Y.-Z., Jin, Z. Design. Synthesis and biological activities of novel pleuromutilin derivatives with a substituted triazole moiety as potent antibacterial agents. *Eur. J. Med. Chem.*, **2020**, 204:112604.
119. Shang, R., Pu, X., Xu, X., Xin, Z., Zhang, C., Guo, W., Liu, Yu., Liang, J. Synthesis and Biological Activities of Novel Pleuromutilin Derivatives with a Substituted Thiadiazole Moiety as Potent Drug-Resistant Bacteria Inhibitors. *J. Med. Chem.*, **2014**, 57(13):5664-78.
120. Shang, R., Wang, S., Xu, X., Yi, Y., Guo, W., Yu, L., Liang, J. Chemical Synthesis and Biological Activities of Novel Pleuromutilin Derivatives with Substituted Amino Moiety. *PLoS ONE*, **2013**, 8(12):e82595.
121. Shang, R.F., Wang, G.H., Xu, X.M., Liu, S.J., Zhang, C., Yi, Y.P., Liang, J.P., Liu, Y. Synthesis and biological evaluation of new pleuromutilin derivatives as antibacterial agents. *Molecules*, **2014**, 19(11):19050-65.
122. Fan, Y., Liu, Y., Wang, H., Shi, T., Cheng, F., Hao, B., Yi, Y., Shang, R. Novel pleuromutilin derivatives with substituted 6-methylpyrimidine: Design, synthesis and antibacterial evaluation. *Eur. J. Med. Chem.*, **2020**, 207:112735.
123. Huang, S.-Y., Wang, X., Shen, D.-Y., Chen, F., Zhang, G.-Y., Zhang, Z., Li, K., Jin, Z., Du, D., Tang, Y.-Z. Design, synthesis and biological evaluation of novel pleuromutilin derivatives as potent anti-MRSA agents targeting the 50S ribosome. *Bioorg. Med. Chem.*, **2021**, 38:116138.
124. Paukner, S., Riedl, R. Pleuromutilins: Potent Drugs for Resistant Bugs-Mode of Action and Resistance. *Cold Spring Harb. Perspect. Med.*, **2017**, 7(1):a027110.
125. Thirring, K., Heilmayer, W., Riedl, R., Kollmann, H., IvezicSchoenfeld, Z., Wicha, W., Paukner, S., Strickmann, D. World Pat., WO2015110481 A1, **2015**.
126. Breugst, M., Reissig, H.U. The Huisgen Reaction: Milestones of the 1,3-Dipolar Cycloaddition. *Angew. Chem. Int. Ed. Engl.*, **2020**, 59(30):12293-307.
127. Kolb, H.C., Finn, M.G., Sharpless, K.B. Click Chemistry: Diverse Chemical Function from a Few Good Reactions. *Angew. Chem. Int. Ed. Engl.*, **2001**, 40(11):2004-21.

128. Singh, M.S., Chowdhury, S., Koley, S. Advances of azide-alkyne cycloaddition-click chemistry over the recent decade. *Tetrahedron*, **2016**, 72(35):5257-83.
129. Kolb, H.C., Sharpless, K.B. The growing impact of click chemistry on drug discovery. *Drug Discov. Today.*, **2003**, 8(24):1128-37.
130. Hoyle, C.E., Bowman, C.N. Thiol-ene click chemistry. *Angew. Chem. Int. Ed. Engl.*, **2010**, 49(9):1540-73.
131. Hoyle, C.E., Lee, T.Y., Roper, T. Thiol-enes: Chemistry of the past with promise for the future. *J. Polym. Sci. A Polym. Chem.*, **2004**, 42:5301-38.
132. Borbás, A. Photoinitiated Thiol-ene Reactions of Enoses: A Powerful Tool for Stereoselective Synthesis of Glycomimetics with Challenging Glycosidic Linkages. *Chem. Eur. J.*, **2020**, 26:6090-101.
133. Kelemen, V., Bege, M., Eszenyi, D., Debreczeni, N., Bényei, A., Stürzer, T., Herczegh, P., Borbás, A. Stereoselective Thioconjugation by Photoinduced Thiol-ene Coupling Reactions of Hexo- and Pentopyranosyl D- and L-Glycals at Low-Temperature-Reactivity and Stereoselectivity Study. *Chem. Eur. J.*, **2019**, 25:14555.
134. Bege, M., Bereczki, I., Herczeg, M., Kicsák, M., Eszenyi, D., Herczegh, P., Borbás, A. A low-temperature, photoinduced thiol-ene click reaction: a mild and efficient method for the synthesis of sugar-modified nucleosides. *Org. Biomol. Chem.*, **2017**, 15(43):9226-33.
135. Fairbanks, B.D., Love, D.M., Bowman, C.N., Efficient Polymer-Polymer Conjugation via Thiol-ene Click Reaction. *Macromol. Chem. Phys.*, **2017**, 218:1700073.
136. Nolan, M.D., Scanlan, E.M. Applications of Thiol-Ene Chemistry for Peptide Science. *Front. Chem.*, **2020**, 8:583272.
137. Nair, D., Podgórski, M., Chatani, S., Gong, T., Xi, W., Fenoli, C.R., Bowman, C. The Thiol-Michael Addition Click Reaction: A Powerful and Widely Used Tool in Materials Chemistry. *Chem. Mater.*, **2014**, 26:724-44.
138. Morgan, C.R., Magnotta, F., Ketley, A.D. Thiol-ene photocurable polymers. *J. Polym. Sci. Polym. Chem. Ed.*, **1977**, 15:627-45.
139. Tasdelen, M.A., Yagci, Y. Light-Induced Click Reactions. *Angew. Chem. Int. Ed.*, **2013**, 52:5930-38.
140. Dadashi-Silab, S., Doran, S., Yagci, Y. Photoinduced electron transfer reactions for macromolecular syntheses. *Chem. Rev.*, **2016**, 116(17):10212-75.
141. Yagci, Y., Jockusch, S., Turro, N.J. Photoinitiated Polymerization: Advances, Challenges, and Opportunities. *Macromolecules*, **2010**, 43(15): 6245-60.
142. Thai Le, S., Malinowska, L., Vašková, M., Mező, E., Kelemen, V., Borbás, A., Hodek, P., Wimmerová, M., Csávás, M. Investigation of the Binding Affinity of a Broad

- Array of L-Fucosides with Six Fucose-Specific Lectins of Bacterial and Fungal Origin. *Molecules*, **2019**, 24(12):2262.
143. Malinovská, L., Thai Le, S., Herczeg, M., Vašková, M., Houser, J., Fujdiarová, E., Komárek, J., Hodek, P., Borbás, A., Wimmerová, M., Csávás, M. Synthesis of β -D-galactopyranoside-Presenting Glycoclusters, Investigation of Their Interactions with *Pseudomonas aeruginosa* Lectin A (PA-IL) and Evaluation of Their Anti-Adhesion Potential. *Biomolecules*, **2019**, 9(11):686.
144. Damalanka, V.C., Maddirala, A.R., Janetka, J.W. Novel approaches to glycomimetic design: development of small molecular weight lectin antagonists. *Expert Opin. Drug Discov.*, **2021**, 16(5):513-36.
145. Jančaříková, G., Herczeg, M., Fujdiarová, E., Houser, J., Kövér, K.E., Borbás, A., Wimmerová, M., Csávás, M. Synthesis of α -L-Fucopyranoside-Presenting Glycoclusters and Investigation of Their Interaction with *Photorhabdus asymbiotica* Lectin (PHL). *Chem. Eur. J.*, **2018**, 24(16):4055-68.
146. Guchhait, G., Misra, A.K. Efficient glycosylation of unprotected sugars using sulfamic acid: A mild eco-friendly catalyst. *Catal. Commun.*, **2011**, 14(1):52-7.
147. Matta, K.L., Girotra, R.N., Barlow, J.J. Synthesis of p-nitrobenzyl and p-nitrophenyl 1-thioglycopyranosides. *Carbohydr. Res.*, **1975**, 43:101-9.
148. Zemplén, G., Kuntz, A. *Ber.*, **1924**, 57B, 1357.
149. Adinolfi, M., Capasso, D., Di Gaetano, S., Iadonisi, A., Leone, L., Pastore, A. A straightforward synthetic access to symmetrical glycosyl disulfides and biological evaluation thereof. *Org. Biomol. Chem.*, **2011**, 9(18):6278.
150. Eszenyi, D., Kelemen, V., Balogh, F., Bege, M., Csávás, M., Herczeg, P., Borbás, A. Promotion of a Reaction by Cooling: Stereoselective 1,2-cis- α -Thioglycoconjugation by Thiol-Ene Coupling at -80 °C. *Chem. Eur. J.*, **2018**, 24(18):4532-36.
151. Chabre, Y.M., Shiao, T.C., Vidal, S., Roy, R. Synthesis of Prop-2-ynyl 2,3,4,6-Tetra-O-Acetyl- α -D-Mannopyranoside. Carbohydrate chemistry proven synthetic method. *CRC Press*, **2012**, 1(31):275-8.
152. Segura, M., Sansone, F., Casnati, A., Ungaro, R. Synthesis of Lower Rim Polyhydroxylated Calix[4]arenes. *Synthesis*, **2001**, 2105-12.
153. Goddard-Borger, E.D., Stick, R.V. An efficient, inexpensive, and shelf-stable diazotransfer reagent: imidazole-1-sulfonyl azide hydrochloride. *Org. Lett.*, **2007**, 9(19):3797-800.
154. Pandiakumar, A.K., Sarma, S.P., Samuelson, A.G. Mechanistic studies on the diazo transfer reaction. *Tetrahedron Lett.*, **2014**, 55(18):2917-20.

155. McPherson, J.C., Runner, R., Buxton, T.B., Hartmann, J.F., Farcasiu, D., Bereczki, I., Róth, E., Tollas, S., Ostorházi, E., Rozgonyi, F., Herczegh, P. Synthesis of osteotropic hydroxybisphosphonate derivatives of fluoroquinolone antibacterials. *Eur. J. Med. Chem.*, **2012**, 47(1):615-8.
156. McCourt, R.O., Scanlan, E.M. A Sequential Acyl Thiol-Ene and Thiolactonization Approach for the Synthesis of δ -Thiolactones. *Org. Lett.*, **2019**, 21(9):3460-4.
157. Zelli, R., Dumy, P., Marra, A. Metal-free synthesis of imino-disaccharides and calix-iminosugars by photoinduced radical thiol-ene coupling (TEC). *Org. Biomol. Chem.*, **2020**, 18:2392-7.
158. Kašáková, M., Malinovská, L., Klejch, T., Hlaváčková, M., Dvořáková, H., Fújdíarová, E., Rottnerová, Z., Mat'átková, O., Lhoták, P., Wimmerová, M., Moravcová, J. Selectivity of original C-Hexopyranosyl Calix[4]arene conjugates towards lectins of different origin. *Carbohydr. Res.*, **2018**, 469:60-72.
159. Sano, K., Ogawa, H. Hemagglutination (inhibition) assay. *Methods Mol Biol.*, **2014**, 1200:47-52.
160. Csávás, M., Malinovská, L., Perret, F., Gyurkó, M., Illyés, Z.T., Wimmerová, M., Borbás, A. Tri- and tetravalent mannoclusters cross-link and aggregate BC2L-A lectin from *Burkholderia cenocepacia*. *Carbohydr. Res.*, **2017**, 437:1-8.
161. Schlick, K.H., Cloninger, M.J. Inhibition binding studies of glycodendrimer-lectin interactions using surface plasmon resonance. *Tetrahedron*, **2010**, 66:5305-10.

8.2 List of publications



UNIVERSITY of
DEBRECEN

UNIVERSITY AND NATIONAL LIBRARY
UNIVERSITY OF DEBRECEN

H-4002 Egyetem tér 1, Debrecen
Phone: +3652/410-443, email: publikaciok@lib.unideb.hu

Registry number: DEENK/535/2021.PL
Subject: PhD Publication List

Candidate: Son Le Thai
Doctoral School: Doctoral School of Pharmacy

List of publications related to the dissertation

1. **Le Thai, S.**, Páll, D., Róth, E., Tran, T., Debreczeni, N., Bege, M., Bereczki, I., Ostorházi, E., Milánkovits, M., Herczegh, P., Borbás, A., Csávás, M.: The Very First Modification of Pleuromutilin and Lefamulin by Photoinitiated Radical Addition Reactions: synthesis and Antibacterial Studies.
Pharmaceutics. 13 (12), 1-21, 2021.
DOI: <http://dx.doi.org/10.3390/pharmaceutics13122028>
IF: 6.321 (2020)
2. **Le Thai, S.**, Malinovská, L., Vaskova, M., Mező, E., Kelemen, V., Borbás, A., Hodek, P., Wimmerová, M., Csávás, M.: Investigation of the Binding Affinity of a Broad Array of I-Fucosides with Six Fucose-Specific Lectins of Bacterial and Fungal Origin.
Molecules. 24 (12), 1-17, 2019.
DOI: <http://dx.doi.org/10.3390/molecules24122262>
IF: 3.267
3. Malinovská, L., **Le Thai, S.**, Herczeg, M., Vaskova, M., Houser, J., Fudiarová, E., Komárek, J., Hodek, P., Borbás, A., Wimmerová, M., Csávás, M.: Synthesis of [beta]-D-galactopyranoside-Presenting Glycoclusters, Investigation of Their Interactions with *Pseudomonas aeruginosa* Lectin A (PA-IL) and Evaluation of Their Anti-Adhesion Potential.
Biomolecules. 9 (11), 1-22, 2019.
DOI: <http://dx.doi.org/10.3390/biom9110686>
IF: 4.082





List of other publications

4. Szűcs, Z., Kelemen, V., **Le Thai, S.**, Csávás, M., Róth, E., Batta, G., Stevaert, A., Vanderlinden, E., Naesens, L., Herczegh, P., Borbás, A.: Structure-activity relationship studies of lipophilic teicoplanin pseudoaglycon derivatives as new anti-influenza virus agents.
Eur. J. Med. Chem. 157, 1017-1030, 2018.
DOI: <http://dx.doi.org/10.1016/j.ejmech.2018.08.058>
IF: 4.833

Total IF of journals (all publications): 18,503

Total IF of journals (publications related to the dissertation): 13,67

The Candidate's publication data submitted to the iDEa Tudóstér have been validated by DEENK on the basis of the Journal Citation Report (Impact Factor) database.

17 December, 2021



9. Keywords

antibiotic resistance, antiadhesive, lectin, lectin inhibitors, multivalents, glycomimetics, quinolone, pleuromutilin, chimeric antibiotic, novel therapy, pharmaceutical chemistry

10. Acknowledgement

First and foremost, I would like to express my sincere gratitude to my supervisor *Dr. Magdolna Csávás* for her understanding and wholehearted support during my research. Her instruction and advice have been invaluable since the first day I joined Ph.D. Her patience and care over the years have been my motivation to complete this research. For me, it has been an honour to be her Ph.D. student.

Secondly, I would like to extend my gratitude to *Dr. Lenka Malinovská*, assistant professor of the National Centre for Biomolecular Research, Faculty of Science, Masaryk University, and *Dr. Eszter Ostorházi*, associate professor of the Department of Medical Microbiology, Semmelweis University, for measuring biological activity, for collaboration and support which are crucial to my Ph.D. work.

I would like to deeply thank *Prof. Anikó Borbás*, Professor and Head of the Department of Pharmaceutical Chemistry, and *Prof. Pál Herczegh*, Professor at the Department of Pharmaceutical Chemistry, for their professional advice that helped me to accomplish my research experiments.

I would like to greatly thank *Dr. Ilona Bakai-Bereczki*, assistant professor at our department, for the MALDI-ToF measurement and the help with my reactions.

I am very grateful to *Dr. Nóra Debreczeni*, *Dr. Miklós Bege*, *Dr. Mihály Herczeg*, *Dr. Zsolt Szűcs*, *Dr. Máté Kicsák*, *Dr. Erika Hevesi-Mező*, *Dr. Fruzsina Demeter*, Department of Pharmaceutical Chemistry, and *Prof. Gyula Batta*, Professor at Department of Organic Chemistry, for their help in the practical work and NMR measurements and interpretations.

I gratefully appreciate *Erzsébet Róth* and *Bodza Márta*, laboratory technician, for their valuable knowledge and practical experience. I also appreciate *Mariann Varga*, laboratory technician, for measuring optical rotation of the compounds, and *Dóra Fekete*, laboratory technician, for her help during my work. I wish to thank *Dr. Eszter Boglárka Lőrincz* for her help with my experiments, *Dr. Zsolt Szűcs* and *Dr. Viktor Kelemen* for helping me since the first day I joined in as a foreign student.

I wish to extend my gratitude to *Zsuzsa Molnár-Koszorus* for her help with the administrative work.

Last but not least, I truly thank my family. Words can not express how much I owe *my parents, my brother and sister, my relatives, and my friends*, for their support, encouragement, care and love. I can never come to this point in my life without them.

This work was supported under the projects NKFIH K119509, EFOP-3.6.1-16-2016-00022 "Debrecen Venture Catapult Program" and EFOP-3.6.3-VEKOP-16-2017-00009.

11. Appendix

1. CARBOHYDRATE-BASED POTENTIAL ANTIMICROBIAL DRUGS AND GLYCOPEPTIDES WITH OLD AND NEW THERAPEUTIC GOALS

M. Csávás, L. Malinovská, G. Jančaříková, Son Thai Le, Zs. Szűcs, P. Herczegh, M. Wimmerová, A. Borbás
Joint Meeting of Medicinal Chemistry, Prága, 2019

2. SYNTHESIS OF ANTIBACTERIAL MULTIVALENT CARBOHYDRATE-ANTIBIOTIC CHIMERAS WITH POTENTIAL AFFINITY TO BACTERIAL LECTINS

Son Le Thai, Anikó Borbás, Magdolna Csávás
International Workshop on Chemistry and Chemical Biology of Carbohydrates, Nucleic Acids and Antibiotics, Mátrafüred, 2019

3. CARBOHYDRATE-ANTIBIOTIC CHIMERAS WITH POTENTIAL ANTIMICROBIAL EFFECTS

Son Thai Le, M. Csávás
Research and Development for Therapeutical Purposes Conference, Debrecen, 2019

4. MULTIVALENS SZÉNHYDRÁTOK SZINTÉZISE ÉS LEKTINEKKEL VALÓ KÖLCSONHATÁSÁNAK VIZSGÁLATA

Csávás Magdolna, Lenka Malinovská, Gita Jancaríková, Son Thai Le, Herczeg Mihály, E. Kövér Katalin, Michaela Wimmerová, Borbás Anikó
International Chemical Conference, Sovata, 2019

5. SYNTHESIS OF CARBOHYDRATE-ANTIBIOTIC CHIMERA: COUPLING OF AN ALPHA-L-FUCOSIDE CONTAINING MULTIVALENT GLYCOCLUSTERS WITH FLUOROQUINOLONE ANTIBIOTICS

Son Thai Le, Gyula Batta, Anikó Borbás, Magdolna Csávás
Chemistry towards Biology, Budapest, 2018

6. SYNTHESIS OF AN ALPHA-L-FUCOSIDES PRESENTING CHIMERIC GLYCOCLUSTER

Son Thai Le, Gyula Batta, Anikó Borbás, Magdolna Csávás

Annual meeting of the Working Committee for Carbohydrates, Nucleic Acids and Antibiotics of the Hungarian Academy of Sciences, Mátrafüred, 2018

7. STRUCTURE-ACTIVITY RELATIONSHIP STUDIES OF LIPOPHILIC TEICOPLANIN PSEUDOAGLYCON DERIVATIVES AS NEW ANTI-INFLUENZA VIRUS AGENTS

Zsolt Szűcs, Viktor Kelemen, Son Thai Le, Magdolna Csávás, Erzsébet Róth, Gyula Batta, Evelien Vanderlinden, Anikó Borbás, Lieve Naesens, Pál Herczegh

Annual meeting of the Working Committee for Carbohydrates, Nucleic Acids and Antibiotics of the Hungarian Academy of Sciences, Mátraháza, 2017